LMSC-F115808

FINAL REPORT

Advanced Planar Array Development For Space Station

Lockheed Missiles & Space Company

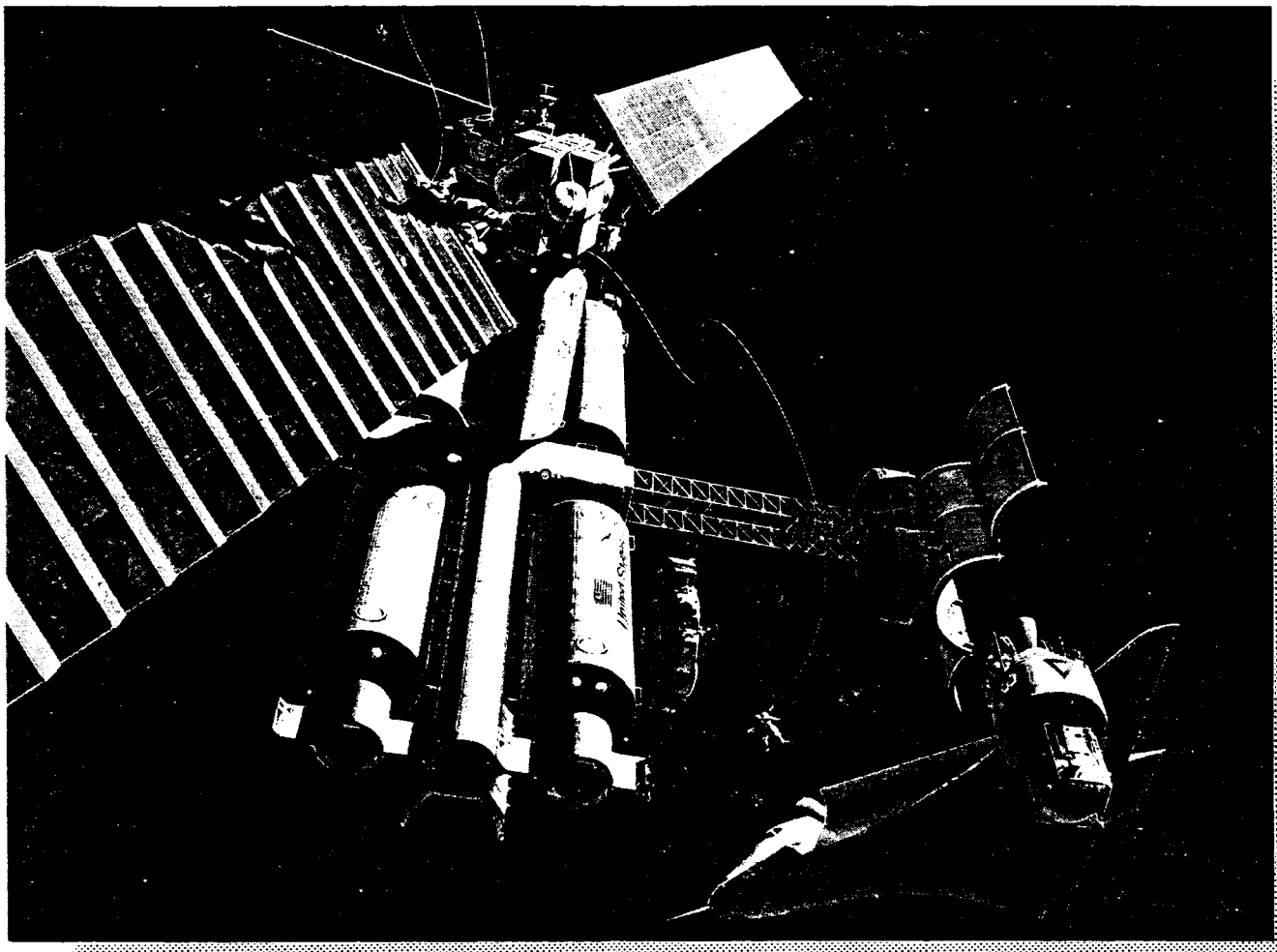

FINAL REPORT

LMSC-F115808

JUNE 1987

Advanced Planar Array Development For Space Station

submitted to:

NASA

MARSHALL SPACE FLIGHT CENTER

National Aeronautics and Space Administration

Lockheed Missiles & Space Company

FOREWORD

This report documents the work performed by Lockheed Missiles & Space Company, Inc., Sunnyvale, California, for Marshall Space Flight Center (MSFC) of the National Aeronautics and Space Administration under contract no. NAS8-36419 on the Advanced Planar Array Development for Space Station project.

The term of this contract was originally 30 months beginning on 1 June 1985 and concluding on 30 November 1987. Due to funding cutbacks, the contract ended on 1 June 1987. This report summarizes the full term effort performed on the subject contract over this entire period.

The Contracting Officer Representative (COR) from NASA/MSFC was originally Ralph Carruth, and then on 30 May 1986, Steve M. Tesney became the COR from NASA/MSFC. These two men provided technical direction for this work.

TABLE OF CONTENTS

TABLE OF CONTENTS (cont.)

LIST OF FIGURES

LIST OF FIGURES (cont.)

LIST OF FIGURES (cont.)

LIST OF TABLES

PRECEDING PAGE BLANK NOT FILMED

Section 1
INTRODUCTION AND SUMMARY

1.1 INTRODUCTION

This report details the results of the Advanced Planar Array Development for the Space Station contract. The original objectives of the contract were (1) to develop a process for manufacturing superstrate assemblies, (2) to demonstrate superstrate technology through fabrication and test, (3) to develop and analyze a preliminary solar array wing design, and (4) to fabricate a wing segment based on the wing design. After funding cutbacks, the major objectives were confined to objectives (1) and (2) as stated above.

The primary tasks completed were designing test modules, fabricating test modules, and testing modules. LMSC performed three tests which included thermal cycle testing for 2000 thermal cycles, thermal balance testing at the Boeing Environmental Test Lab in Kent, Washington, and acceptance testing a 15" x 50" panel segment for 100 thermal cycles.

The superstrate modules performed well during both thermal cycle testing and thermal balance testing. The successful completion of these tests demonstrates the technical feasibility of a solar array power system utilizing superstrate technology. This final report describes the major elements of this contract including the manufacturing process used to fabricate modules, the tests performed, and the results and conclusions of the tests.

1.2 APPROACH

The project was managed by the Astronautics Division's Space Station program office headed by R. P. Marcellini. The original project organization is shown in Figure 1-1. Several organizational changes were made during the contract. Because of funding

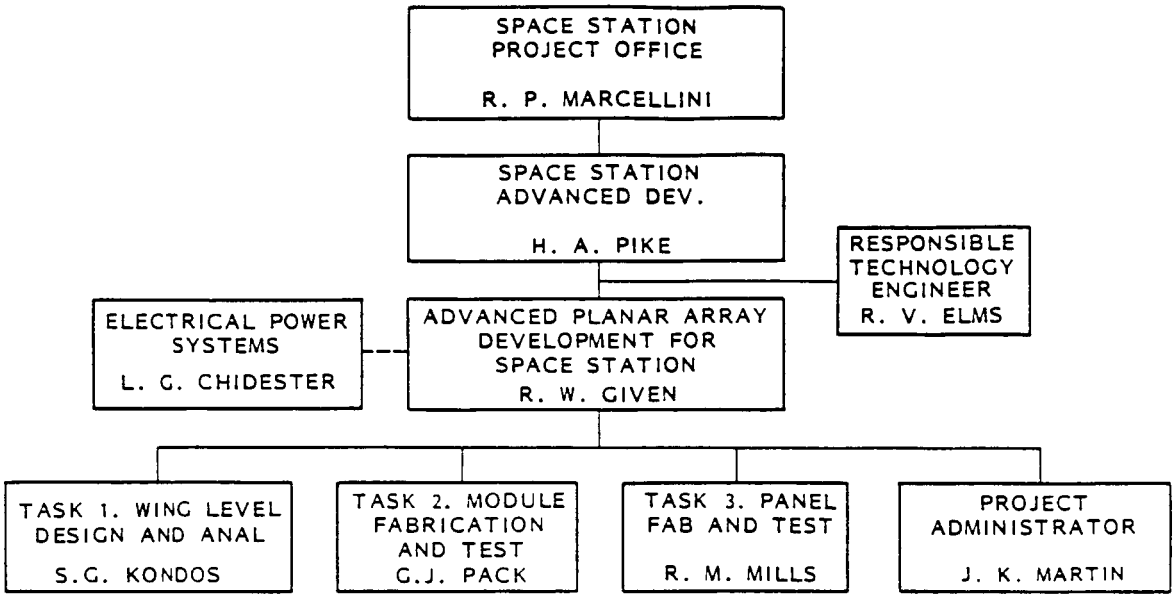

Figure 1-1 Space Station Project Reporting Relationship

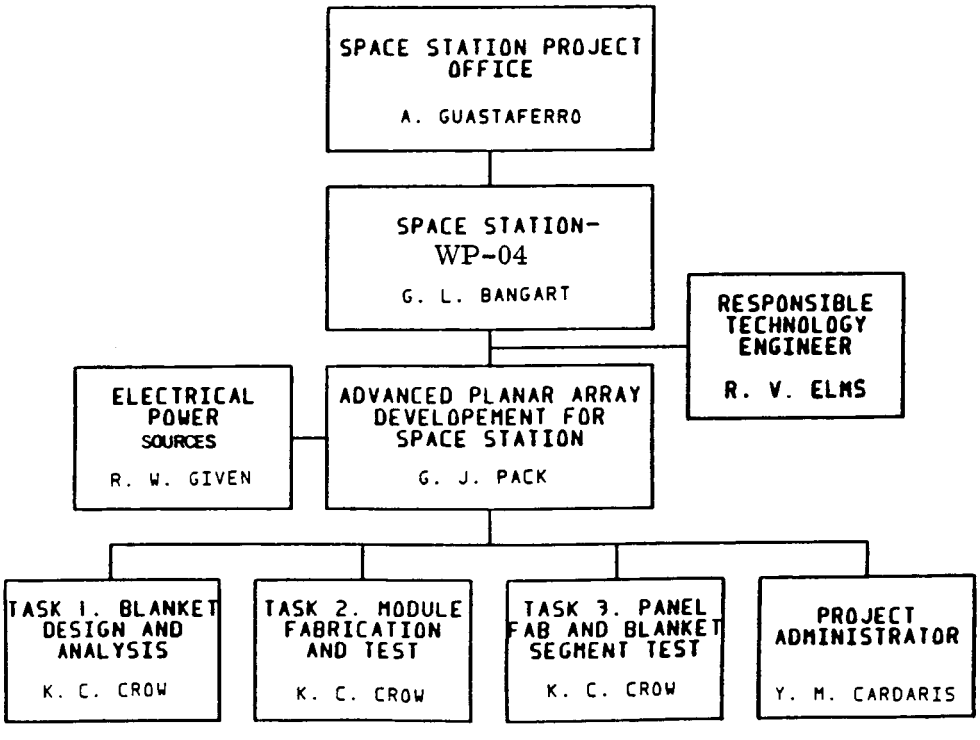

Figure 1-2 Final Space Station Project Reporting Relationship

cutbacks, the manpower level was reduced to one engineer, Mr. Ken Crow. Also, there were upper management changes on the Space Station program resulting in a program organization structure as shown in Figure 1-2.

1.3 TASK DESCRIPTION

A work breakdown by Tasks is shown in Figure 1-3. With the reduction in funding on this contract, several items in the original work breakdown were not completed. Those items not completed were discussed and agreed upon at the time of contract renegotiation. Those items completed were all tasks related to module level analysis, design, fabrication, and test, and the items not completed were all tasks related to wing level analysis, design, fabrication, and test.

1.4 PROJECT FLOW DIAGRAM

A revised work flow diagram is shown in Figure 1-4 which incorporates changes from the work flow diagram presented in the original contract proposal. These changes were the result of contract cutbacks. The main intent of the project flow diagram is to show how contract requirements lead to developing modules, to testing modules, to delivering modules, and to reporting results.

1.5 SCHEDULE

The original term of this contract was a 30 month period from 1 June 1985 to 30 November 1987, but with funding cutbacks the contract period was reduced to 15 months ending 30 August 1986. LMSC requested an extension to close off the contract which was granted. The contract was extended through 1 June 1987 to prepare a final report, to present a final oral report, to complete thermal balance analysis, and to deliver tested modules. The contract schedule appears in Figure 1-5.

TASK 1.0 WING DESIGN AND ANALYSIS

- *1.1 DEVELOP PRELIMINARY DESIGN OF A SOLAR ARRAY WING
- 1.2 DETAIL DESIGN
- 1.3 ENVIRONMENT/ANALYSIS
  - 1.3.1 Ground Handling Environment
  - 1.3.2 Shuttle Orbiter Launch and Reentry Environments
  - 1.3.3 Low Earth Orbit Operational Environment
  - 1.3.4 Resultant Electrical Performance

TASK 2.0 MODULE FABRICATION AND TESTS

- *2.1 THERMAL CYCLE TESTING
- *2.2 THERMAL BALANCE TESTING
- *2.3 15" x 50" DELIVERABLE MODULE

TASK 3.0 PANEL FABRICATION AND TESTING

- 3.1 FABRICATE SOLAR ARRAY PANELS
- 3.2 DEVELOPMENT TESTING
- 3.3 STOWAGE AND SMALL SEGMENT TESTING

TASK 4.0 DELIVERABLES

- *4.1 FINAL REPORT
- *4.2 ALL MODULES TESTED IN TASK 2.0
- *4.3 15" x 50" MSFC TEST MODULE
- 4.4 WING SEGMENT AND DEPLOYER

TASK 5.0 REPORTING

- *5.1 MONTHLY PROGRESS REPORTS AND MANAGEMENT (FINANCIAL) REPORTS
- *5.2 MID-TERM ORAL PRESENTATIONS
- *5.3 FINAL ORAL PRESENTATION
- *5.4 FINAL COMPREHENSIVE REPORT

*COMPLETED

Figure 1-3 Task Description

ORIGINAL PAGE IS
OF POOR QUALITY

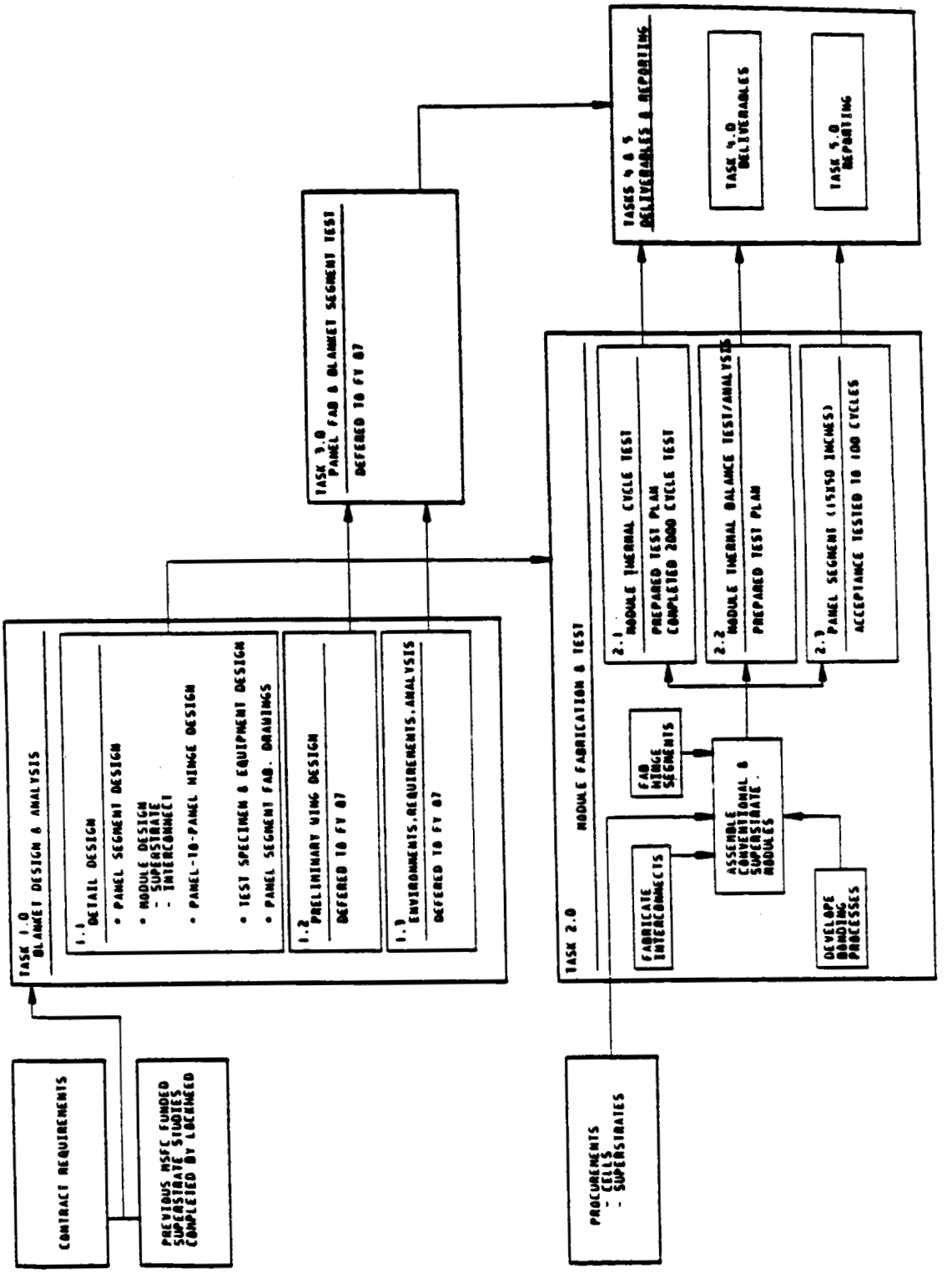

Figure 1-4 Project Flow Diagram

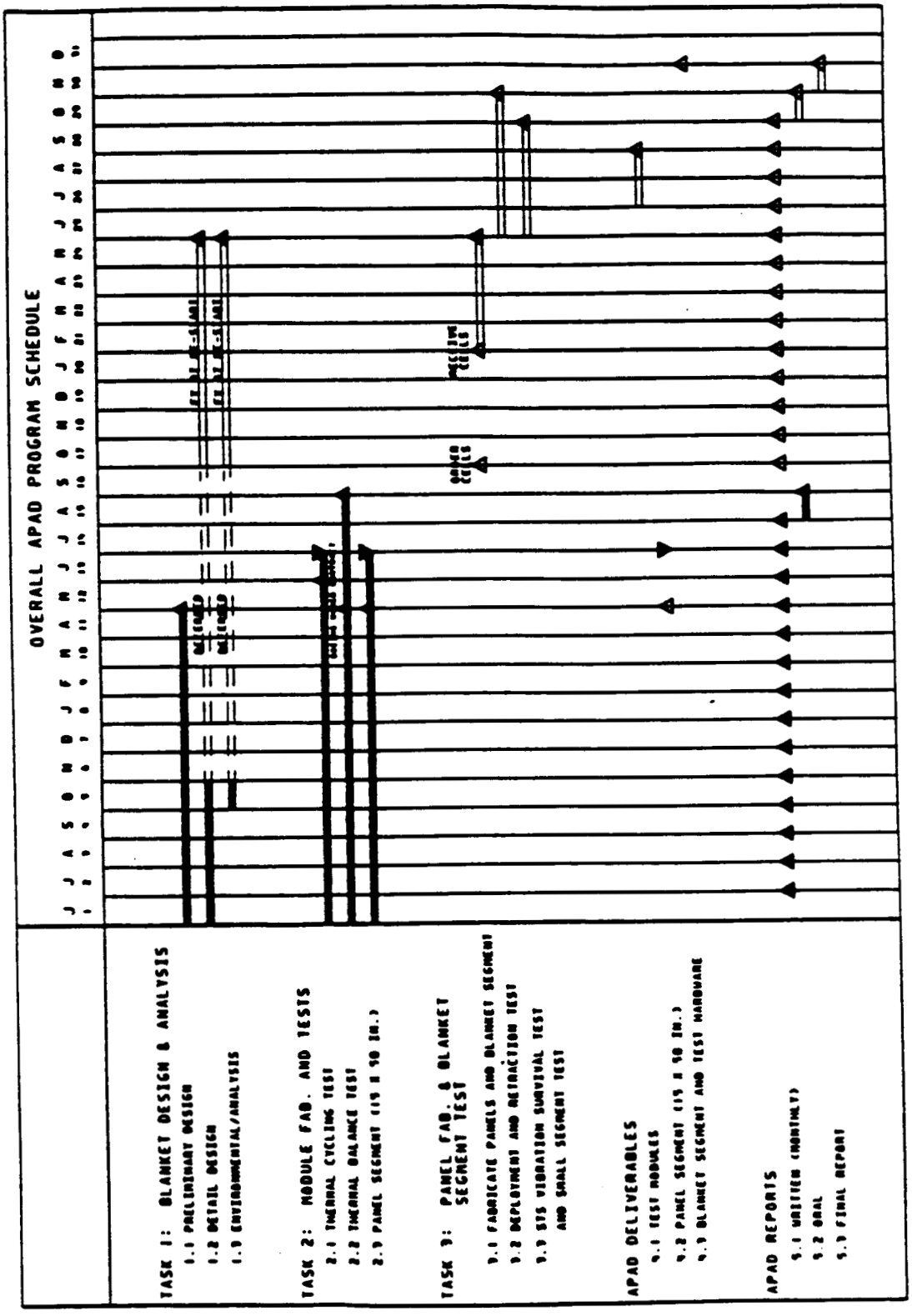

Figure 1-5 Schedule

ORIGINAL PAGE IS
OF POOR QUALITY

1.6 SUMMARY

A total of twelve (12) modules were fabricated for test purposes. The three uses of these modules included thermal cycling a five (5) module panel segment at MSFC, thermal cycling four (4) modules for 2000 cycles at LMSC, and thermal balance testing three (3) modules at Boeing in Kent, Washington.

Section 2
MODULE DESIGN DESCRIPTION

There were two types of modules tested on this contract. One type used the conventional Solar Array Flight Experiment (SAFE) technology, and the other used an advanced superstrate technology. A description of the two types of modules follows and includes a description of the solar cells, interconnects, superstrate hinges, and the module assemblies.

2.1 LARGE AREA SOLAR CELL ASSEMBLY

The solar cells used to fabricate the superstrate were made of 2 ohm-cm, wraparound contact (WAC) design. The cells were 5.9 x 5.9 cm^2 and 8 mils thick with a gridded "p" contact. The electrical efficiency of the cells was 13.2% at AM0 and 25°C. The back surface treatment was an optical coating to enhance IR transmission.

The solar cells used to fabricate the SAFE type module were the same as the solar cells described above except the back surface treatment was an aluminum 2000-4000 angstrom reflector. Figure 2-1 shows an IR transparent cell and an aluminum back surface reflector cell. Figure 2-2 describes the different components of both types of solar cell assemblies.

2.2 MODULE INTERCONNECTS

Two new interconnect designs were developed to maximize the IR transmission of the cell by having the traces follow the "p" contacts and grids and by routing the traces in-between cells where possible. In addition, some kapton was cut away to further enhance IR transmission. Two interconnect designs were needed to support the two different kinds of testing, thermal cycling and thermal balance testing. Figure 2-3 shows the thermal cycle module interconnect design and Figure 2-4 shows the thermal balance module interconnect design.

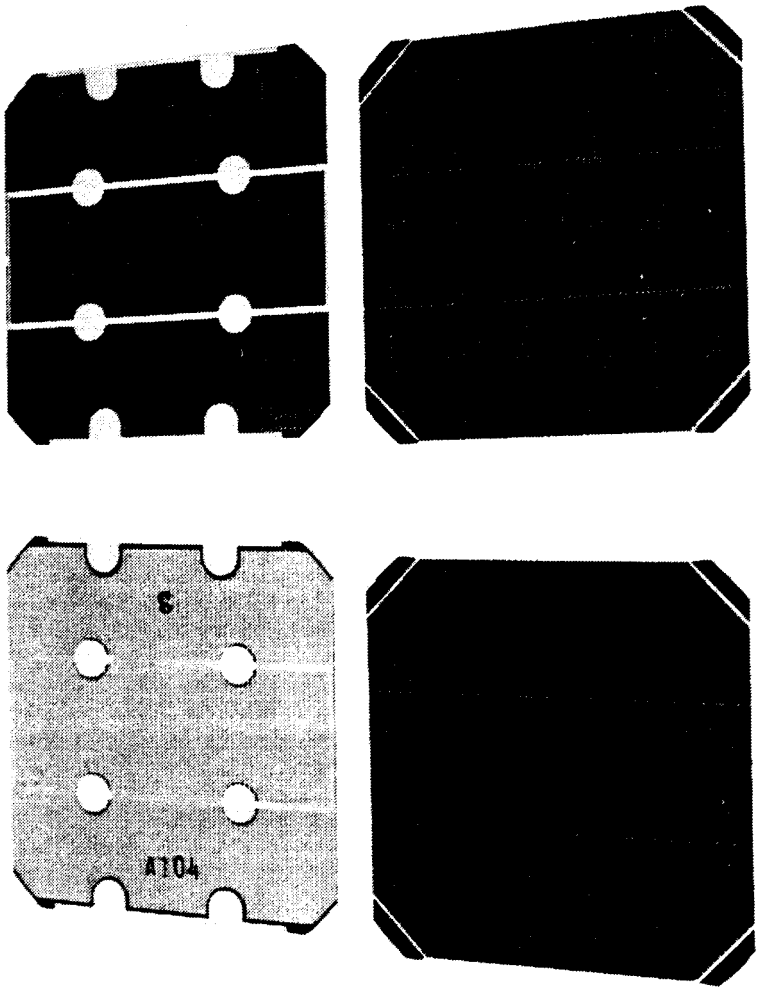

Figure 2-1 Solar Cell Comparison

ORIGINAL PAGE IS
OF POOR QUALITY

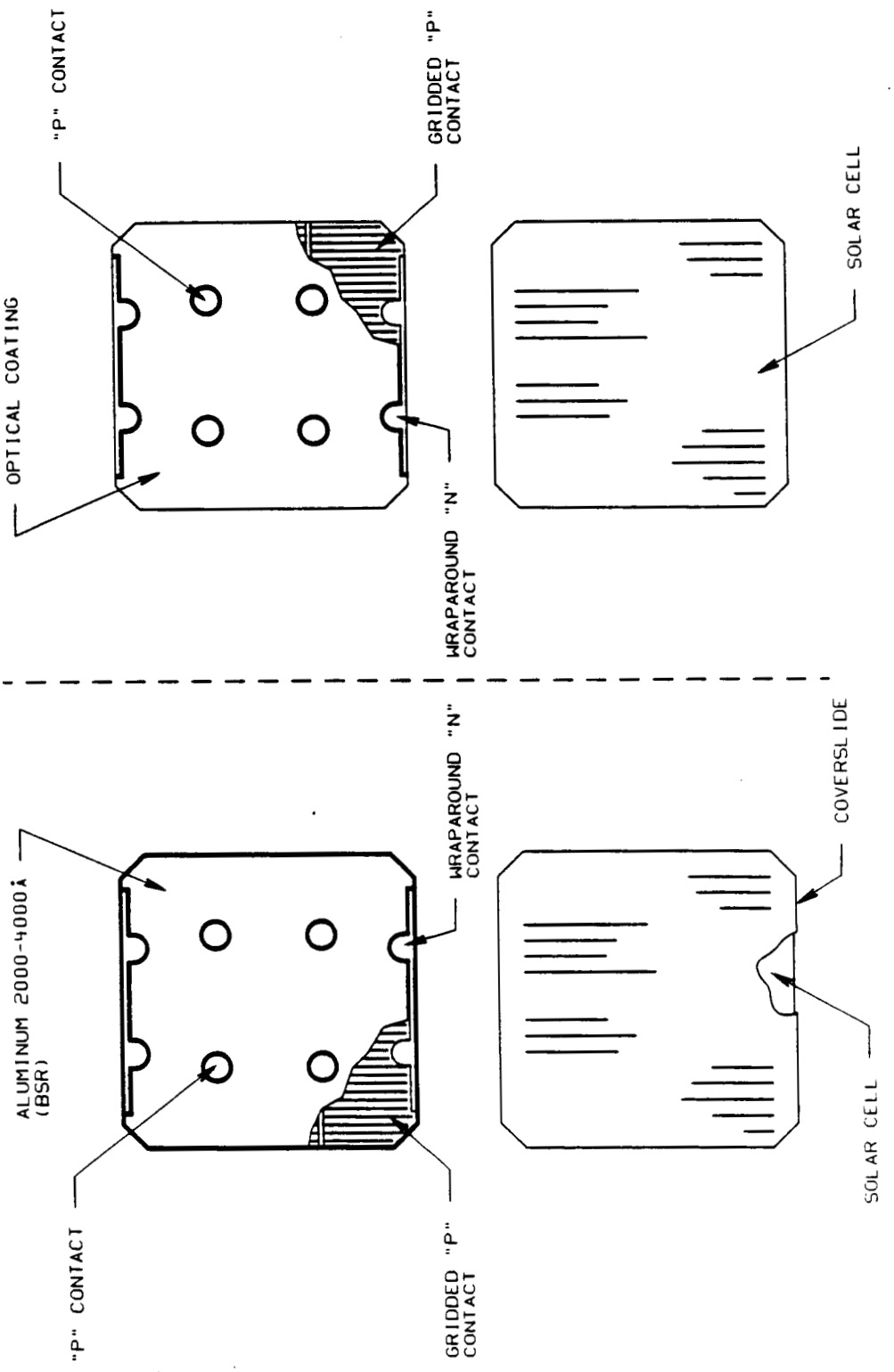

Figure 2-2 Solar Cell Components

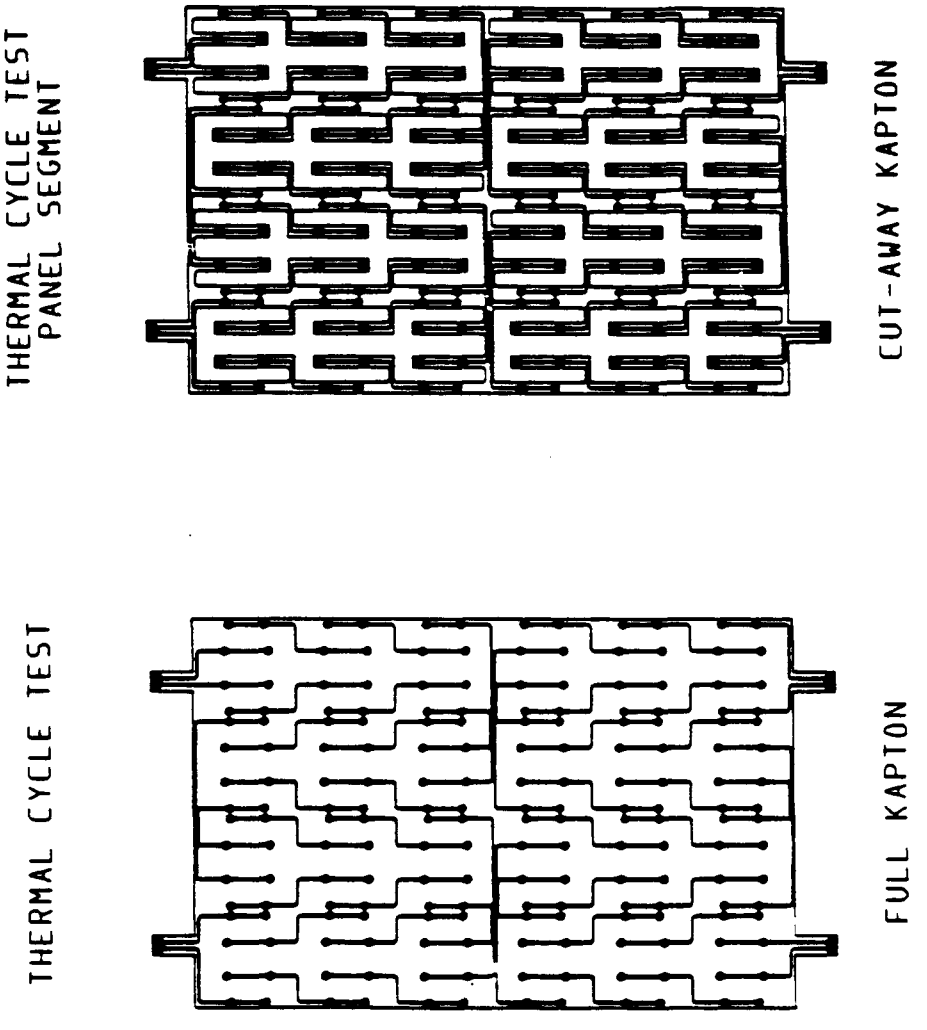

Figure 2-3 Module Interconnects

THERMAL BALANCE TEST MODULES

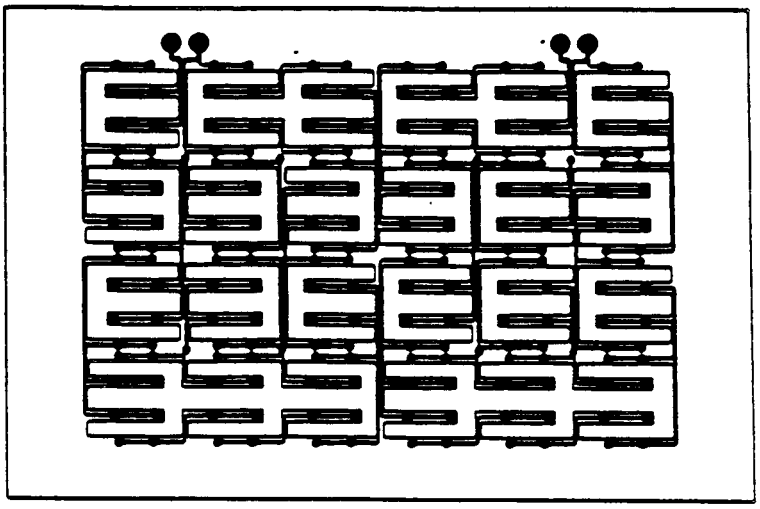

CUT-AWAY KAPTON

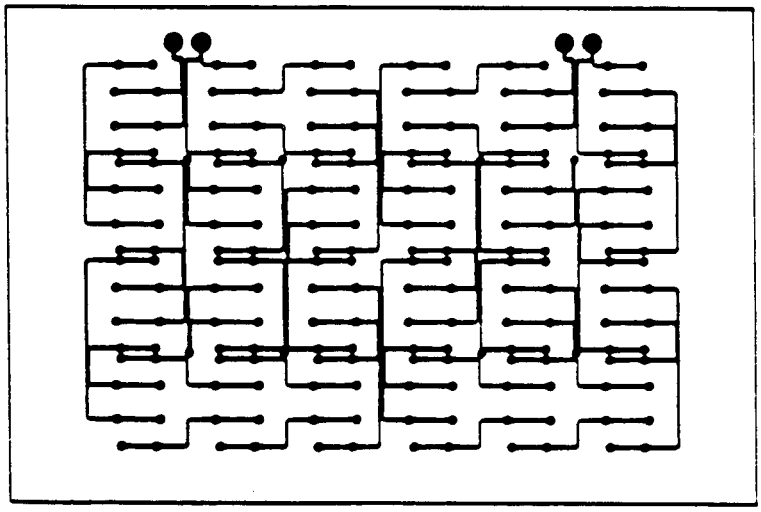

FULL KAPTON

Figure 2-4 Module Interconnects

2.3 SUPERSTRATE HINGE

Figure 2-5 shows the hinge design developed under a previous MSFC contract. The hinge elements consist of 1 mil moly with an upper and lower configuration. Two fiberglass hinge stiffeners are sandwiched between the two hinge elements of opposing superstrate modules. A hinge pin is used to hold the hinge assembly together and to allow for freedom of rotation about the hinge pin.

The superstrate hinge was used on the five unit panel segment. Each superstrate module had an upper and lower hinge element bonded to the superstrate glass.

2.4 SUPERSTRATE MODULE ASSEMBLY

The superstrate module assembly differs from the conventional SAFE-type module as shown in Figure 2-6. The conventional module bonds an individual coverslide (microsheet glass) on each solar cell with silicone adhesive (DC 93-500). The superstrate module consists of a sheet of microsheet glass bonded to twenty-four solar cells using silicone adhesive (DC 93-500). A sheet of scrim cloth is sandwiched between the glass and solar cells for the superstrate assembly. The scrim cloth is 3 mils thick and is made of S-glass fibers. The function of the scrim cloth is to control bondline thickness and to hold the assembly together if a crack should occur.

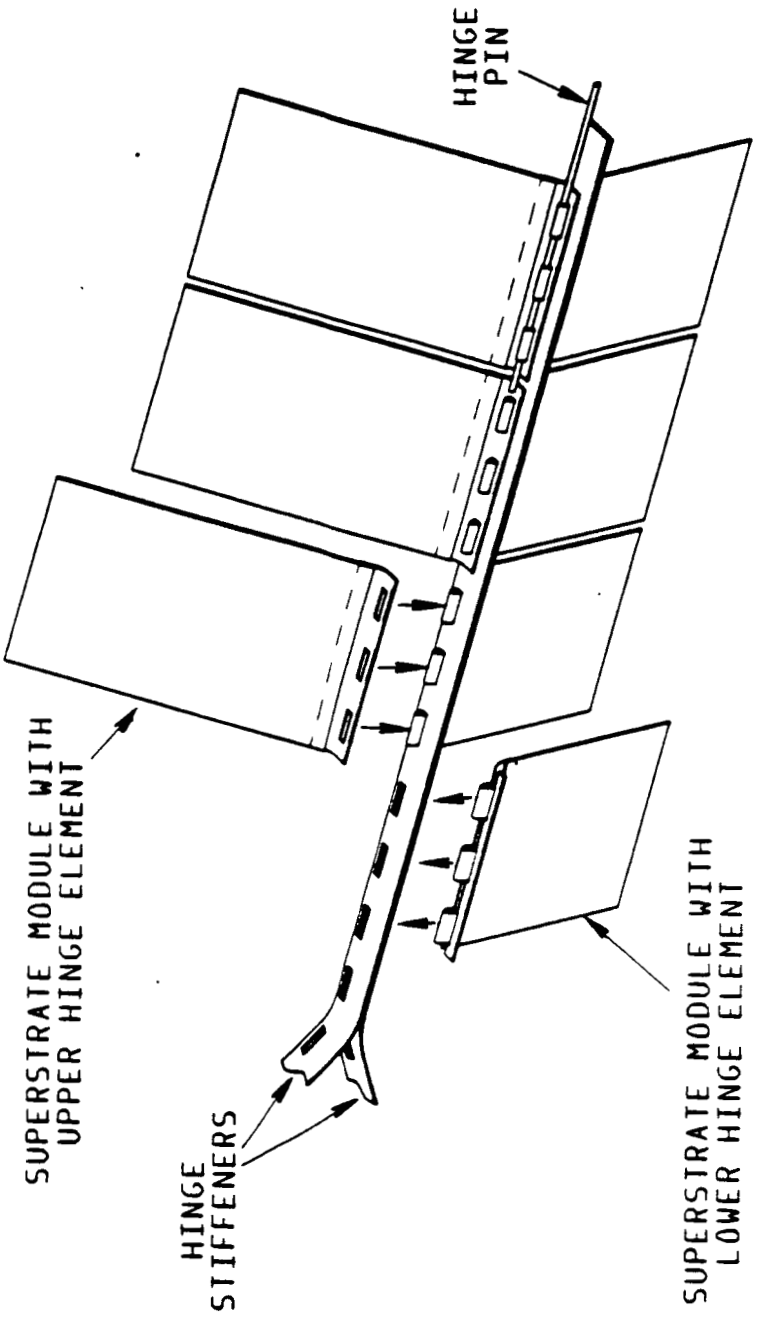

Figure 2-5 Superstrate Hinge

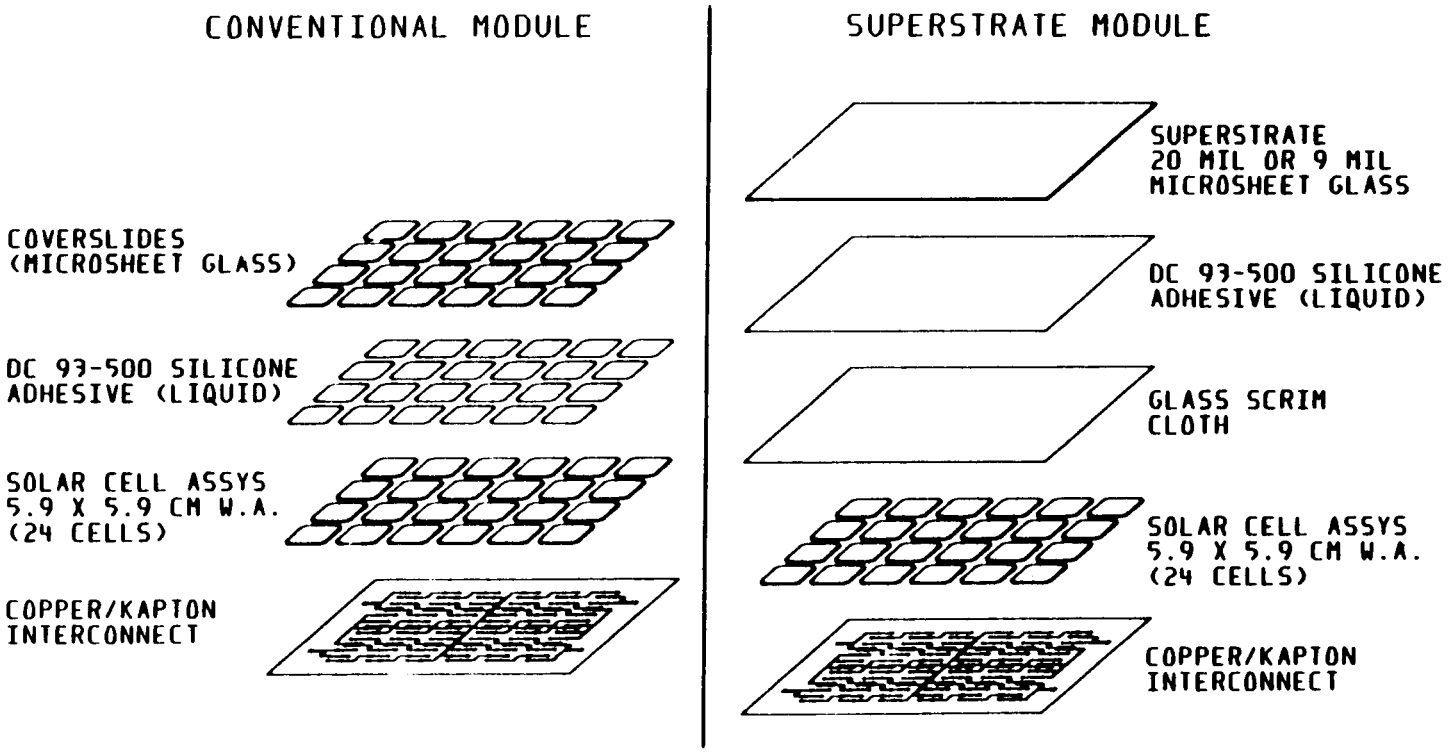

Figure 2-6 Module Assembly - Superstrate vs Conventional

Section 3
MANUFACTURING PROCESS DEVELOPMENT

3.1 BONDING GLASS TO SOLAR CELLS

In order to develop a successful process for bonding superstrates to solar cells, our LMSC process engineers started by bonding four solar cells to a sheet of glass. When the bonding process was sufficient to produce no bubbles during lay up or cure time, we designed the fabrication tooling for the full sized samples.

3.2 TOOLING

There were three major tools as well as various shop aids. Figure 3-1 shows one of the major tools, the superstrate bonding tool. The tool was made of aluminum and its overall dimensions were 1" x 14.5" x 20". To maintain the proper solar cell registration during bonding, small aluminum dividers were milled into the tool. In addition, .25" diameter pins were press fit into the tool to locate the superstrate glass with respect to the solar cells. The tool was also designed to provide a vacuum to hold the solar cells in place. By milling a cavity in the back of the tool, drilling vacuum ports in the front of the tool, attaching a vacuum nozzle on the side of the tool, and sealing the edge of the tool with a silicone rubber, we were able to establish a vacuum system. The front of the tool was teflon coated to allow for easy superstrate removal after bonding and to allow for easy tool cleaning.

The second major tool was a hinge forming die, see Figure 3-2. The hinge forming die was used to form a ridge in the moly, lower hinge element. The ridge in the lower hinge element fits into the slotted upper hinge element as was shown in Figure 2-5.

The third major tool was the hinge bonding tool, see Figure 3-3. After the solar cells were bonded to a sheet of superstrate glass, the upper and lower hinge elements are bonded to the superstrate assembly. The superstrate glass was located in the hinge tool by butting the glass against two perpendicular edges which were machined

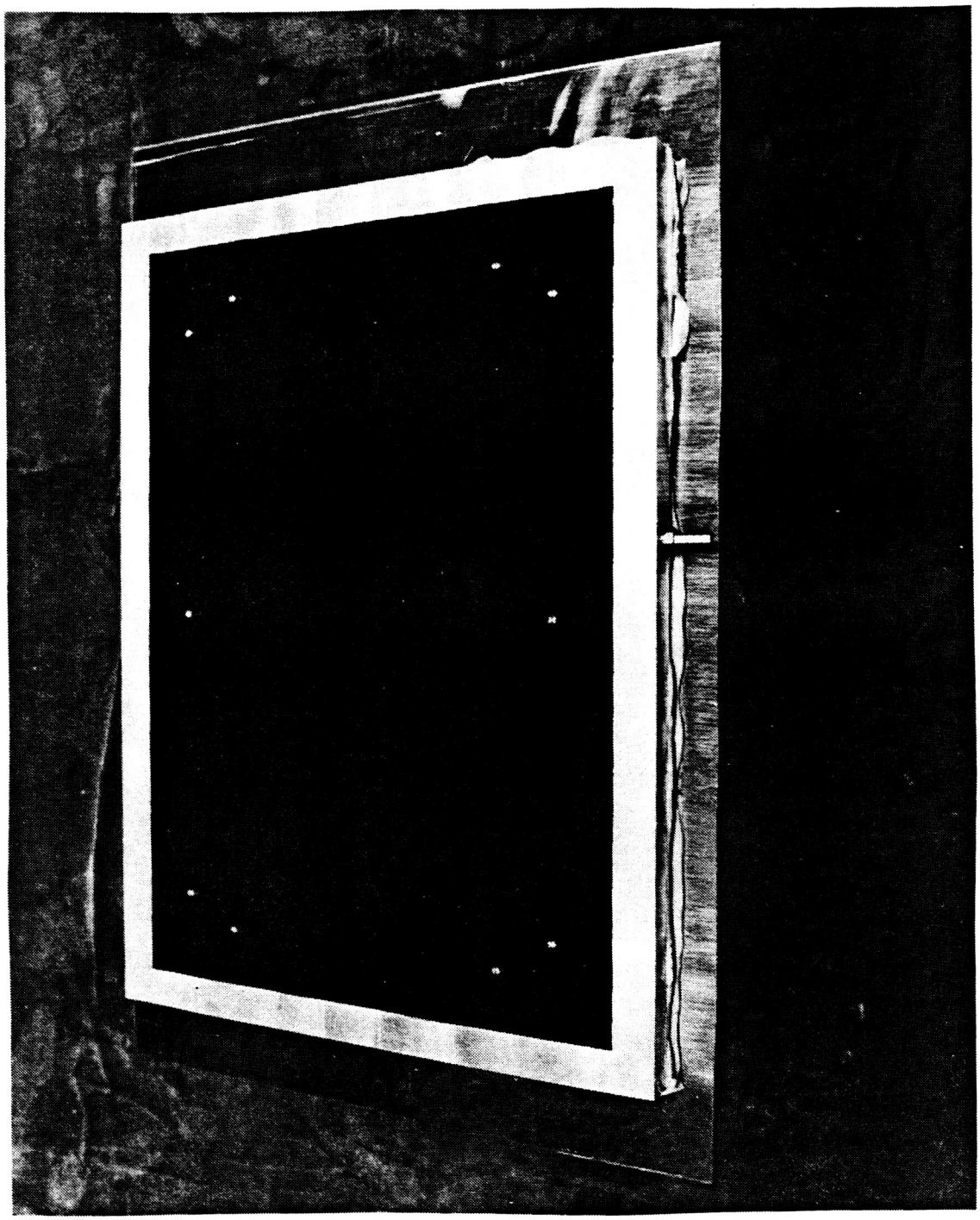

Figure 3-1 Superstrate Bonding Tool

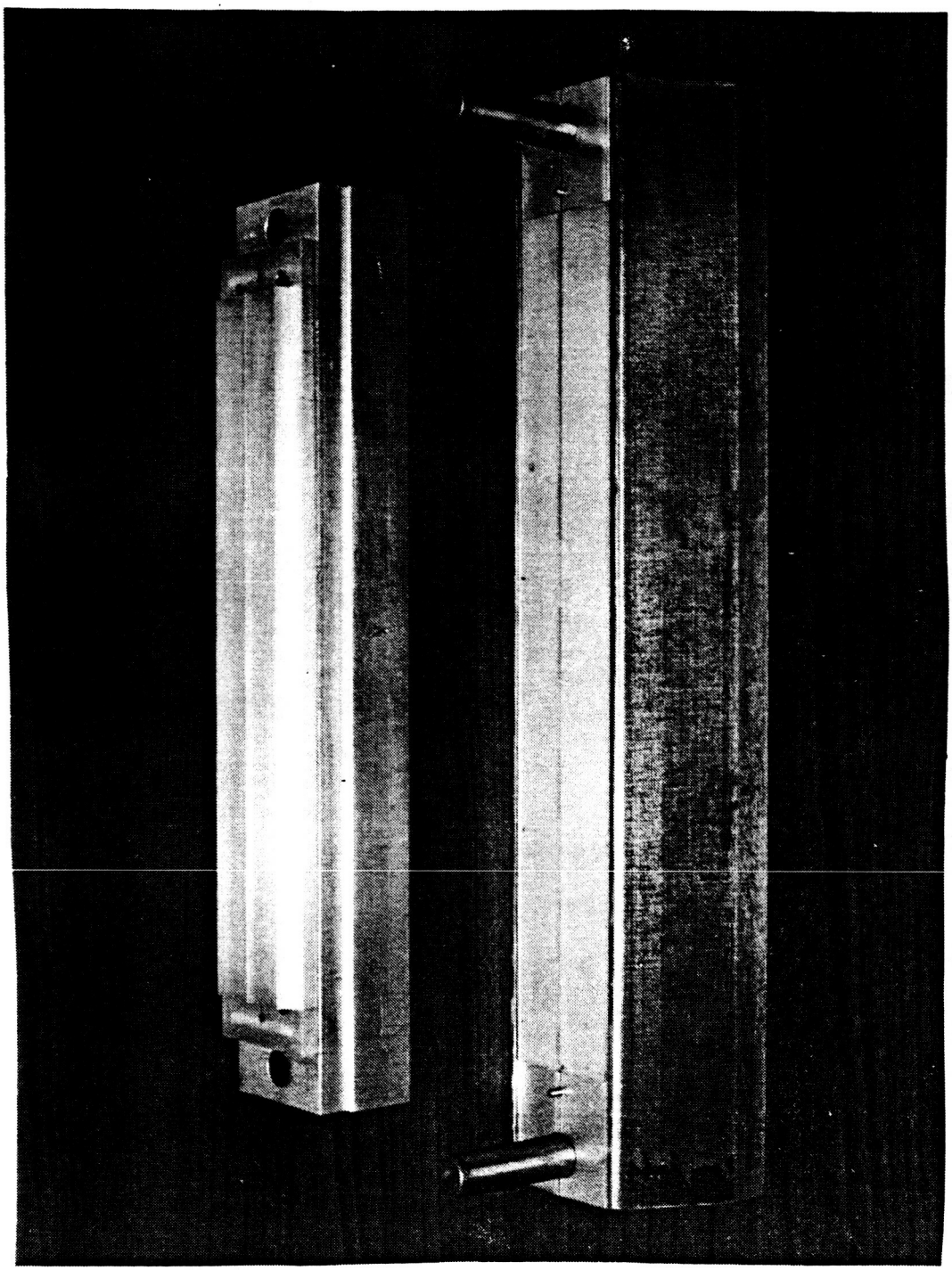

Figure 3-2 Hinge Forming Die

ORIGINAL PAGE IS
OF POOR QUALITY

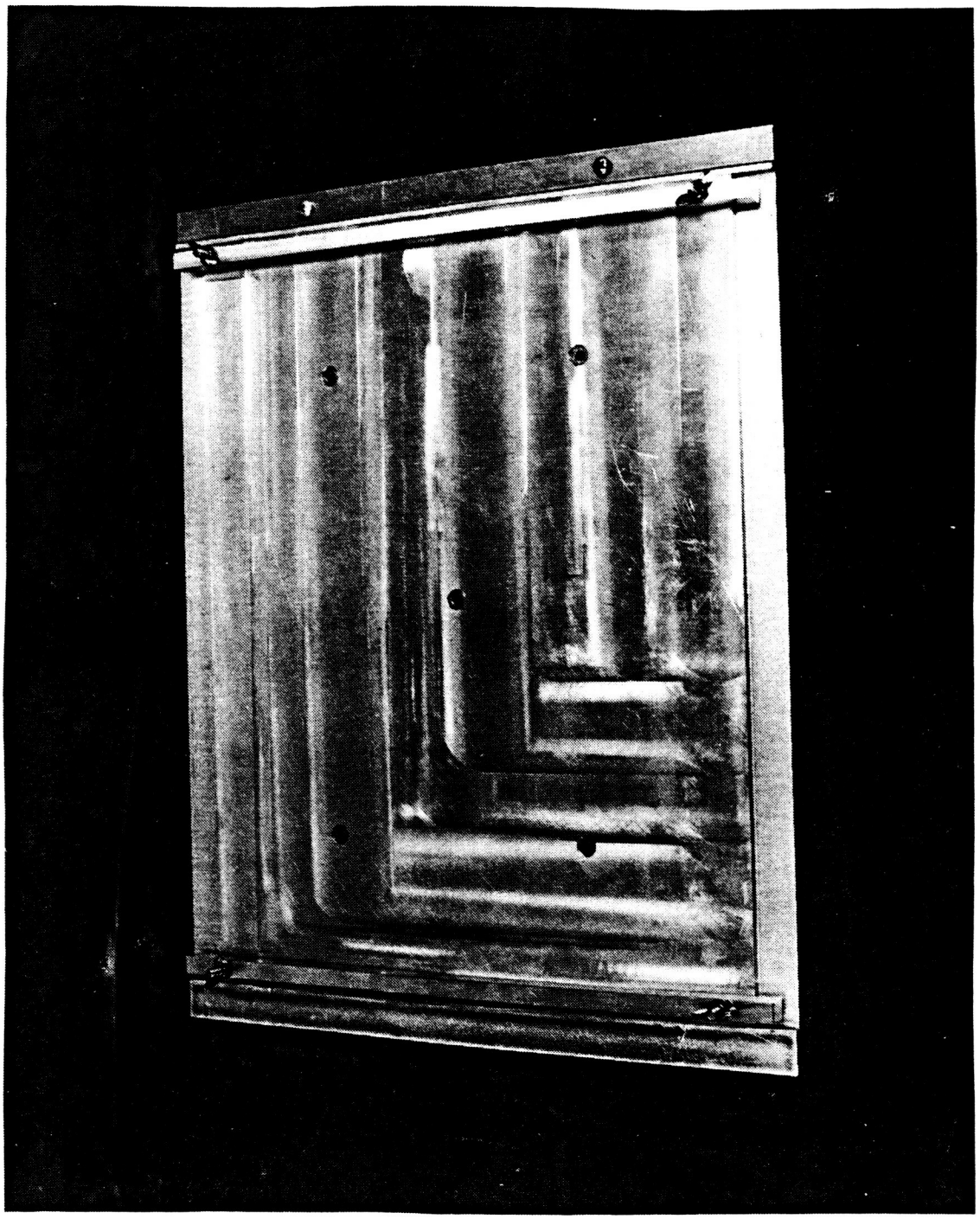

Figure 3-3 Hinge Bonding Tool

into the tool. By applying pressure along the hinge bondline using aluminum bars and locating the hinges with respect to the glass using pins, the hinges were bonded in place.

3.3 MANUFACTURING PROCESS

Two manufacturing processes were considered in bonding solar cells to superstrate glass. One approach was welding solar cells to a copper/kapton interconnect, applying adhesive to the superstrate glass and scrim cloth, placing the welded solar cell module on top of the superstrate glass, applying a vacuum bag to the assembly, and autoclaving the assembly to cure the adhesive and to drive adhesive bubbles out from between the solar cells and superstrate glass. This approach had been used on previous superstrate work, but was not used on this contract because this approach required using an autoclave instead of an oven and this approach allowed adhesive squeeze out to embed "n" contact wrap-around weld joints with adhesive.

The second approach considered in fabricating superstrate assemblies required bonding solar cells to the superstrate glass prior to welding the copper/kapton interconnect to the solar cells. This approach was the manufacturing process used on this contract because the process used a conventional oven and eliminated adhesive squeeze out problems with "n" contact weld areas. This process is described below in detail beginning with superstrate glass preparation.

3.4 SUPERSTRATE GLASS PREPARATION

The following steps were used to insure a good bond between the superstrate glass and the solar cells with no bubbles.

- Mask edges of glass on the side not to be bonded with 3M336 tape ~2" wide.
- Clean the bonding surface of glass with TX409 wetted with 2-propanol and place on flat block.
- Cut quartz paper (scrim cloth) to a size slightly larger (~1" each dimension) than the glass.

- Mix 50 g of DC 93-500 (50 g resin, 5 g curing agent) and degas until no bubbles are present.
- Pour the mixed and degassed adhesive in center on the glass.
- Place the quartz paper (scrim cloth) over the puddle and place clean sheet of Mylar on top.
- Using a rubber roller distribute the adhesive over the whole surface by rolling over Mylar. Start from the center and move roller out toward edges, pushing the air toward edges and assuring complete wetting of quartz paper by the adhesive.
- Cure the superstrate assembly with weight ($\sim$20 lb) applied to it for 4 hrs/150 $\pm$ 10°F.
- Cool to room temperature with weight on top.
- When cooled, remove weight and carefully peel off the Mylar film.
- Trim excess paper and adhesive by running razor blade carefully around edges of glass.

3.5 PREPARE SOLAR CELLS

- Position cells into bonding fixture--bonding side down (Figure 3-4). Pull vacuum to hold cells in place.
- Mask the top surface with single piece of 3M336 tape; provide cutouts for spacers and pins (Figure 3-5).
- Release vacuum, apply strip of paper to tape edges, and remove cells from tool.
- Mold release tool using MS122 teflon spray.
- Place cells back into tool--taped side down and pull vacuum (Figure 3-6).
- Clean bonding surfaces of cells with TX409 wetted with 2-propanol. Air dry for 10 minutes.

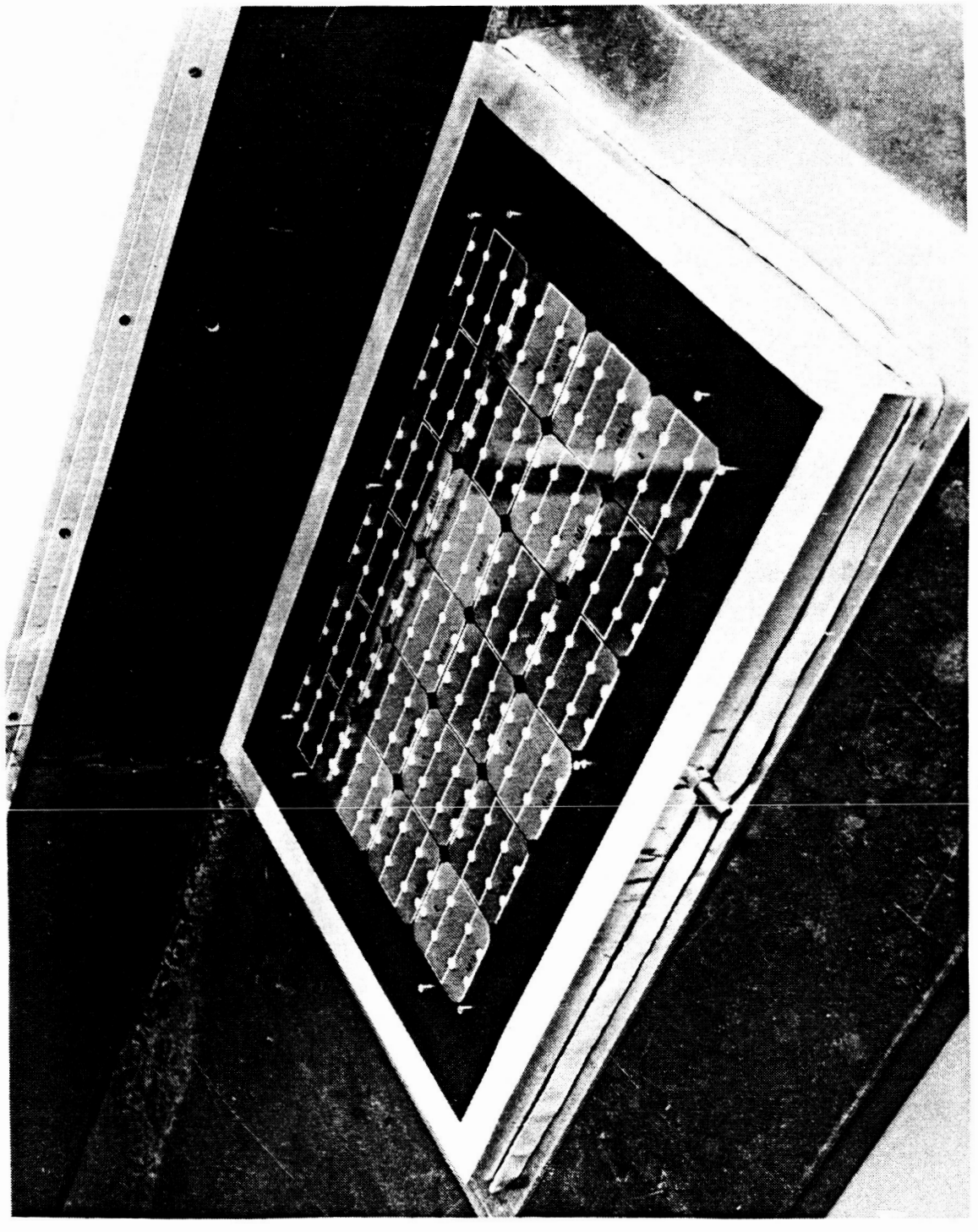

Figure 3-4 Solar Cells Positioned in Bonding Tool

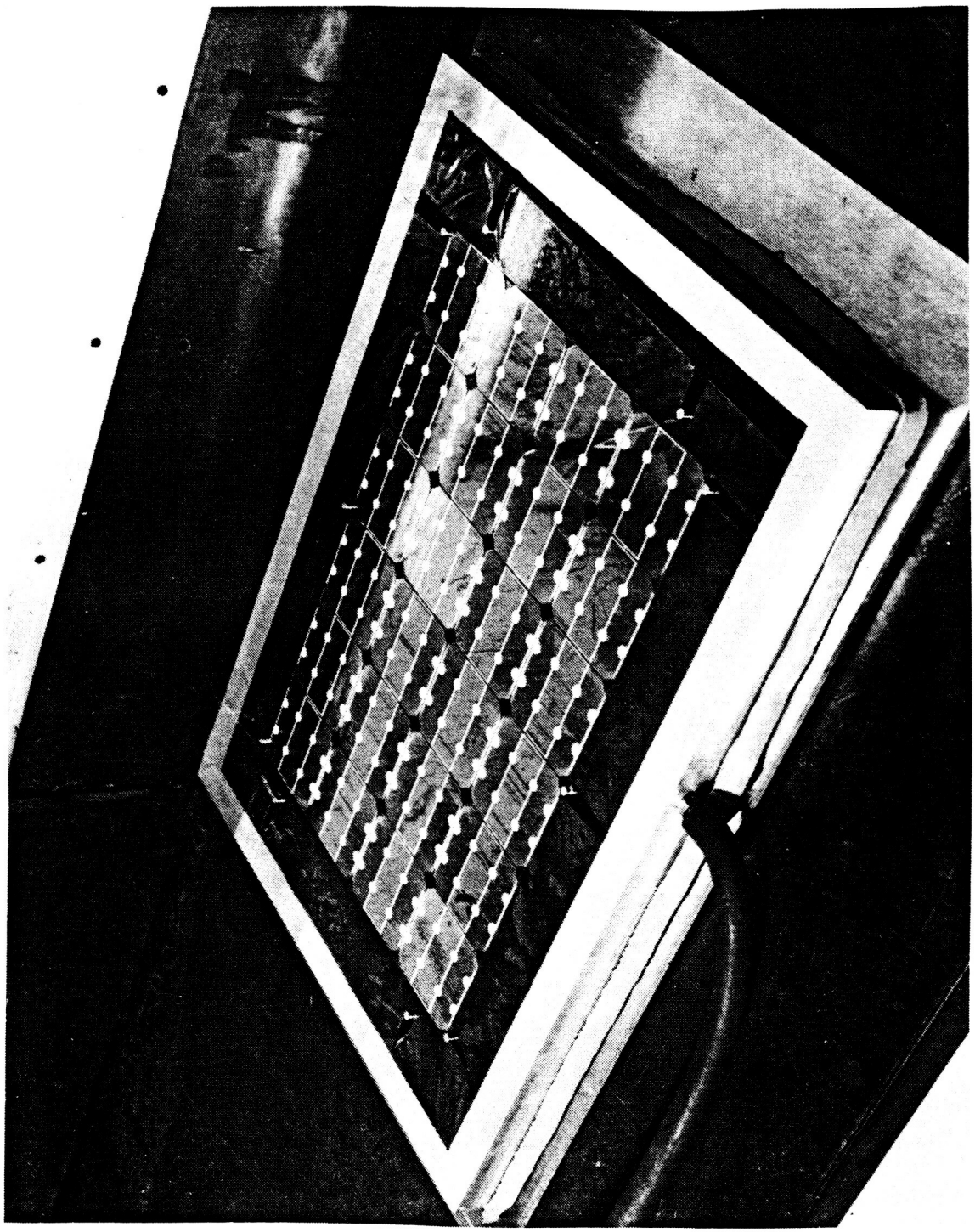

Figure 3-5 Masked Solar Cells Using Low Tack Tape

ORIGINAL PAGE IS
OF POOR QUALITY

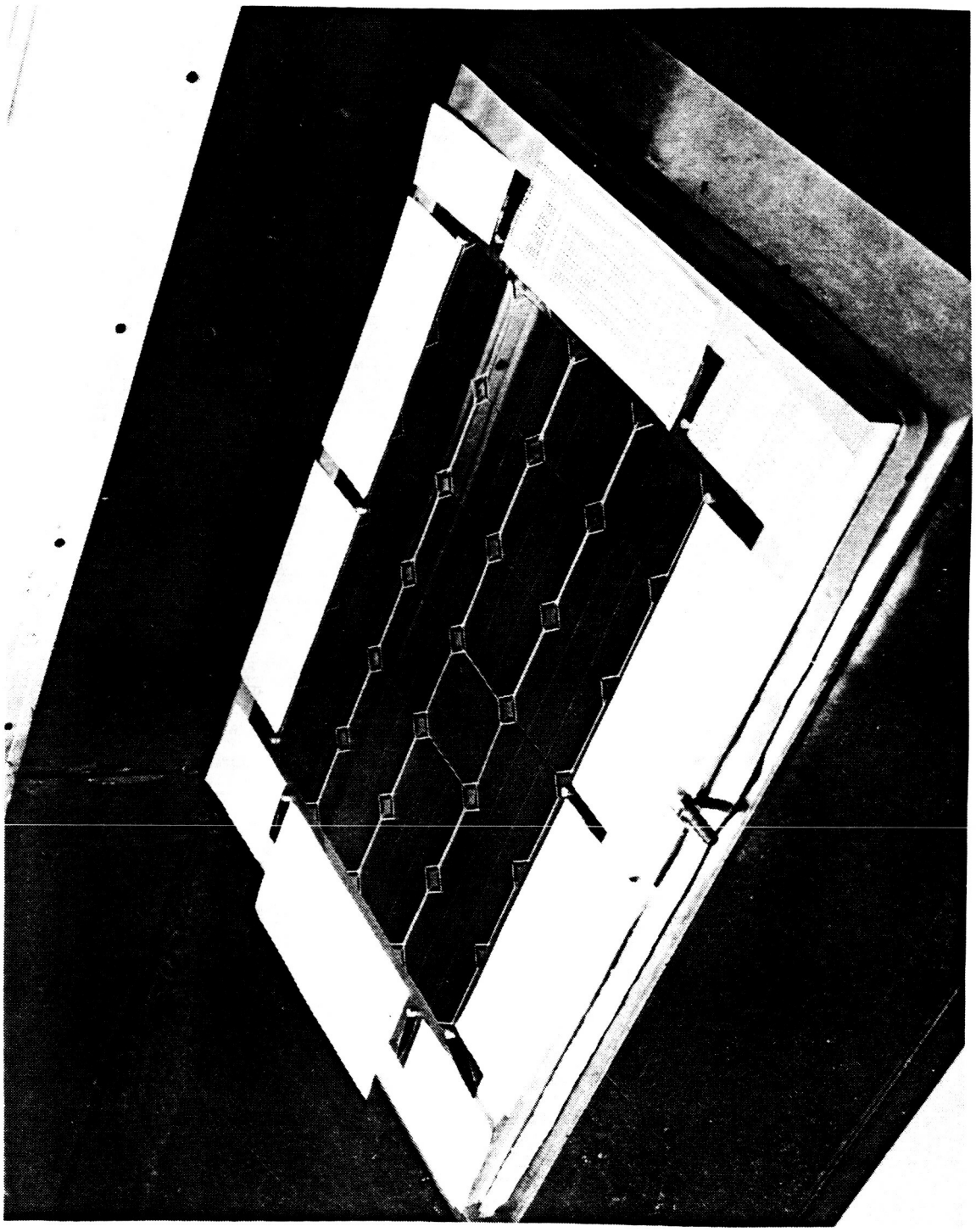

Figure 3-6 Solar Cells Face Up In Bonding Tool

3.6 ASSEMBLE SUPERSTRATE AND CELLS

- Mix 40 g of DC 93-500 (40 g resin, 4 g curing agent) and degas bubble free.
- Wipe the bonding surfaces (superstrate and cells) with TX409 wetted with 2-propanol.
- Pour the mixed and degassed adhesive across the cells held in tool (Figure 3-7). Form a puddle in the middle of cells running along the long dimension (Figure 3-8).
- Place the prepared superstrate over the puddle--laminated paper down (Figure 3-9).
- Allow the adhesive to spread as much as possible.
- Use a rubber roller to complete the spread, rolling from center out, pushing air to edges. Prevent forming dry spots which is caused by applying too much pressure (Figure 3-10).
- When complete spread is achieved and glass is positioned within locating pins (Figure 3-11), place flat plate with weight ($\sim$40 lb) over the assembly and release vacuum from tool. (Foam must be placed under the plate), see Figure 3-12.
- Place assembly in the oven and cure 4 hours minimum/150 $\pm$ 10°F. Cool to room temperature with weight on top.
- Remove weight and assembly from tool. In case of sticking, blow a stream of air under cells to release them from the tool.
- Remove masking tape and clean any excess adhesive from top of superstrate and back of cells with 2-propanol.

Figure 3-7 Apply DC 93-500 Adhesive to Solar Cells

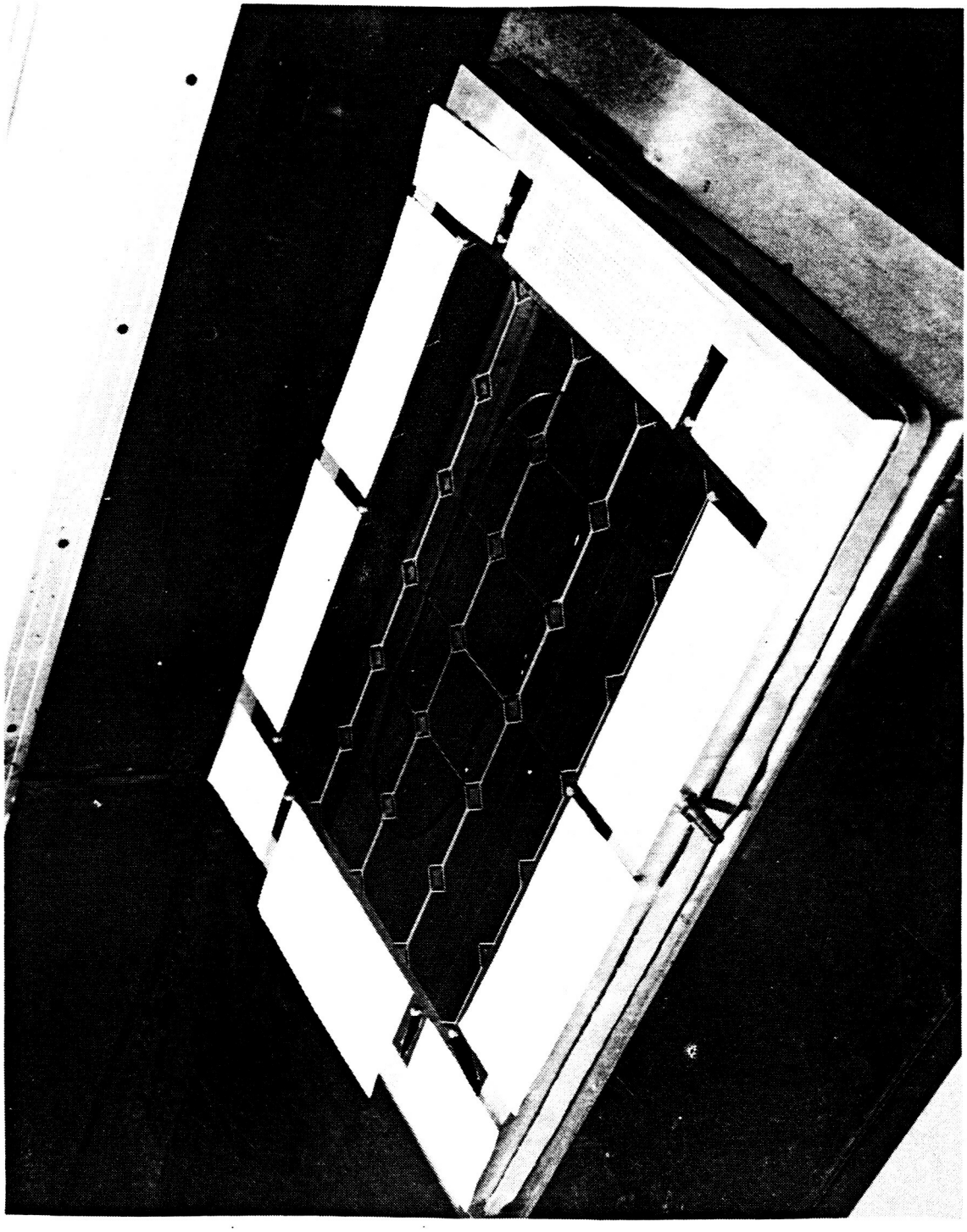

Figure 3-8 Puddle of DC 93-500 Adhesive

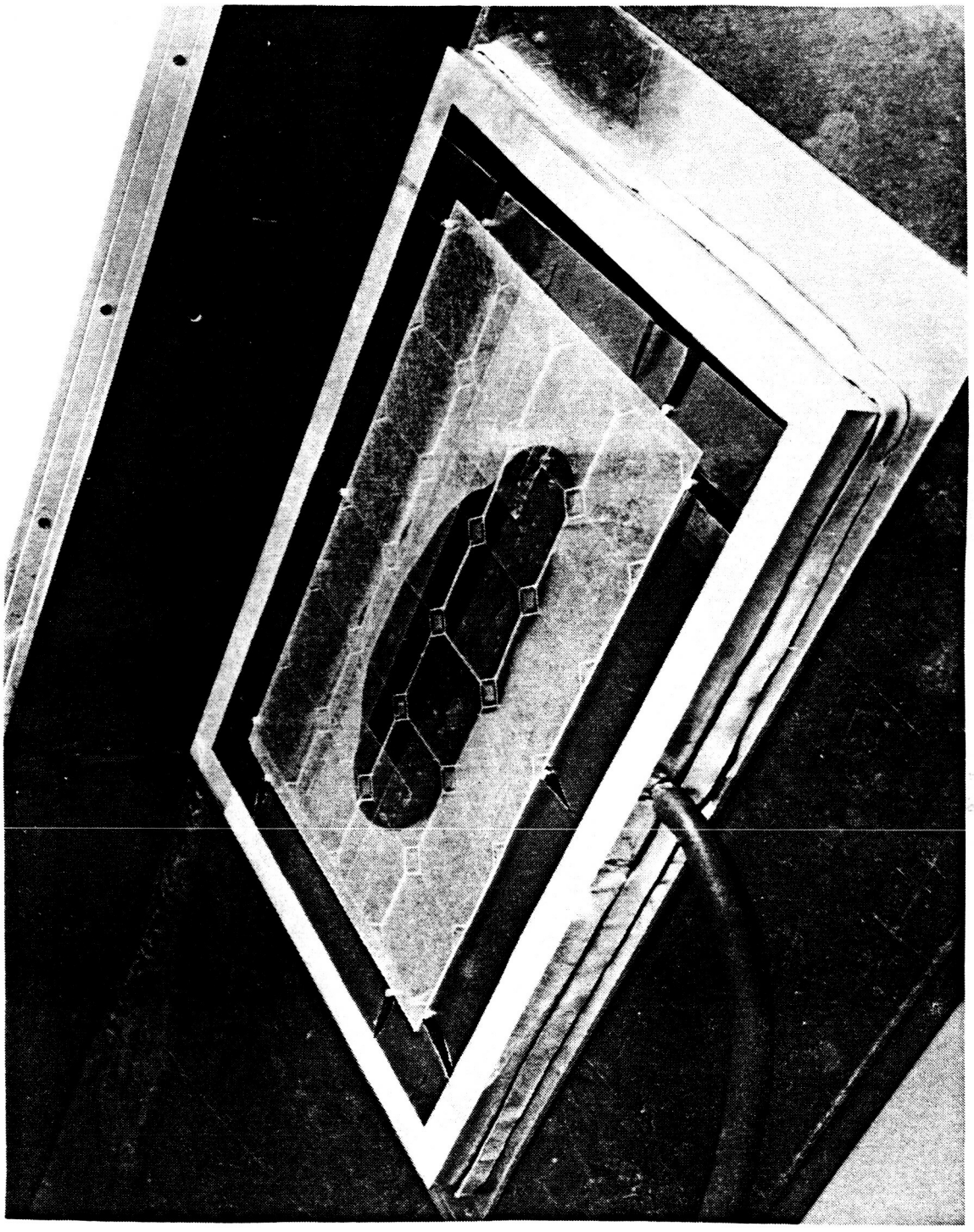

Figure 3-9 Superstrate Glass with Pre Cured Scrim Cloth Positioned Over Solar Cells

Figure 3-10 Distribute Adhesive Using Roller

ORIGINAL PAGE IS
OF POOR QUALITY

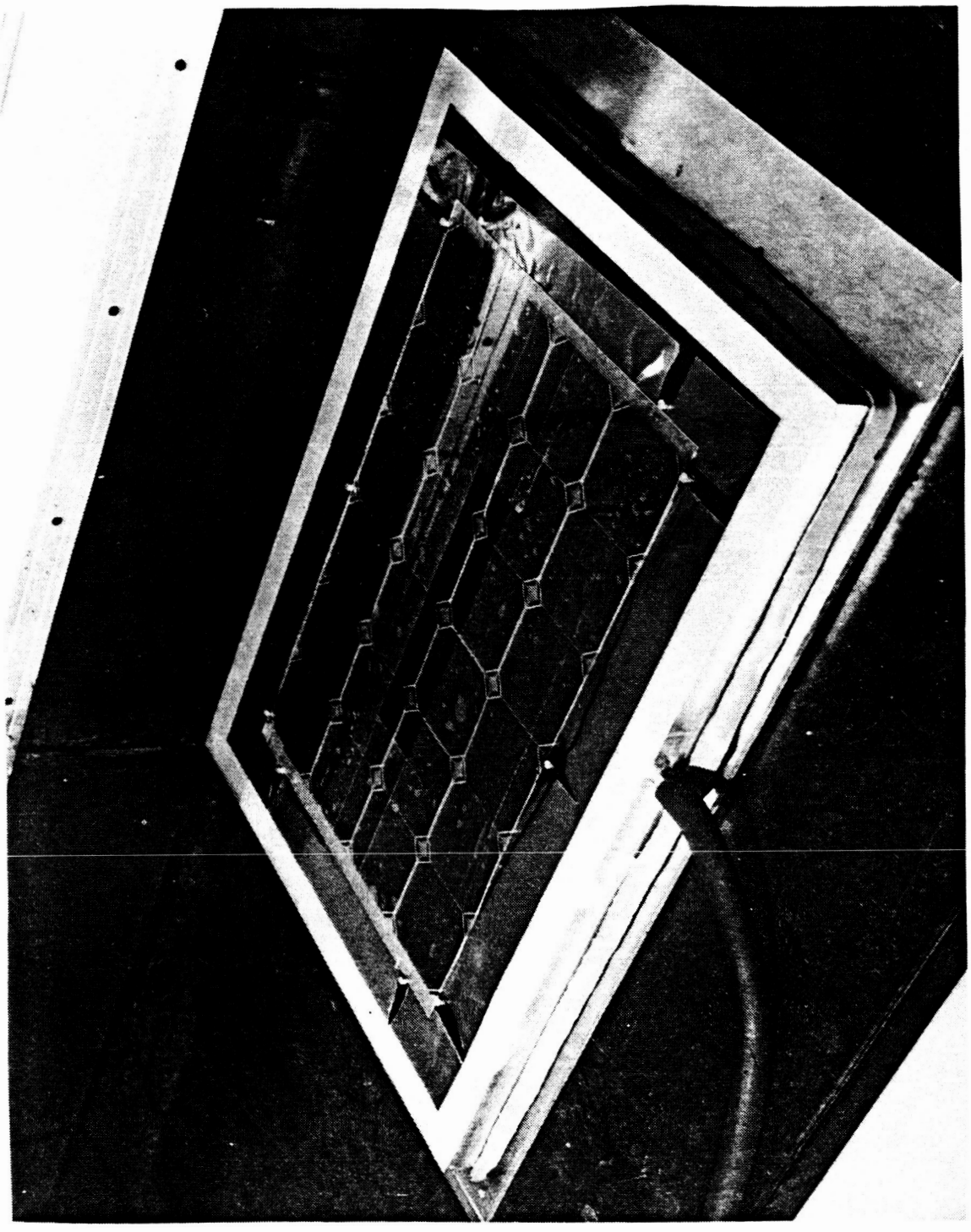

Figure 3-11 Superstrate Assembly with Adhesive Evenly Distributed

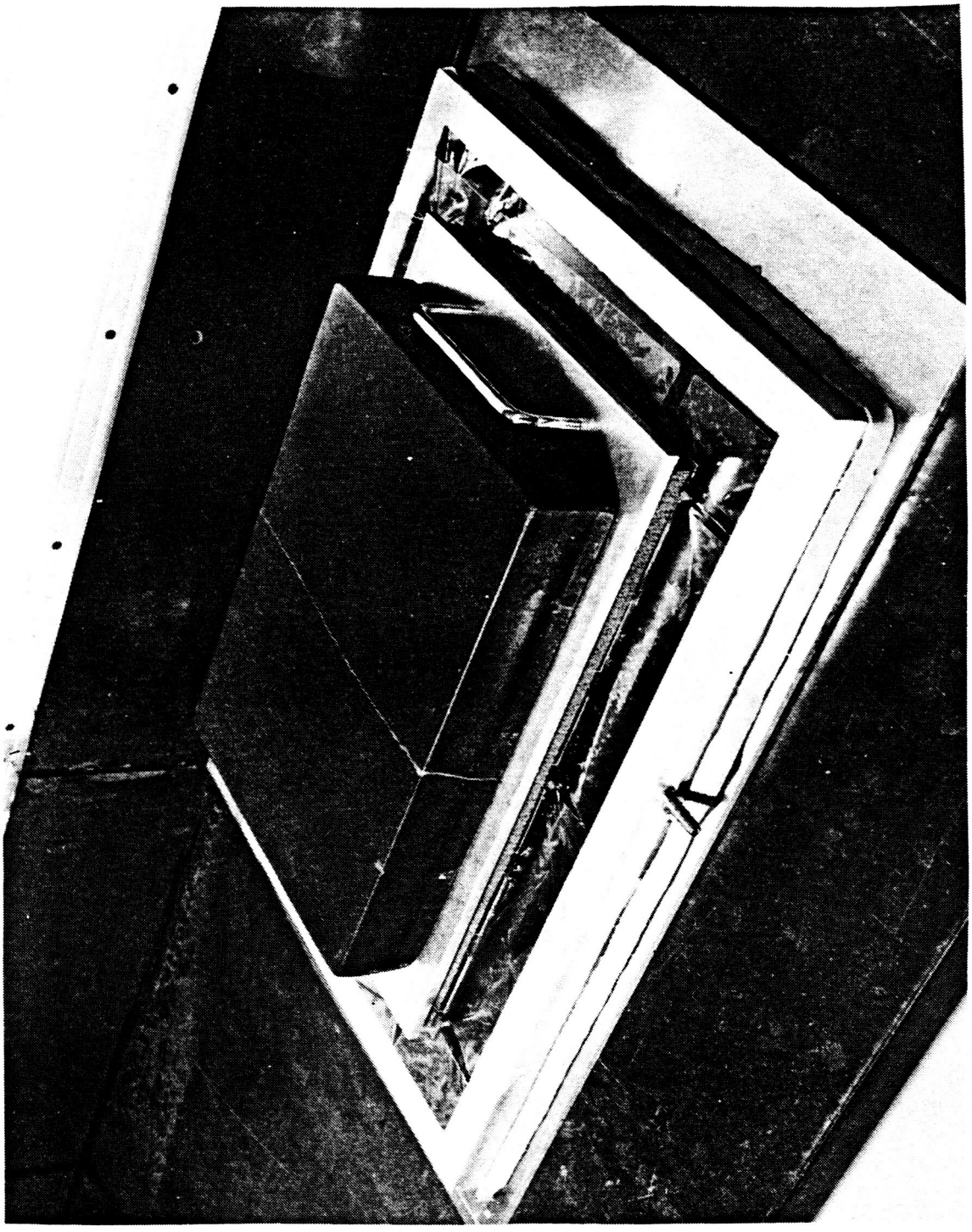

Figure 3-12 Weight Placed on Superstrate Assembly Before Oven Cure

3.7 HINGE BONDING

The bonding of the upper and lower elements of the moly hinges is accomplished in a separate bonding step. Although simultaneous curing of the cells and hinges to the superstrate glass was considered, a two step curing process was used because the tooling and development work were more straightforward. By keeping the tools and process development work simple, we reduced our tooling and development costs. The following steps were used to bond hinges to the superstrate assembly.

- Mask the moly hinge with 3M336 tape in areas not to be bonded.
- Clean the bonding surface of hinge with 2-propanol.
- Prime the bonding surface of hinge with Sylgard primer. Cure primer for 2 hours at room temperature.
- Place superstrate assembly in bonding tool, bonding surface facing up. Bonding tool must be mold released with MS122.
- Clean the bonding surfaces (laminated quartz paper on glass) with 2-propanol.
- Mix 10 g of DC 93-500 (10 g resin, 1 g curing agent) and degas until bubble free.
- Pour a bead of mixed and degassed adhesive on the bonding surface of superstrate.
- Position the primed hinge over the bead of adhesive, using locating pins in the hinge bonding tool.
- Place FEP film over the bond and apply foam pad and crossbar over hinge. Figure 3-13 shows crossbars positioned over hinges and superstrate assembly; however, FEP film and foam pads are not shown.
- Place 5 lb weight on a plate positioned over crossbars (bridge-like).
- Allow to cure at room temperature for 24 hours minimum before removing from tool. Full cure is obtained after 7 days at room temperature. Do not heat cure hinge assembly because the aluminum tool expands and misaligns hinges.
- Remove tape from masked areas of part.

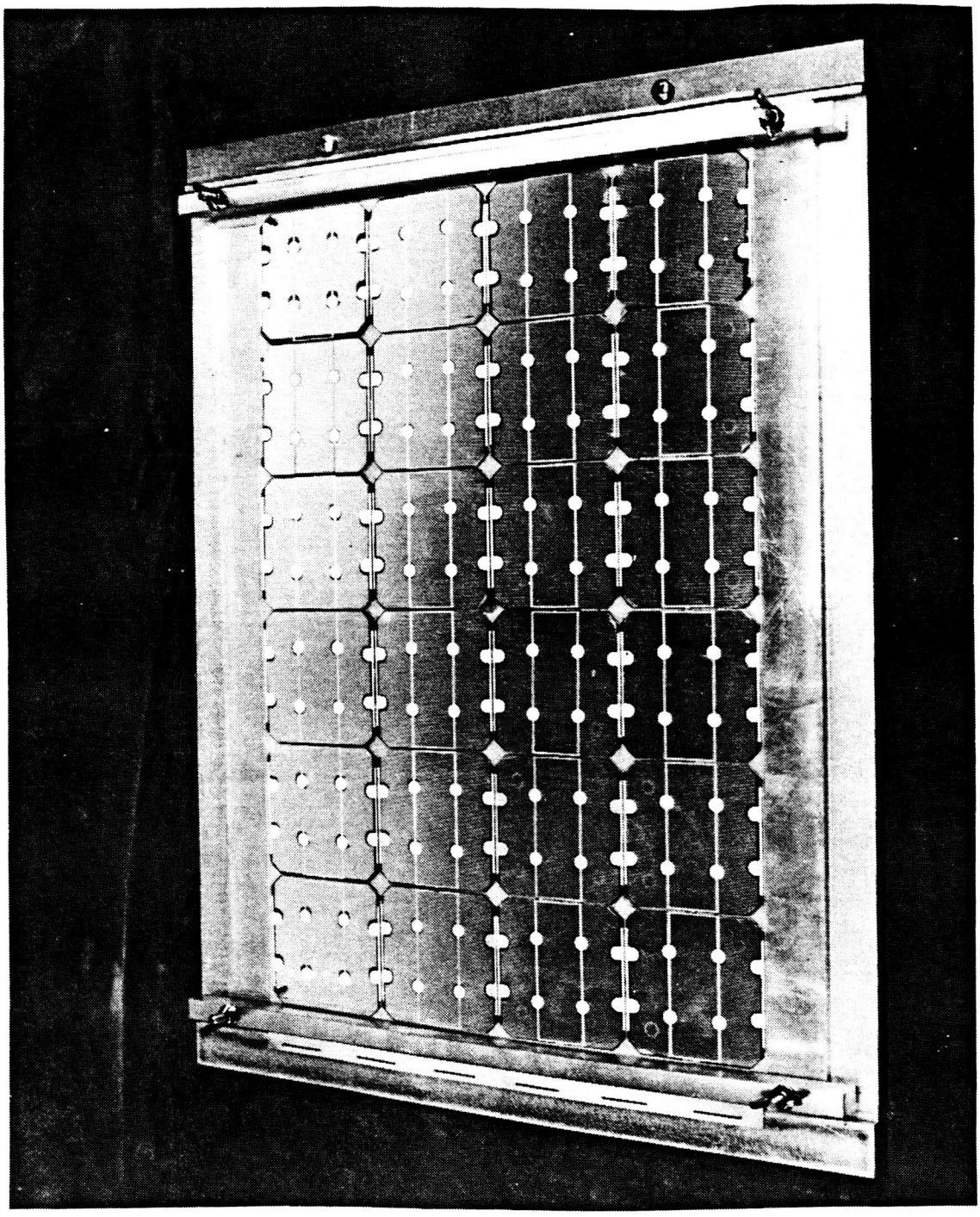

Figure 3-13 Superstrate Assembly Positioned in Bonding Tool

3.8 WELDING INTERCONNECT TO SOLAR CELLS

After the twenty four solar cells and two hinge elements had been bonded to the superstrate glass, a copper/kapton interconnect was welded to the superstrate module. The welder and setup are shown in Figures 3-14 and 3-15. Although the funding of this contract was not sufficient to conduct an extensive weld schedule development program, the weld schedule developed was adequate for the requirements of this contract.

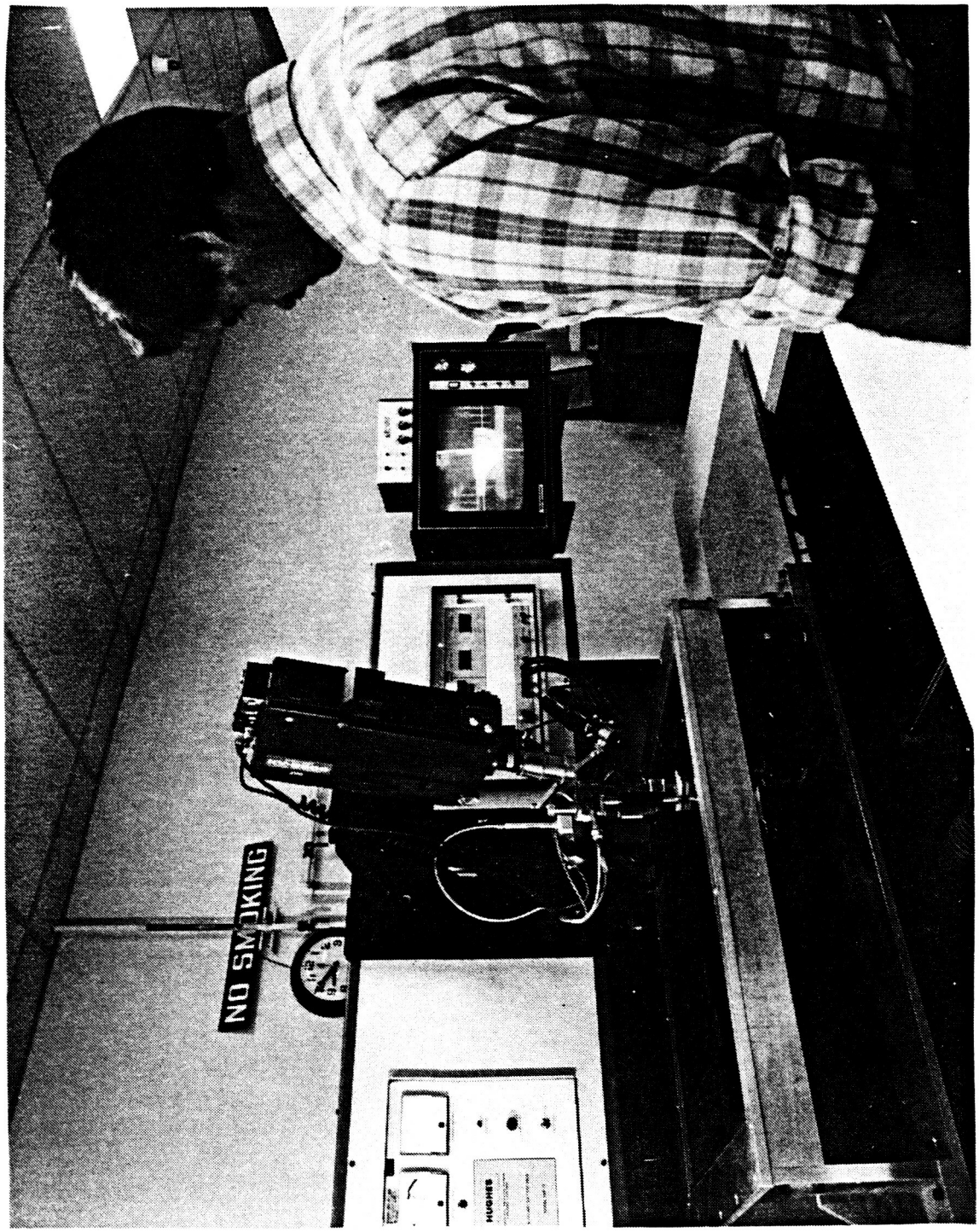

Figure 3-14 Welder Set Up for Welding Superstrate Assembly

ORIGINAL PAGE IS
OF POOR QUALITY

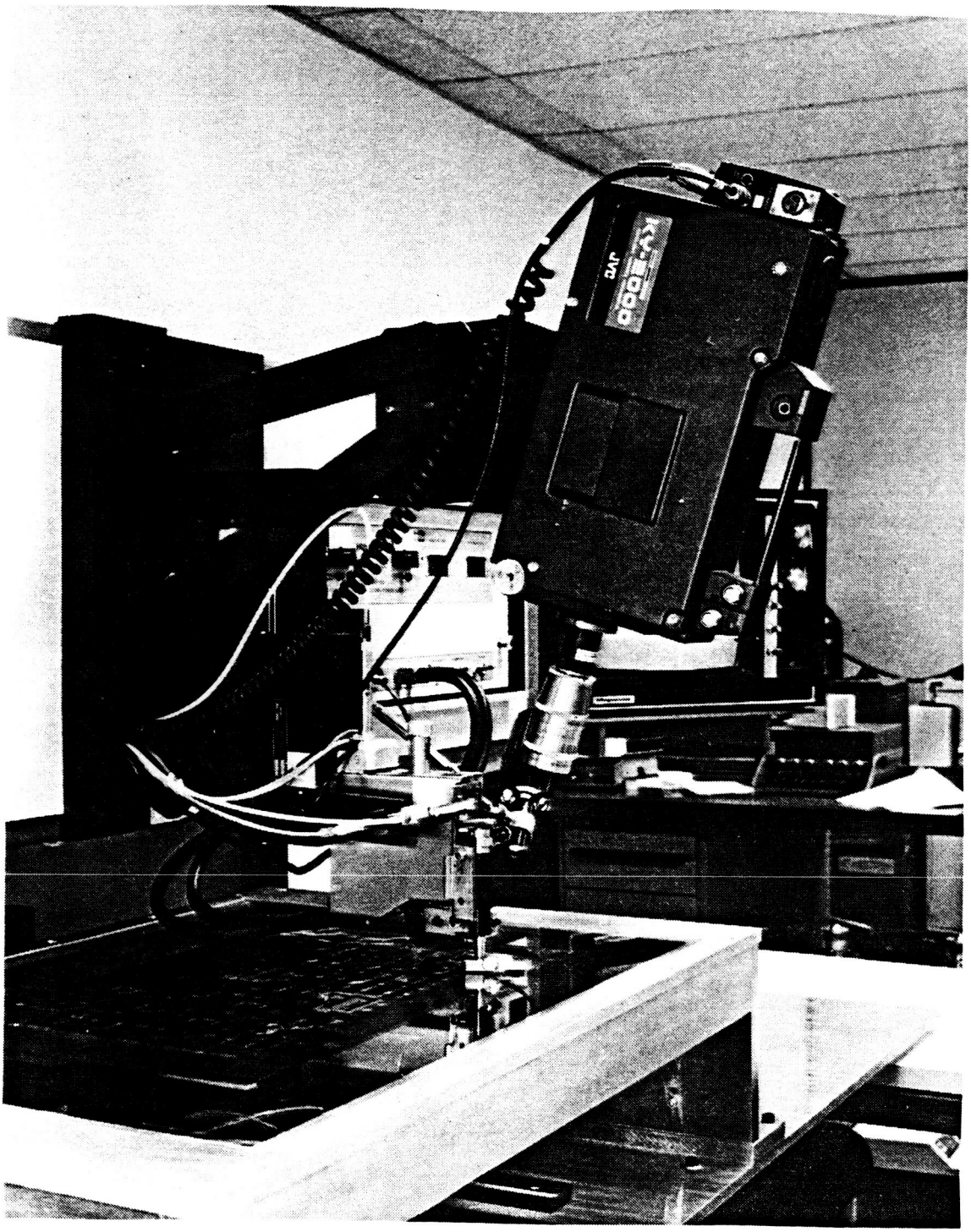

Figure 3-15 Welding of Copper/Kapton Interconnect to Superstrate Assembly

Section 4
FABRICATION AND TEST (TASK 2.0)

Task 2.0 included the fabrication and testing of superstrate modules. This task was divided into three sub-tasks which were designated Tasks 2.1, 2.2 and 2.3. Task 2.1 included fabricating a five unit panel segment for MSFC and performing a 100 thermal cycle acceptance test. Task 2.2 included fabricating and thermal cycling four modules for 2000 cycles. Task 2.3 included fabricating and thermal balance testing three modules at Boeing in Kent, Washington. The module fabrication breakdown is described in Table 4-1. The modules in the table are designated as either superstrate or conventional. The superstrate module was described earlier in this report, and the conventional module refers to the SAFE-type configuration with individual solar cell assemblies welded to a copper/kapton interconnect.

TABLE 4-1
MODULE FABRICATION BREAKDOWN

ITEM	USE	NUMBER OF 24-CELL MODULES (SUPERSTRATE)	(CONVENTIONAL)
1 Panel Segment (Good Electrical)	Thermal Cycle at MSFC	5	0
4 Modules (Good Electrical)	Thermal Cycle at LMSC	3	1
3 Modules (Good Electrical)	Thermal Balance at Boeing	2	1
	Total 24-Cell Modules:	10	2

4.1 THERMAL CYCLE TESTING (TASK 2.1)

4.1.1 Description of Test

Four modules were thermal cycled for 2000 cycles in the Electrical Power System's thermal cycle chamber. This chamber uses a combination of cold GN_2 and controllable fans to thermal cycle samples at an accelerated rate. The test temperature range was -90°C to 50°C which was based on a conservative prediction of a Space Station Low Earth Orbit (LEO). The four samples which were tested included 1) a conventional flexible array using SAFE typical technology, 2) superstrate covered, IR transparent module mounted on a continuous kapton blanket, 3) superstrate covered, IR transparent module with cut-away kapton to allow for maximum IR transmission, and 4) twenty-four solar cells welded to a copper/kapton interconnect sandwiched by two sheets of superstrate glass.

The module thermal cycle test sequence is shown in Figure 4-1. Photographs of the test samples mounted in the test chamber are shown in Figures 4-2 and 4-3. The four test samples mounted in the test frame are shown in Figures 4-4 and 4-5.

4.1.2 Test Results and Conclusions

Electrical performance measurements were made using a Pulse Light Simulator System. Electrical measurements were taken prior to thermal cycling, after 100 thermal cycles, and after 2000 thermal cycles. When adjusted for temperature effects and test uncertainty, the results show no loss in electrical performance for the three superstrate modules. The conventional SAFE-type module did experience an electrical loss of 10% because of interconnect/solar cell joint failure. Nineteen of the 192 joints experienced fatigue type failures on the conventional SAFE-type module. This was attributed to a less than adequate weld schedule. As previously mentioned in this report, funding limitations did not allow us to conduct an extensive weld schedule development plan for the two types of solar cells used. The weld schedule used on the IR transparent solar cells bonded to the superstrate glass appears to have been an adequate schedule, but the weld schedule used for the solar cell assemblies with the aluminum back surface reflector was not adequate for long term thermal cycling.

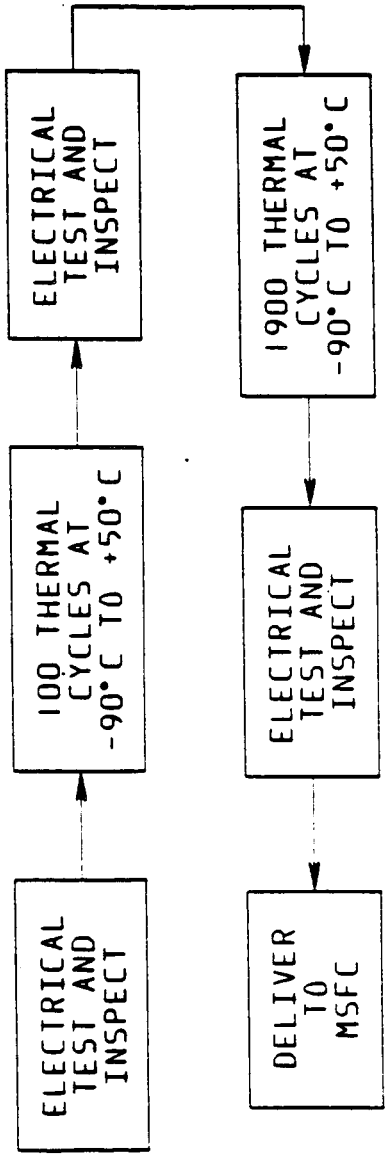

Figure 4-1 Module Thermal Cycle Test Sequence

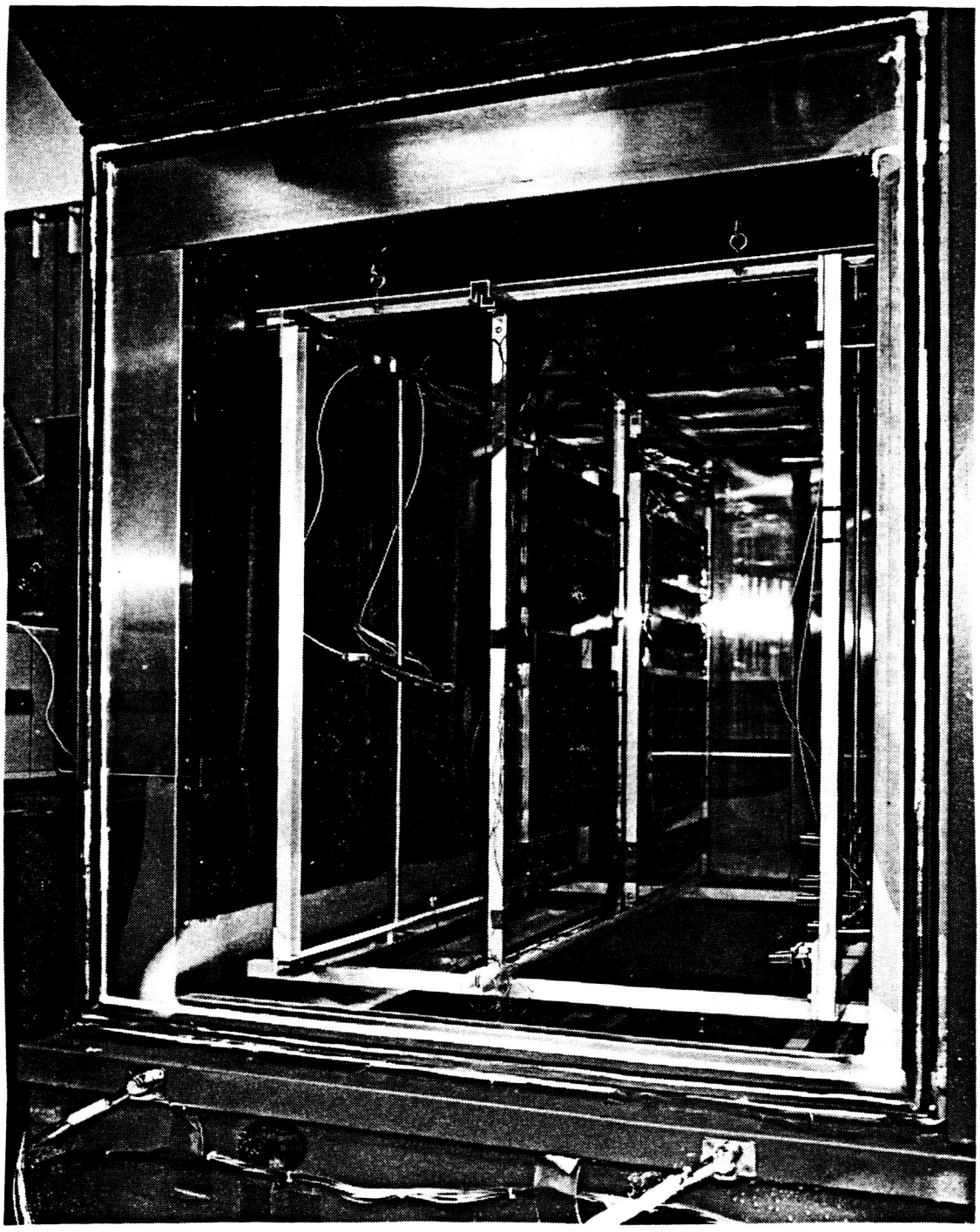

Figure 4-2 Thermal Cycle Test Setup - Front Side

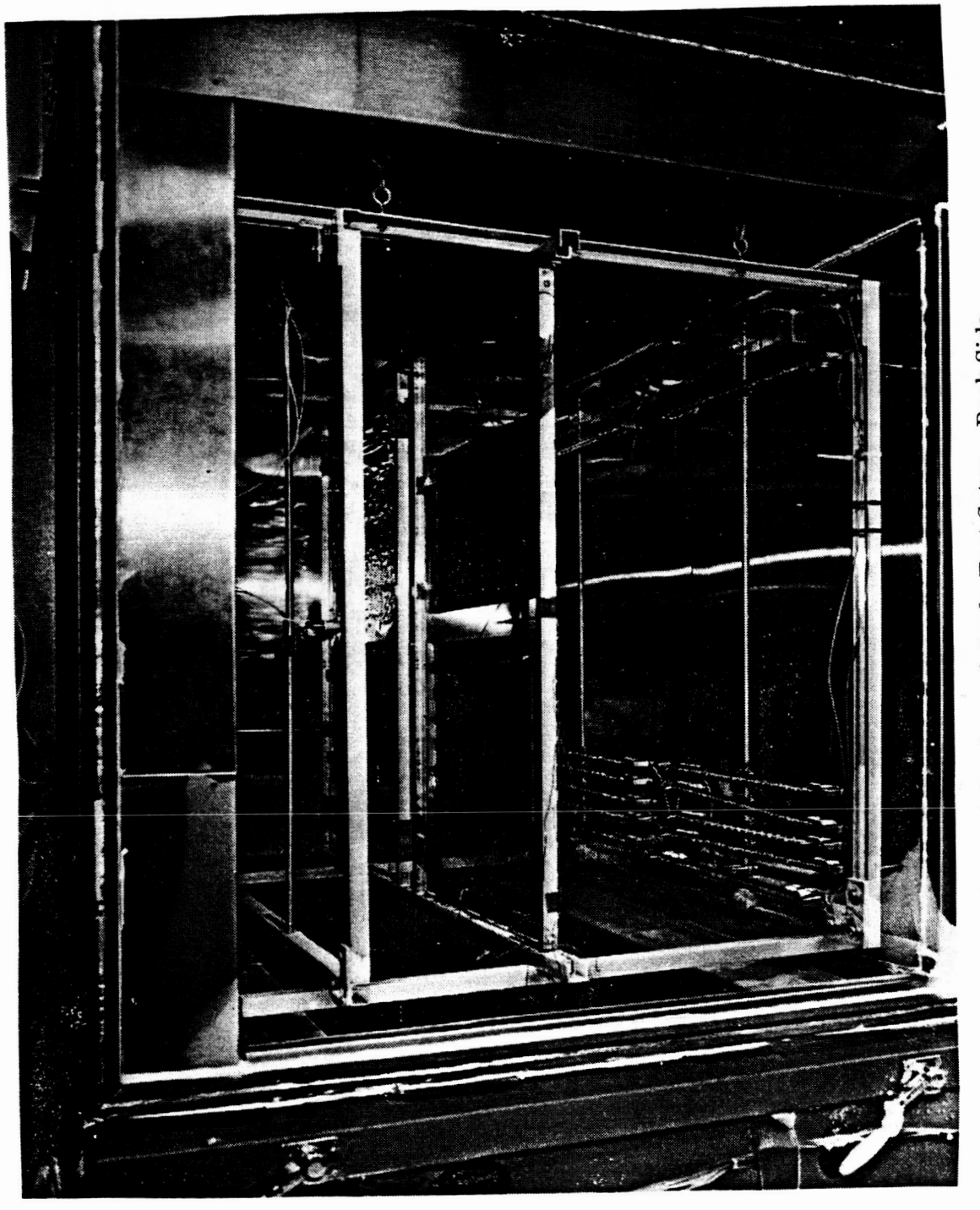

Figure 4-3 Thermal Cycle Test Setup - Back Side

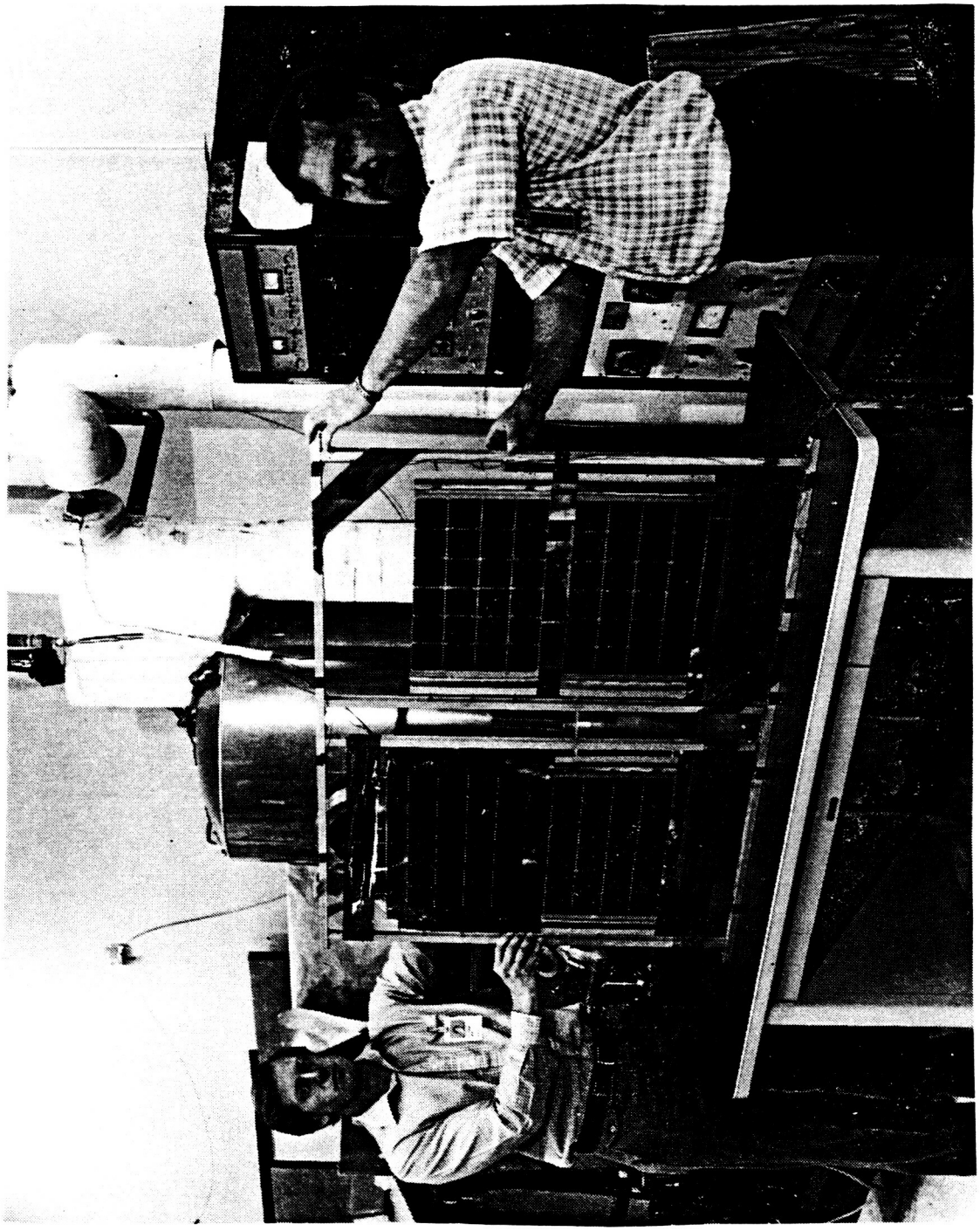

Figure 4-4 Thermal Cycle Samples - Front Side

ORIGINAL PAGE IS
OF POOR QUALITY

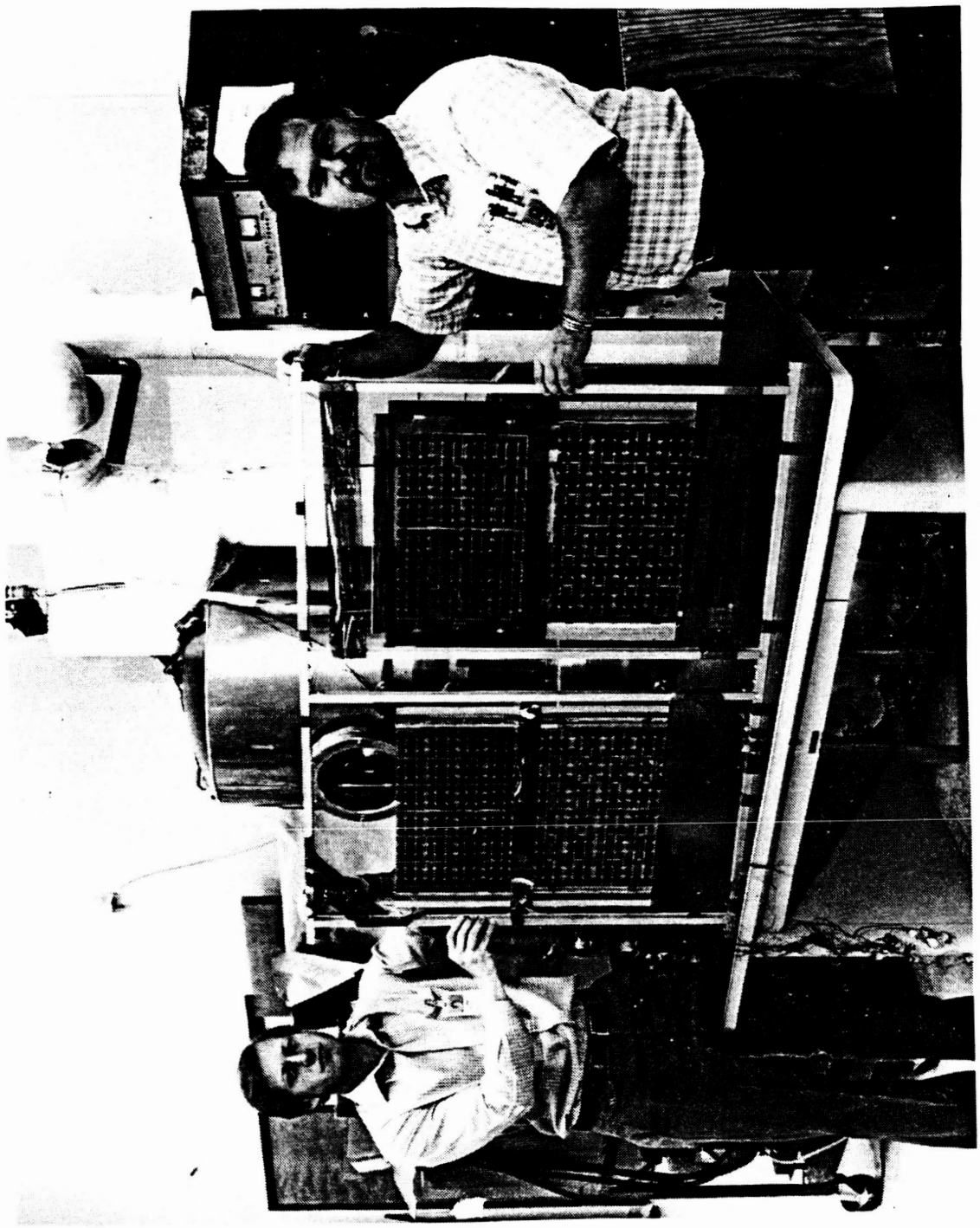

Figure 4-5 Thermal Cycle Samples - Back Side

4.2 THERMAL VACUUM TESTING

4.2.1 Test Objective

LMSC conducted a radiative thermal balance test at the Boeing Space Environmental Laboratory. The objective of this test was to verify the predicted performance of IR transparent solar array modules when exposed to a simulated Low Earth Orbit environment.

4.2.2 Test Facilities

Testing was conducted in Chamber "B" at Boeing. Figure 4-6 shows the chamber used while Figures 4-7 and 4-8 show schematically the key chamber provisions required for this test. In order to minimize convective losses, the test chamber needed to be evacuated to a pressure of $<10^{-5}$ torr. The shrouds were filled with LN_2 to provide a low background radation temperature. A heated conical shroud shown in Figure 4-9 was installed in the base of the chamber to allow adjustment of the IR flux incident on the array back surface to simulate the earth IR source. Two ports were used for solar and solar albedo simulation sources. Direct solar radiation was simulated by an A-1200L solar simulator. The beam entered through a vacuum port and was reflected from an off-axis parabolic mirror onto the test plane. At the test plane, the beam was 42 inches in diameter with a uniformity of $\pm$ 5% and a collimation angle <2 degrees. Albedo was simulated by using an X-25 solar simulator. The beam was introduced through a port in the base of the chamber and directed onto the sample.

The test article was located at the center of the chamber approximately 29 inches above the hard points. Two TRW Differential Radiometers, Model DR-2, were used to monitor the solar and albedo simulation intensity. The test article and temperature controlled cone were attached to a support fixture extending from the chamber base hard points. A non-temperature controlled shroud was located at the test plane to absorb stray energy from the A-1200 and the chamber walls.

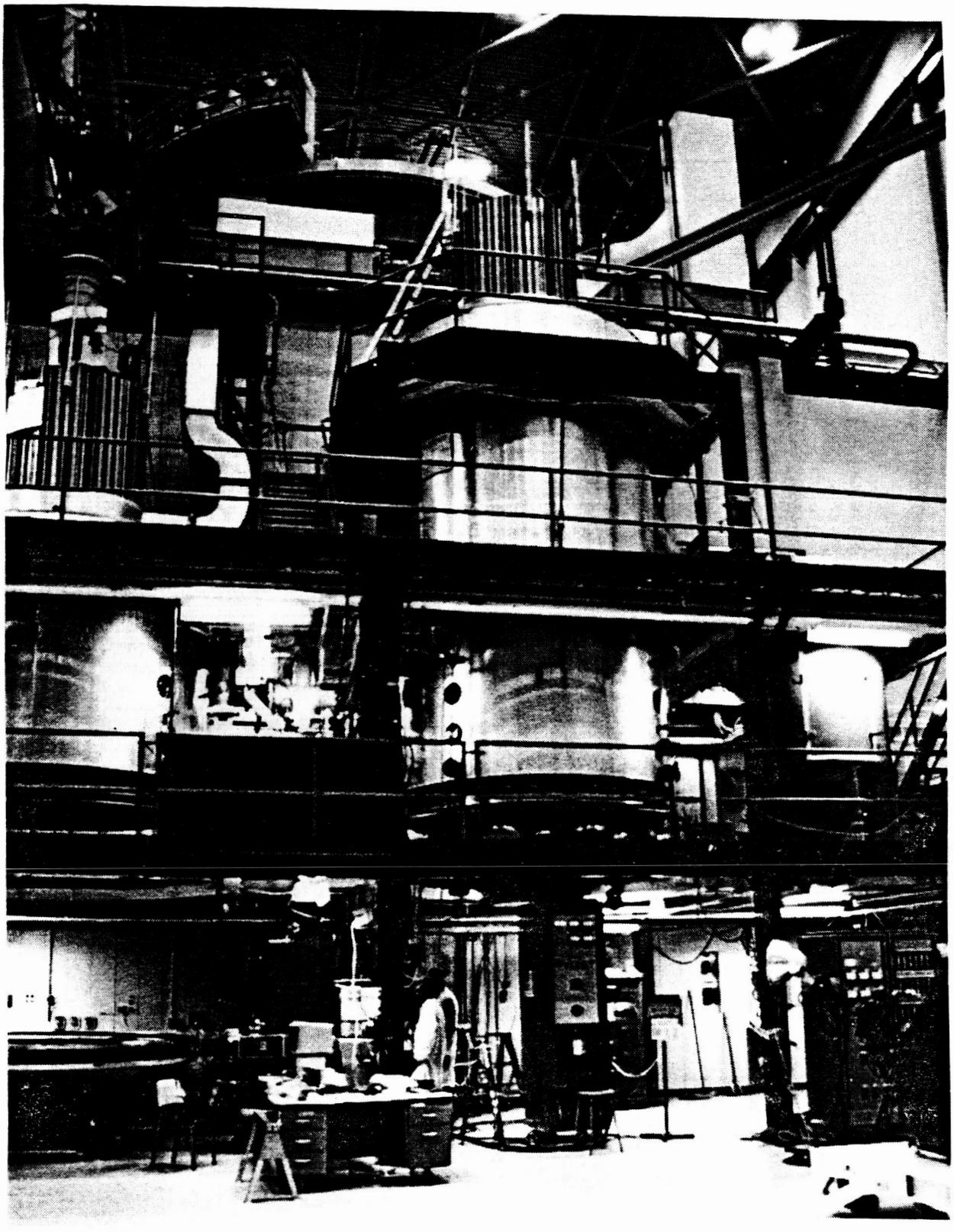

Figure 4-6 Thermal Vacuum Chamber at Boeing Facility

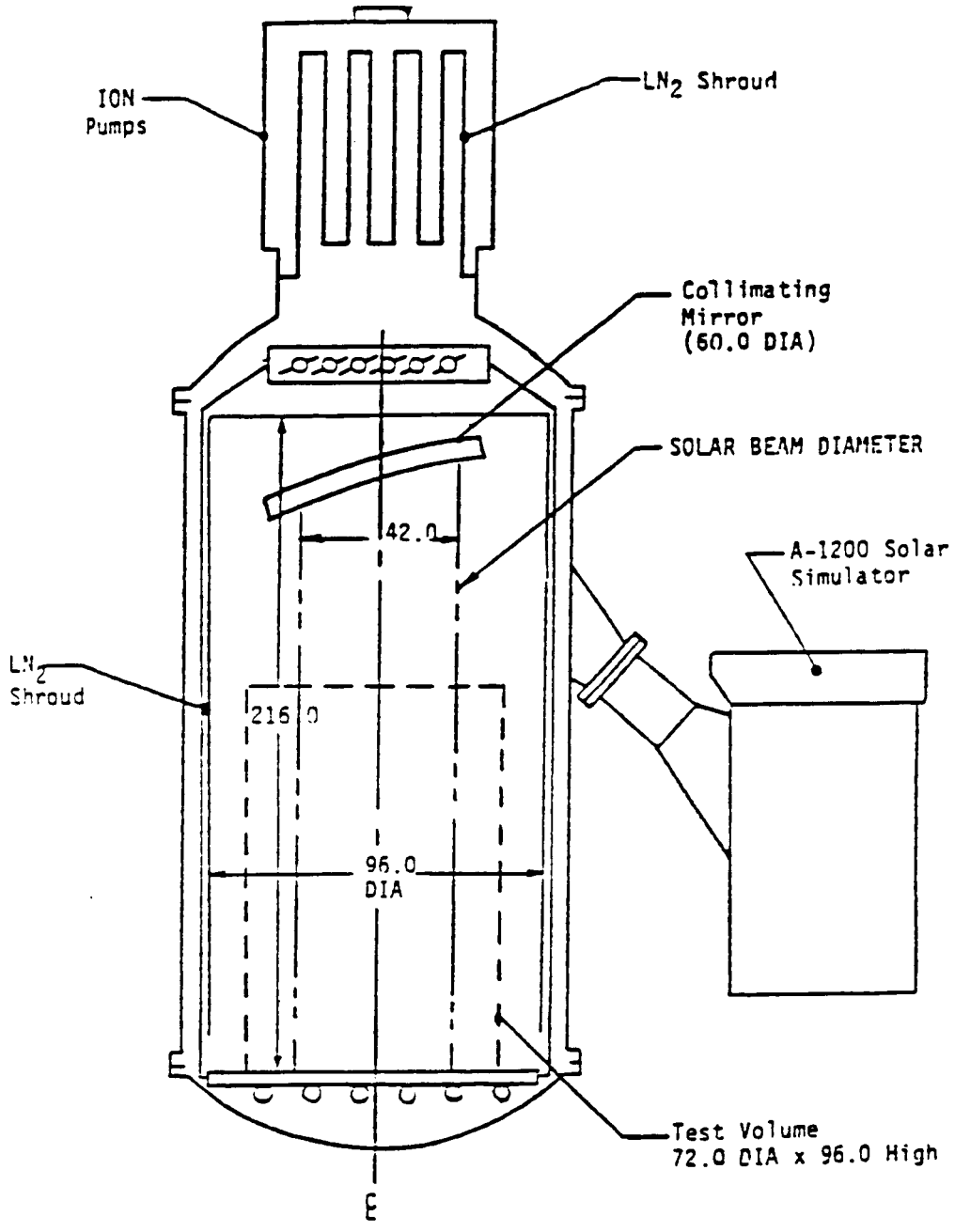

Figure 4-7 Space Chamber B

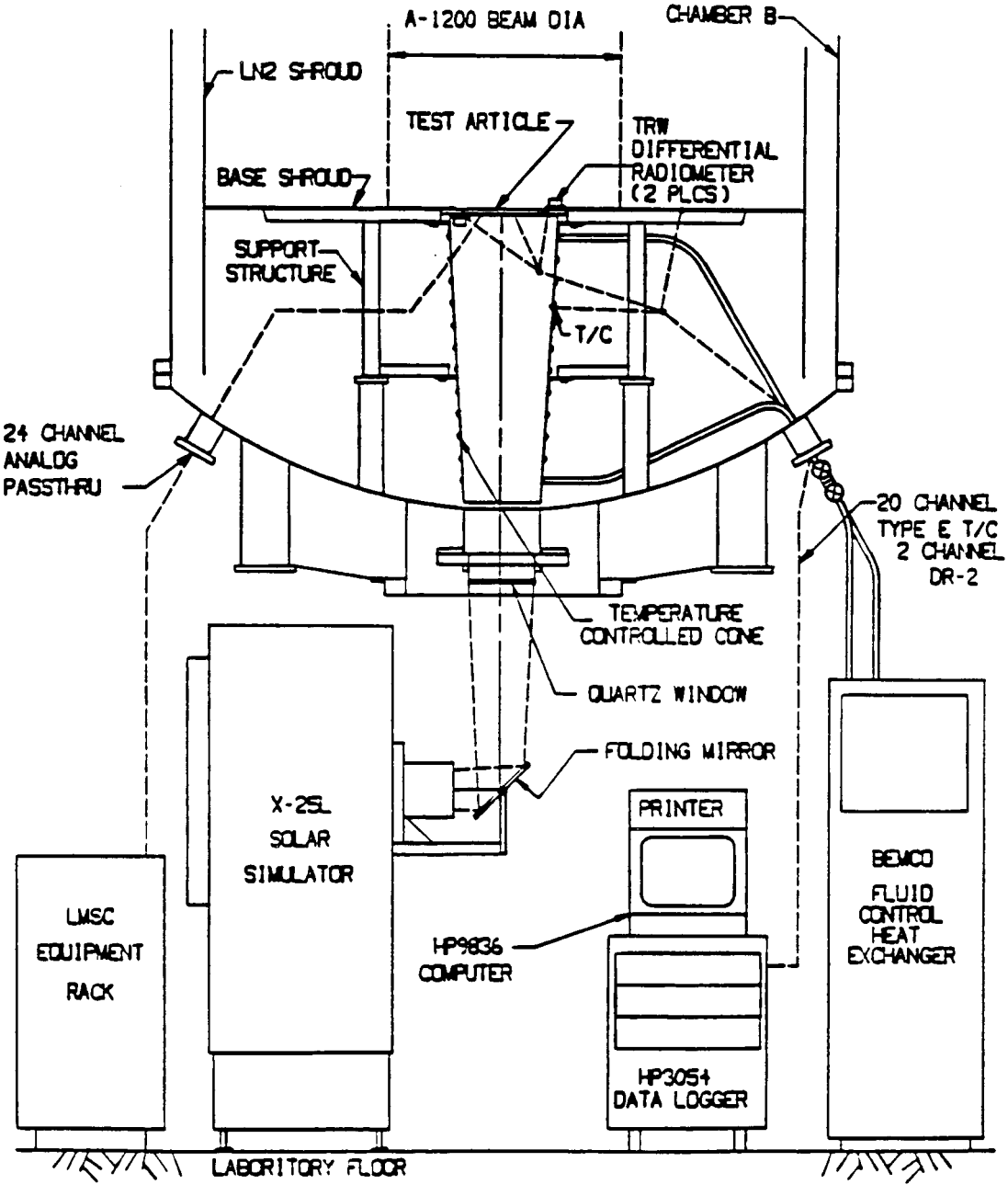

Figure 4-8 Test Setup

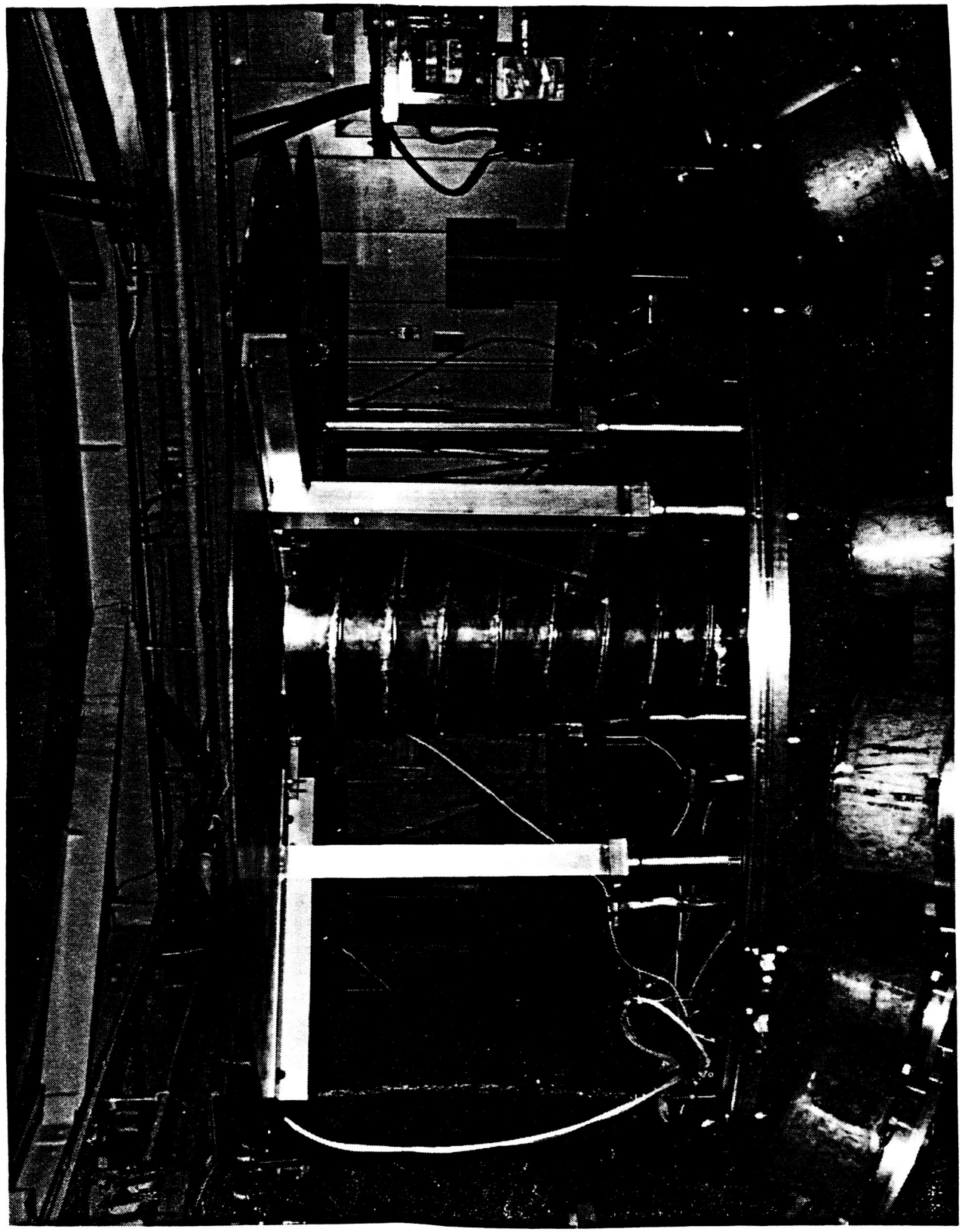

Figure 4-9 Thermal Balance Base Plate and Earth Shine Simulator

The X-25L albedo simulator was located directly below the chamber. The albedo beam was projected from the X-25L and reflected off a 10 inch diameter folding mirror through a 12 inch diameter quartz vacuum window in the chamber base. (See Figure 4-10).

The earth emission cone temperature was controlled using a Bemco fluid controlled heat exchanger.

The solar and albedo beam intensity incident on the radiometers, all thermocouples located in the test article, one thermocouple located on the chamber base shroud and two thermocouples located on the temperature controlled cone were monitored and recorded on an HP 9836 computer and an HP 3054 data acquisition system. The solar panel load wires were monitored and controlled by the LMSC computer and equipment rack.

The A-1200 and the X-25L solar simulators were calibrated per Boeing documents D180-10571-1 and D180-15115-1, Operation and Calibration Procedures for The A-1200 and X-25L, respectively. The A-1200 was calibrated at the test plane 29 inches above the hard points and at chamber center line. The X-25L was calibrated using a mock setup with the chamber window and folding mirror located in their respective positions. Figures 4-11 through 4-15 show the uniformity scans of the A-1200 and X-25L solar simulators. The spectral characteristics of the A-1200 and X-25L are shown in Tables 4-2 and 4-3.

A total of four thermal vacuum tests were performed at a rate of one per 24 hour period. Temperature data was recorded on the HP 9836 computer at a frequency of once per 5 minutes during the 4 hour pump down and 11 hour repressurization periods. Temperature data was recorded at 1 minute intervals during the actual test period of approximately 8 hours. The LMSC computer and equipment rack recorded solar cell performance characteristics during the test.

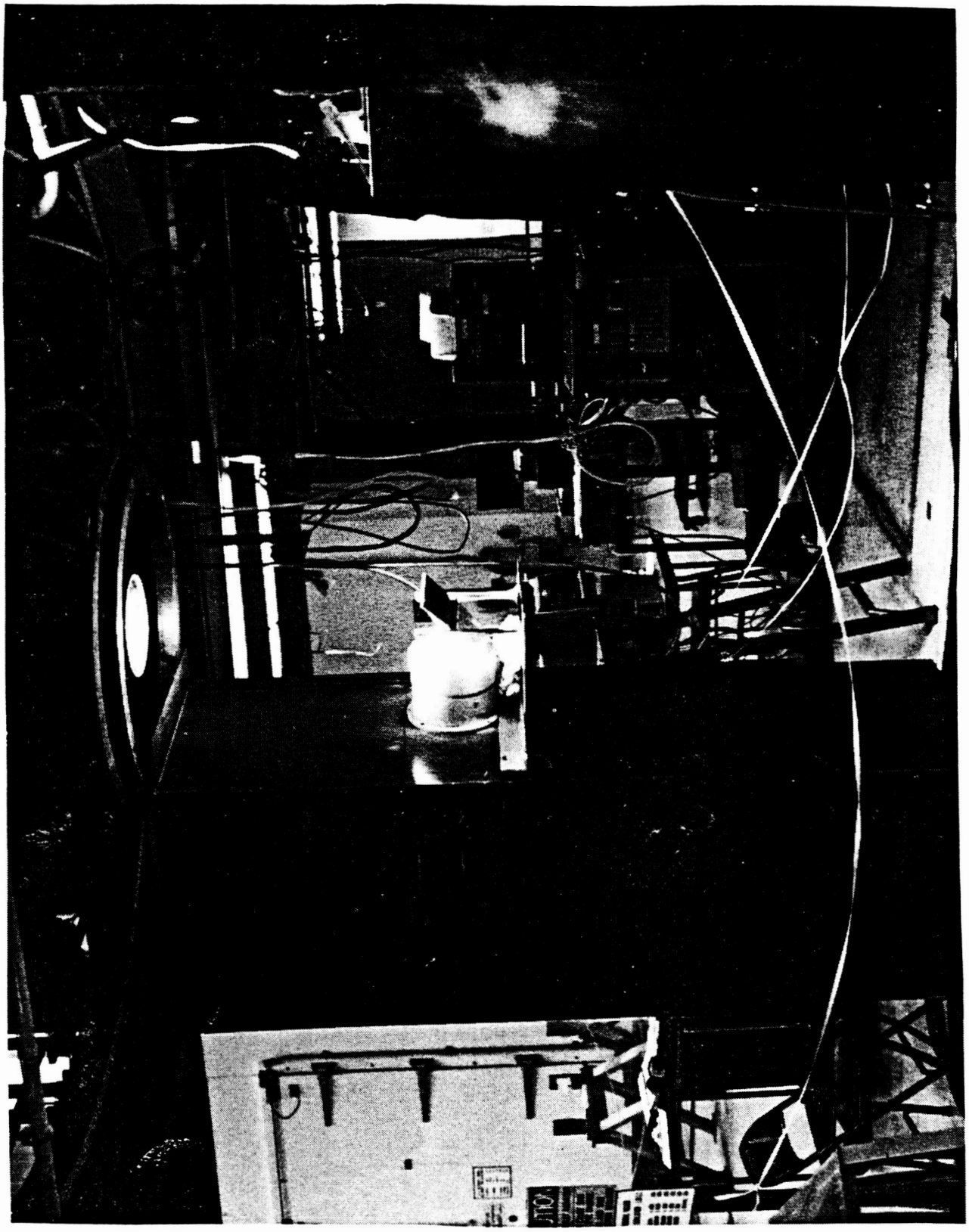

Figure 4-10 X-25 Solar Simulator Used to Simulate Albedo

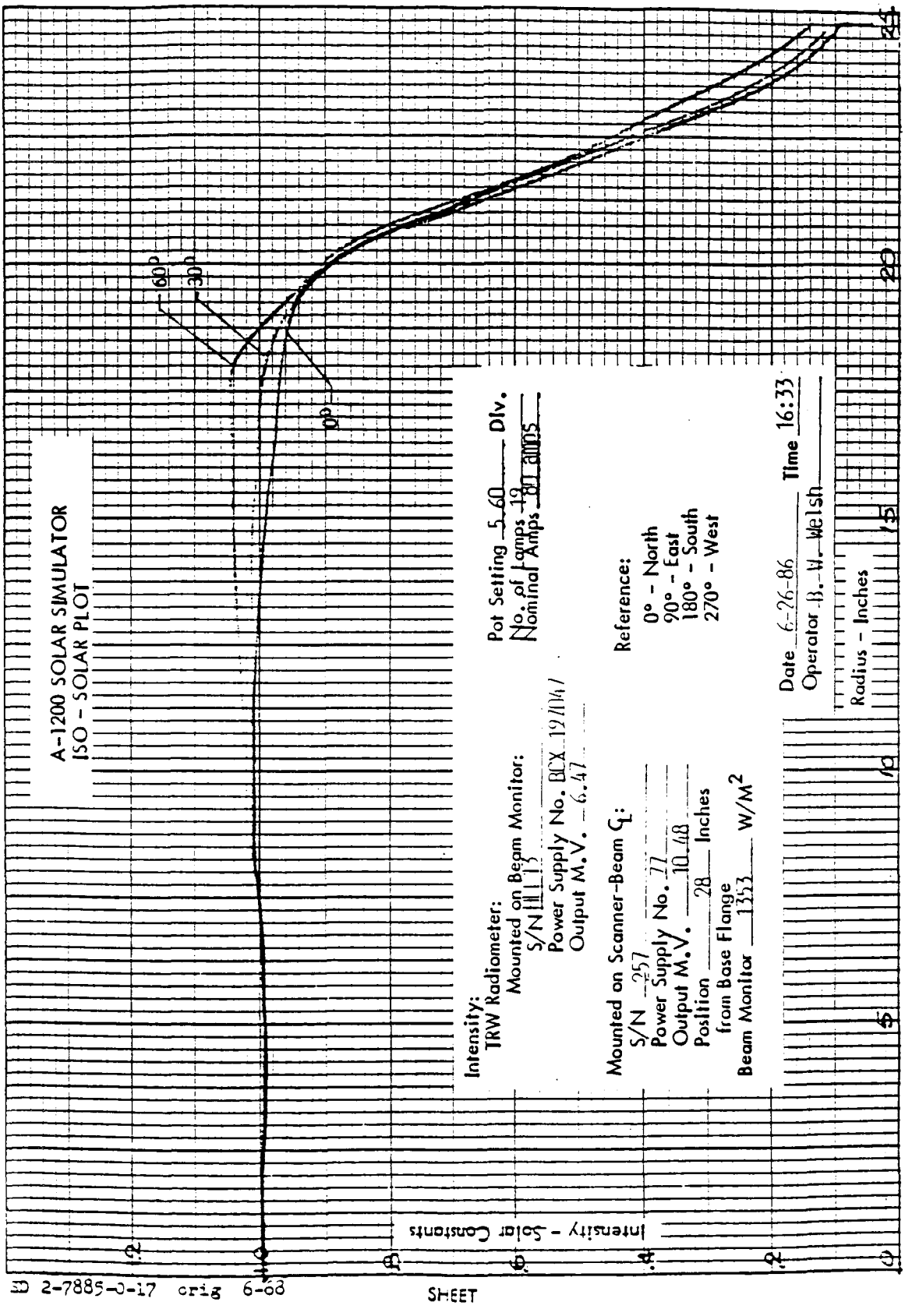

Figure 4-11 A-1200 Solar Simulator ISO-Solar Plot, 0°-60° Azimuth

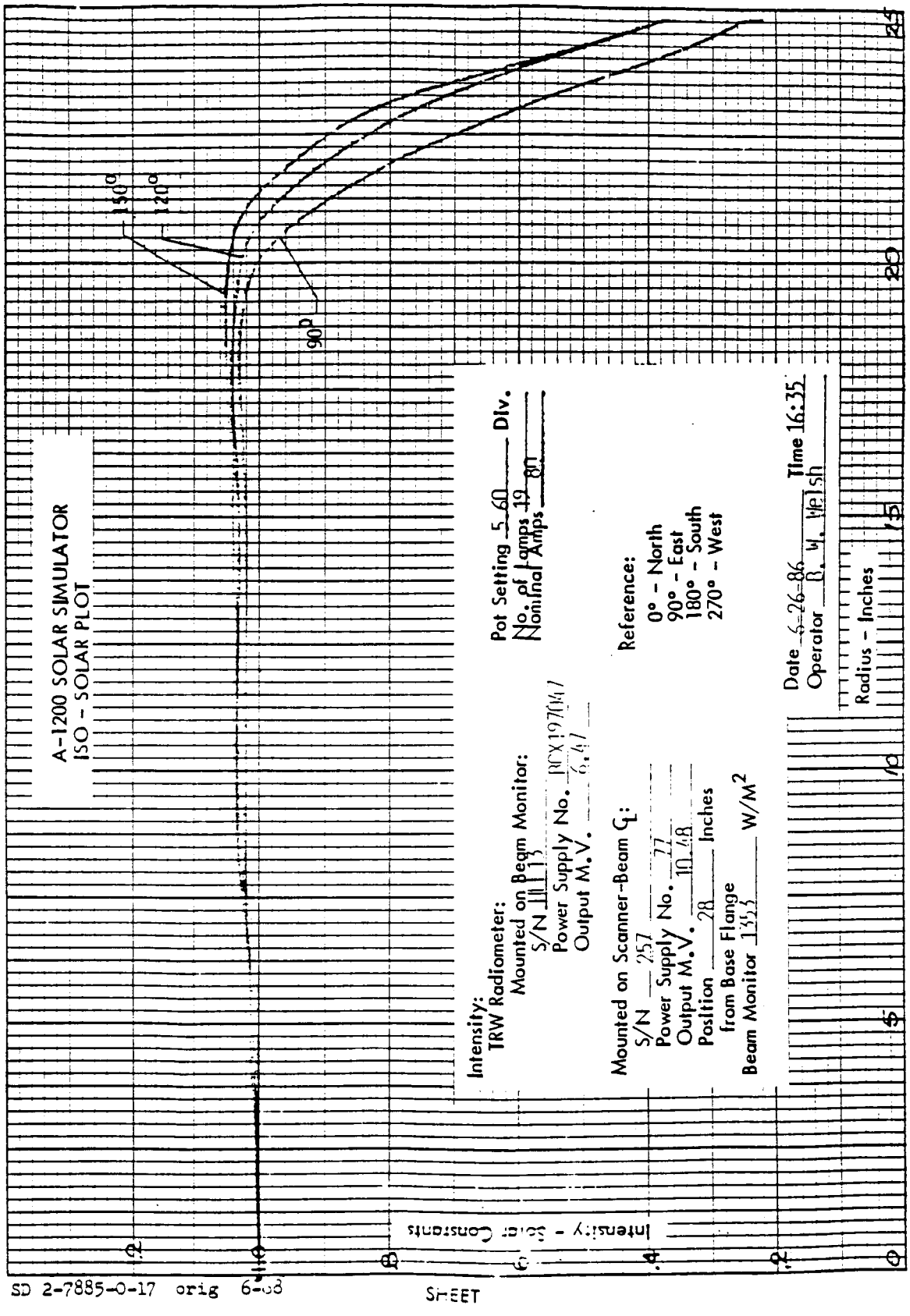

Figure 4-12 A-1200 Solar Simulator ISO-Solar Plot, 90°-150° Azimuth

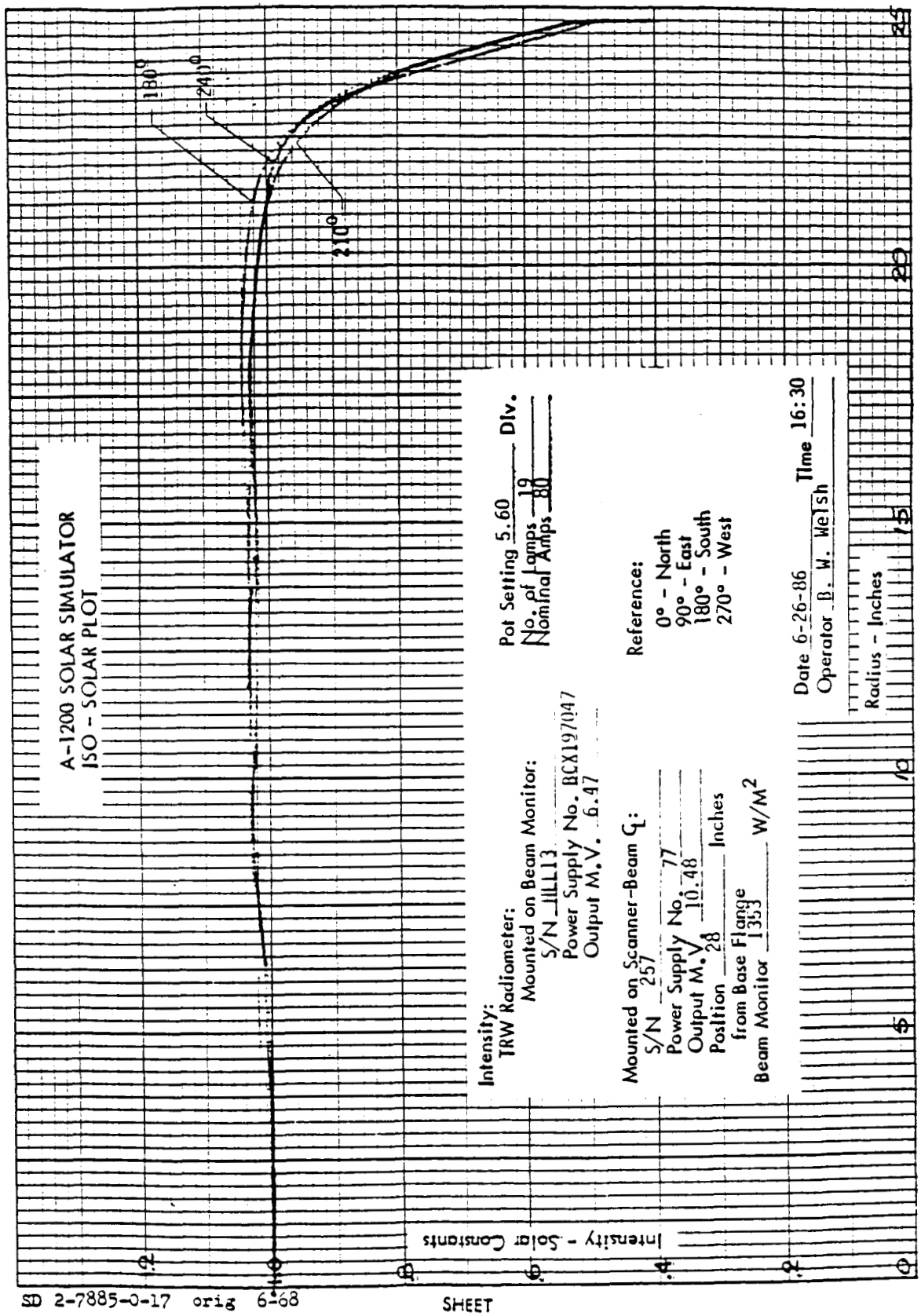

Figure 4-13 A-1200 Solar Simulator ISO-Solar Plot, 180°-210° Azimuth

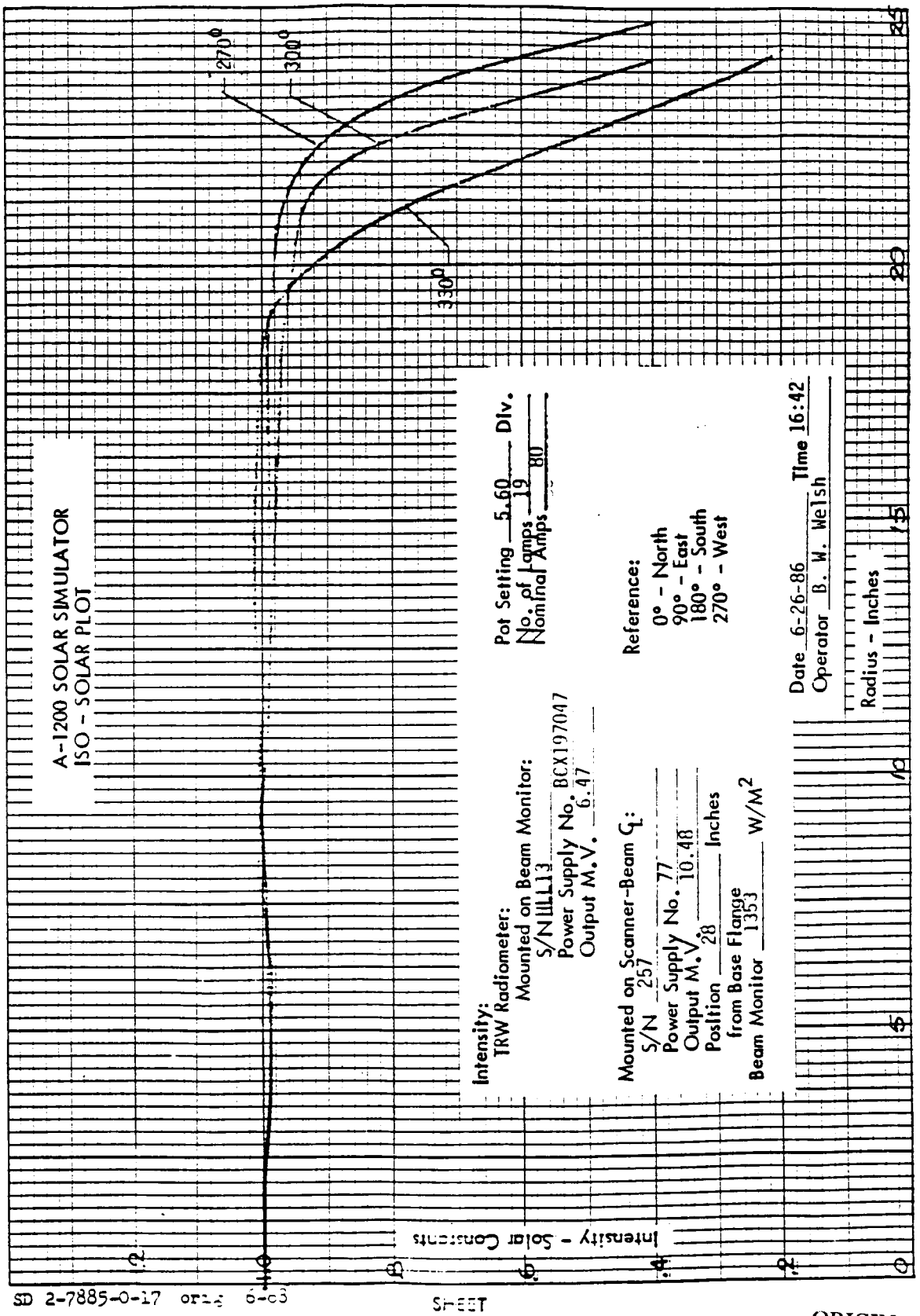

Figure 4-14 A-1200 Solar Simulator ISO-Solar Plot, 270°-330° Azimuth

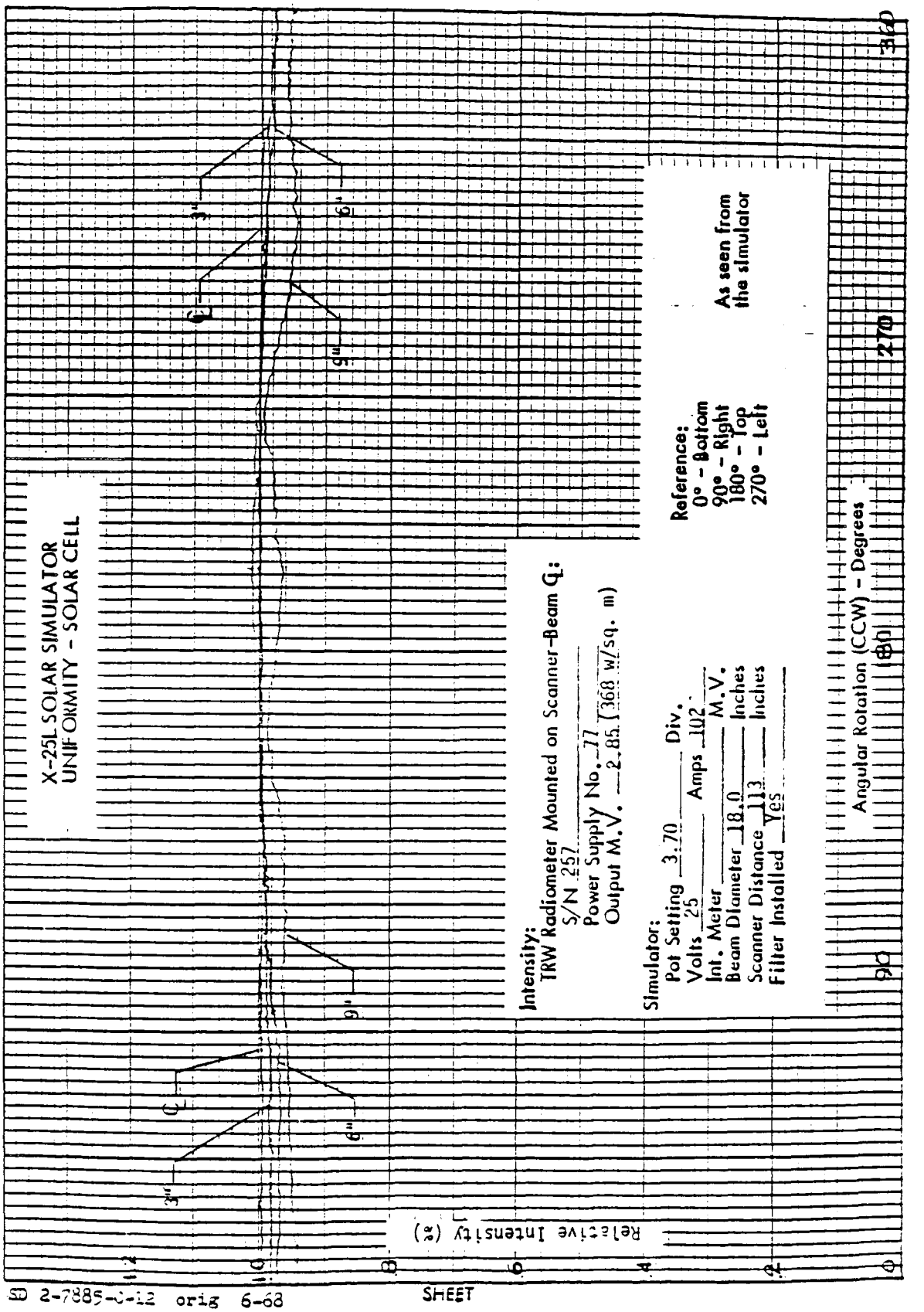

Figure 4-15 X-25L Solar Simulator Uniformity

TABLE 4-2

Date: JUN-30-86

SPECTRAL ENERGY DISTRIBUTION MEASUREMENT

Customer: LMSC Thermal/Vacuum Solar Simulation Test

Solar Simulation Model No: A-1200

Configuration: Chamber center line, floor level
Spectral filter installed

Operator: B. W. Welsh

Chck BWW

Date of Measurement: JUN-27-86

Computer File (Boeing): LMSC1200

The table below depicts spectral data both relatively and in watts/m**2 for the solar simulator. The percent deviation with respect to the engineering standard for the solar constant and solar spectrum (ASTM E490-73a) are given in column 6.

Band No.	Bandwidth (microns)	Matched Data	Normalized Matched Data To One Solar Constant (w/m**2)	Eng Standard	% Deviation
1	0.25-0.35	4.3	19.9	58.5	-65.9
2	0.35-0.40	13.2	61.2	56.9	7.5
3	0.40-0.45	17.9	83.0	86.8	-4.4
4	0.45-0.50	21.8	101.0	100.9	0.1
5	0.50-0.60	44.7	207.2	177.0	17.1
6	0.60-0.70	38.0	176.1	151.5	16.3
7	0.70-0.80	29.0	134.4	123.7	8.7
8	0.80-0.90	21.5	99.7	99.3	0.4
9	0.90-1.00	16.4	76.0	82.9	-8.3
10	1.00-1.20	25.0	115.9	120.6	-3.9
11	1.20-1.50	22.4	103.8	111.4	-6.8
12	1.50-1.80	14.5	67.2	67.0	0.3
13	1.80-2.20	8.4	38.9	43.8	-11.1
14	2.20-2.50	3.4	15.8	19.8	-20.4
		280.5	1300.1	1300.1	

Rev: 2/85

TABLE 4-3

Date: JUL-07-8=

SPECTRAL ENERGY DISTRIBUTION MEASUREMENT

Customer: LMSC Thermal/Vacuum Solar Simulation Test

Solar Simulation Model No: X-25L

Configuration: Reflected off 10 inches mirror through 12 inches vacuum window, spectral filter installed

Operator: C. T. Tran

Chck

Date of Measurement: JUL-03-86

Computer File (Boeing): LMSC25L

The table below depicts spectral data both relatively and in watts/m**2 for the solar simulator. The percent deviation with respect to the engineering standard for the solar constant and solar spectrum (ASTM E490-73a) are given in column 6.

Band No.	Bandwidth (microns)	Matched Data	Normalized Matched Data To One Solar Constant (w/m**2)	Eng Standard	% Deviation
1	0.25-0.35	3.4	17.9	58.5	-69.4
2	0.35-0.40	9.1	47.9	56.9	-15.9
3	0.40-0.45	13.6	71.5	86.8	-17.6
4	0.45-0.50	15.3	80.5	100.9	-20.3
5	0.50-0.60	32.0	168.3	177.0	-4.9
6	0.60-0.70	28.3	148.8	151.5	-1.8
7	0.70-0.80	23.5	123.6	123.7	-0.1
8	0.80-0.90	20.7	108.9	99.3	9.6
9	0.90-1.00	18.2	95.7	82.9	15.5
10	1.00-1.20	27.0	142.0	120.6	17.7
11	1.20-1.50	26.5	139.4	111.4	25.1
12	1.50-1.80	16.2	85.2	67.0	27.2
13	1.80-2.20	9.5	50.0	43.8	14.1
14	2.20-2.50	3.9	20.5	19.8	3.6
		247.2	1300.1	1300.1	

Rev: 2/85

During the thermal performance tests the chamber pressure was maintained at less than 3.0×10^{-7} torr and the chamber wall temperature was held between -303 and -305 degrees F. The earth emission cone temperature was kept constant at approximately -50 degrees F during all tests. The A-1200 solar simulator was operated at irradiance levels of 0.97, 1.00, 1.03 and 1.10 S.C. (1.0 S.C. = 1353 w/m-sq). The X-25L albedo simulator was operated at irradiance levels of 0.30, .35 and .40 S.C.

4.2.3 Test Environments Requirements - Summary

Test environments were selected to span the range encountered in LEO. Simulation was included of the direct solar, reflected solar (albedo) and the earth IR (earth shine). Key parameters and their values were:

- Pressure $<10^{-5}$ torr
- LN_2 Controlled Shrouds
- Solar and Albedo Simulation
  - Solar:
    $1298 \leq Q_S \leq 1418$ W/m^2 adjustable
    1353 W/m^2 nominal
  - Albedo:
    $150 \leq Q_A \leq 563$ W/m^2, adjustable
- Solar and albedo simulations must be within ± 10% of NASA standard solar spectrum.
- Earthshine Simulation
  - $150 \leq Q_E \leq 315$ W/m^2, adjustable
    Verified by thermocouple measurement on source

4.2.4 Sample Description

Three different module designs were fabricated and tested: 1) conventional flexible array using SAFE typical technology, 2) superstrate covered, IR transparent module mounted on a continuous kapton blanket, and 3) superstrate covered module with minimal kapton blanket intruding into the optical path. Several design features were common to the three test modules. Each module consisted of 24, 5.9 x 5.9 cm WAC solar cells configured in a 4 x 6 cell matrix as shown in Figure 4-16. Careful attention was paid to selecting cells with similar electrical and optical characteristics.

The conventional module used typical flight quality back surface reflector (BSR) solar cells. SAFE typical design practice was used in the fabrication of this module with one exception. The acrylic transfer tape which had previously been used was inadvertently left off resulting in slightly higher temperatures.

The other two modules used gridded back contact solar cells. Optical coating was applied to maximize the transmittance of IR through the module. In the case of the full kapton backing, the desired adhesive layer was also missing, which, though resulting in higher temperatures gave a direct comparison with the conventional module. The second IR transparent module had a majority of the kapton cut away exposing the back of the cell. A thin DC93-500 layer was applied to raise the emissivity. Post test measurements showed this layer to be too thin to be effective and no increase in emittance was achieved.

Circuitry and instrumentation were identical for all modules as shown in Figure 4-17.

4.2.5 Testing

The modules were tested at three simulated solar intensities corresponding to equinox and summer and winter solstice. At each intensity, the temperature was monitored until steady state was achieved. After a 0 power output steady state temperature was determined, several cases were run where load resistors were placed across the cell and a new equilibrium temperature was determined. The load resistors were selected to bracket the maximum power point of the cell.

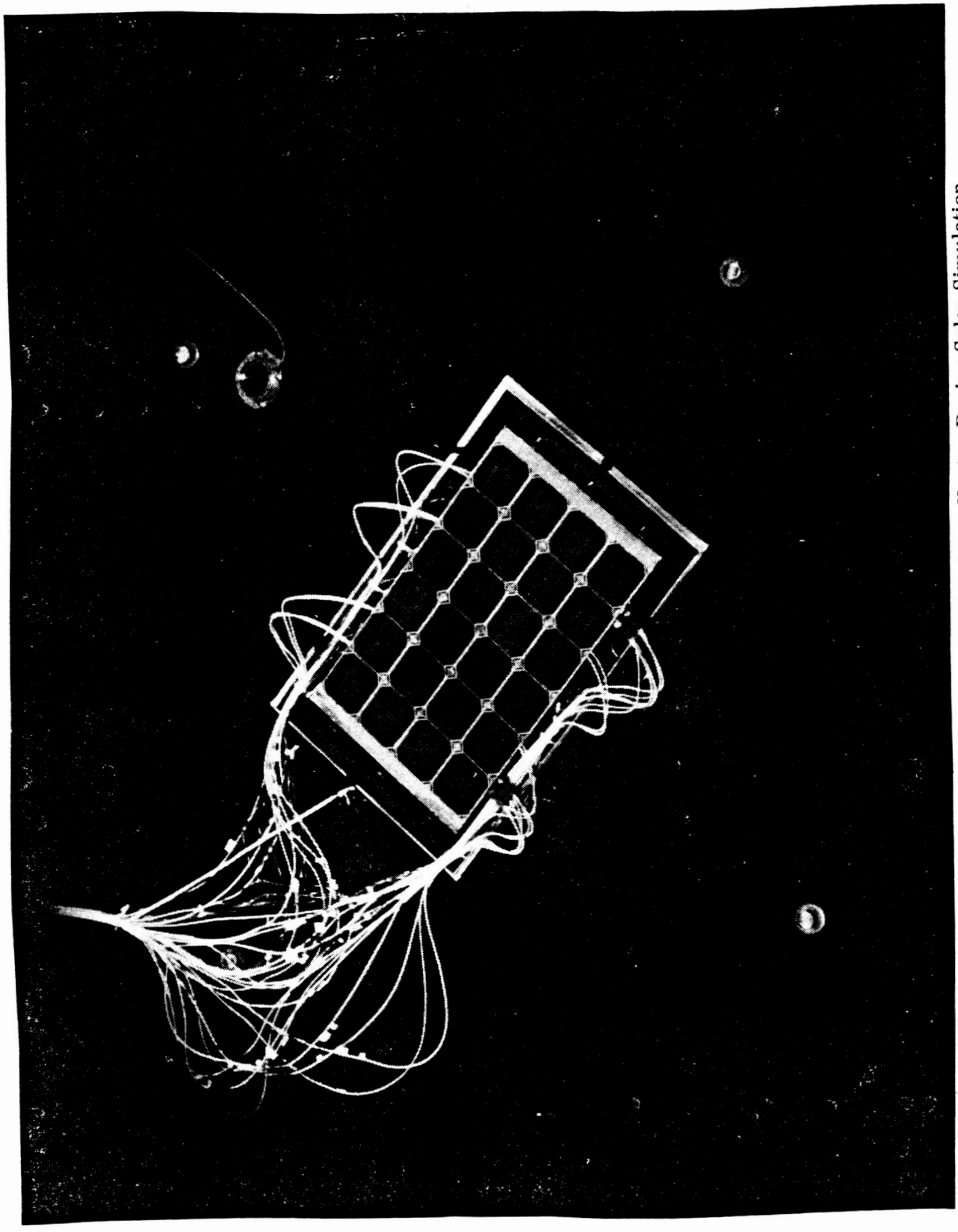

Figure 4-16 Superstrate Module with Cut-Away Kapton During Solar Simulation

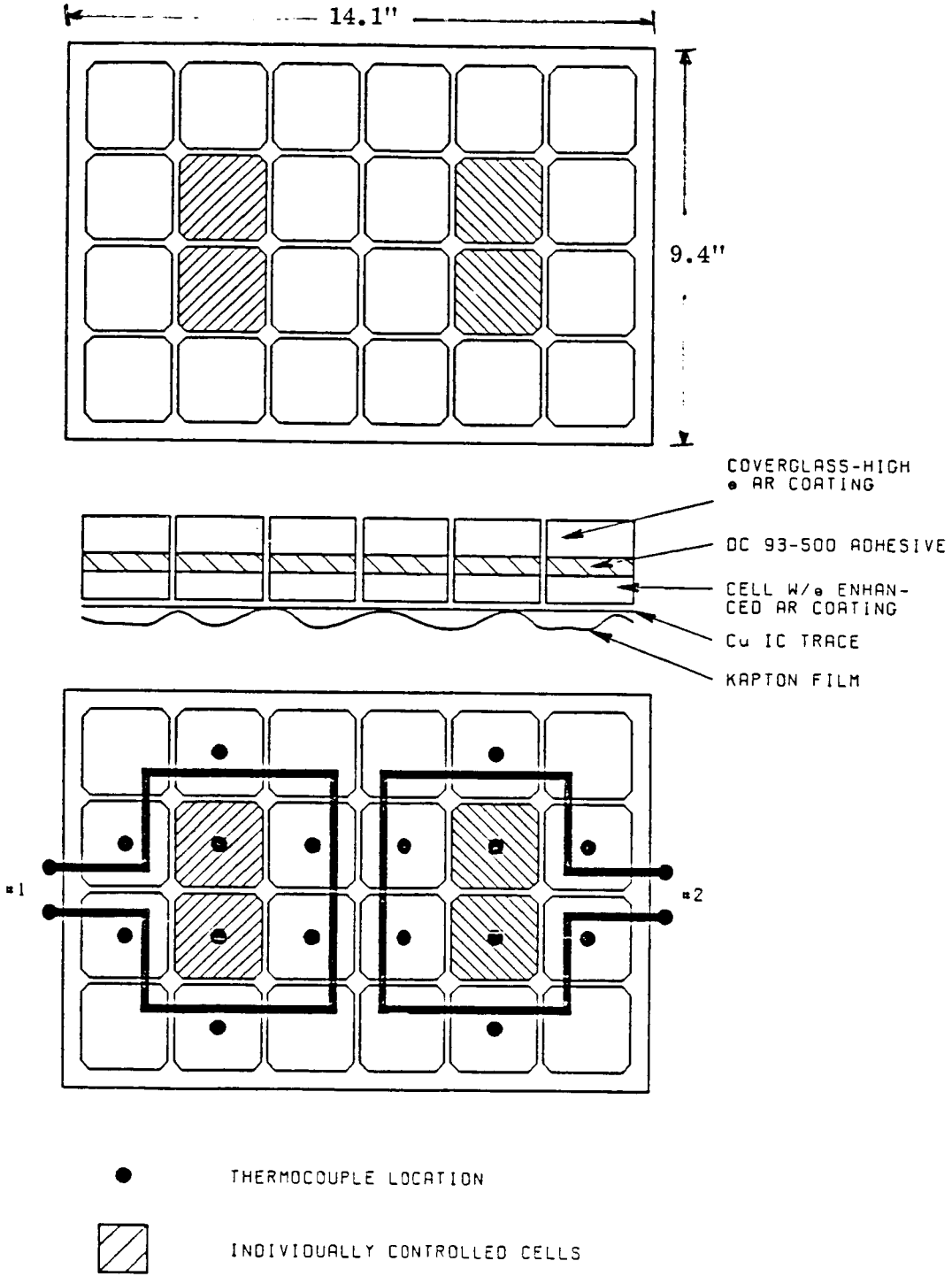

Figure 4-17 Module Circuitry and Thermocouple Locations

At the completion of the direct solar test, the solar simulator was set at 1.0 solar constant (1353W/m^2) and two albedo simulations were simulated. Both no load and loaded cases were run through.

For all tests, the earth emission cone temperature was kept at a constant temperature of approximately -50°F.

4.2.6 Thermal Analysis

A detailed thermal model of the solar cells and test chamber was created. The objective of the modeling was to compare model results with test data. When the two compare closely, one has more confidence that both the modeling techniques and the test results are valid.

4.2.6.1 Thermal Model. The radiation environments seen by the two faces of the test modules were modelled separately. The chamber surfaces above the test plane were modelled using Lockheed's HEATRATE computer program to calculate view factors and to create a radiation interchange network. The back faces of the test module radiated to only two surfaces: the earth IR-simulating cone and the albedo simulator window. The view factor from the cells to the albedo window was about 1% and was neglected. All chamber surfaces that had a significant influence on the solar cells were temperature controlled and were treated as sink nodes in the thermal modeling.

To simplify the analysis, only one solar cell was modelled. This simplification was possible for two reasons. First, all 24 cells were exposed to the same thermal environment and as a result they operated at similar temperatures. Second, the conduction and radiation resistance between cells prevented significant heat transfer between cells. The solar and albedo loads provided by the A1200 and X25L solar simulators were uniform over the entire test module. View factors to chamber surfaces above and below the test plane were similar for each of the cells. Heat leaks through thermocouple leads, electrical leads and test module suspension wires were too small to create significant temperature differences between cells. The electrical power extracted from each of the cells at a given time was similar (i.e.,

all cells open circuited, or all cells near maximum power). The 24 cells were co-planar. Therefore, radiation between cells could occur only by reflecting off chamber surfaces. Heat could conduct between cells through the glass superstrate, the kapton substrate, and the copper interconnects. Kapton (K = 0.3 Btu/hr ft F) and glass (K = 0.5 Btu/hr Ft F) are poor conductors. The small cross-sectional area of the high conductivity copper interconnects (.04 in x .0014 in) created a high conduction resistance between cells.

The schematic in Figure 4-18 shows the cell thermal model. The cell was modelled in an equivalent, ideal manner. The cell, the superstrate and the adhesive layer between the two were treated as a single node. The thin material layers (6 mils of glass, 2 mils of adhesive and 8 mils of silicon) resulted in little conduction resistance across the assembly. The temperature difference from the solar cell to the front of the superstrate glass was expected to be less than 1°F for these tests. Lateral temperature gradients (i.e., in the plane of the cell) existed in the solar cell due to conduction from the cell into the copper interconnects. However, the substrate design used in these tests resulted in lateral temperature differences of less than 1°F in the cell.

In all three test modules, the substrate was not adhered to the back of the cell. The substrate was attached only at the weld pads. Contact conductance between the cell and substrate was neglected. The copper interconnects were modelled with a single equivalent fin. The length of the equivalent fin equaled the average length of the copper interconnect fins on the substrate (1.1 in.). The fraction of the back surface area of the cell that the equivalent fin covers equaled the fraction of total substrate area that copper interconnects covered (10%). The copper fin was broken into five nodes along its length. Each of these nodes had a radiation hookup with the solar cell and also radiated to the earth IR simulating cone. Heat conducted laterally from each of the copper fin nodes into a series of four kapton nodes. The conduction resistors and radiation constants for these kapton nodes were effective values due to the use of the equivalent copper fin. The remainder of the kapton substrate was unaffected by the copper fin. Heat transfer into and out of this section was by radiation only. The cell radiated from its front face to the sink nodes above the test plane. The cell back face radiated to the nodes of the substrate, and also the earth IR simulating core.

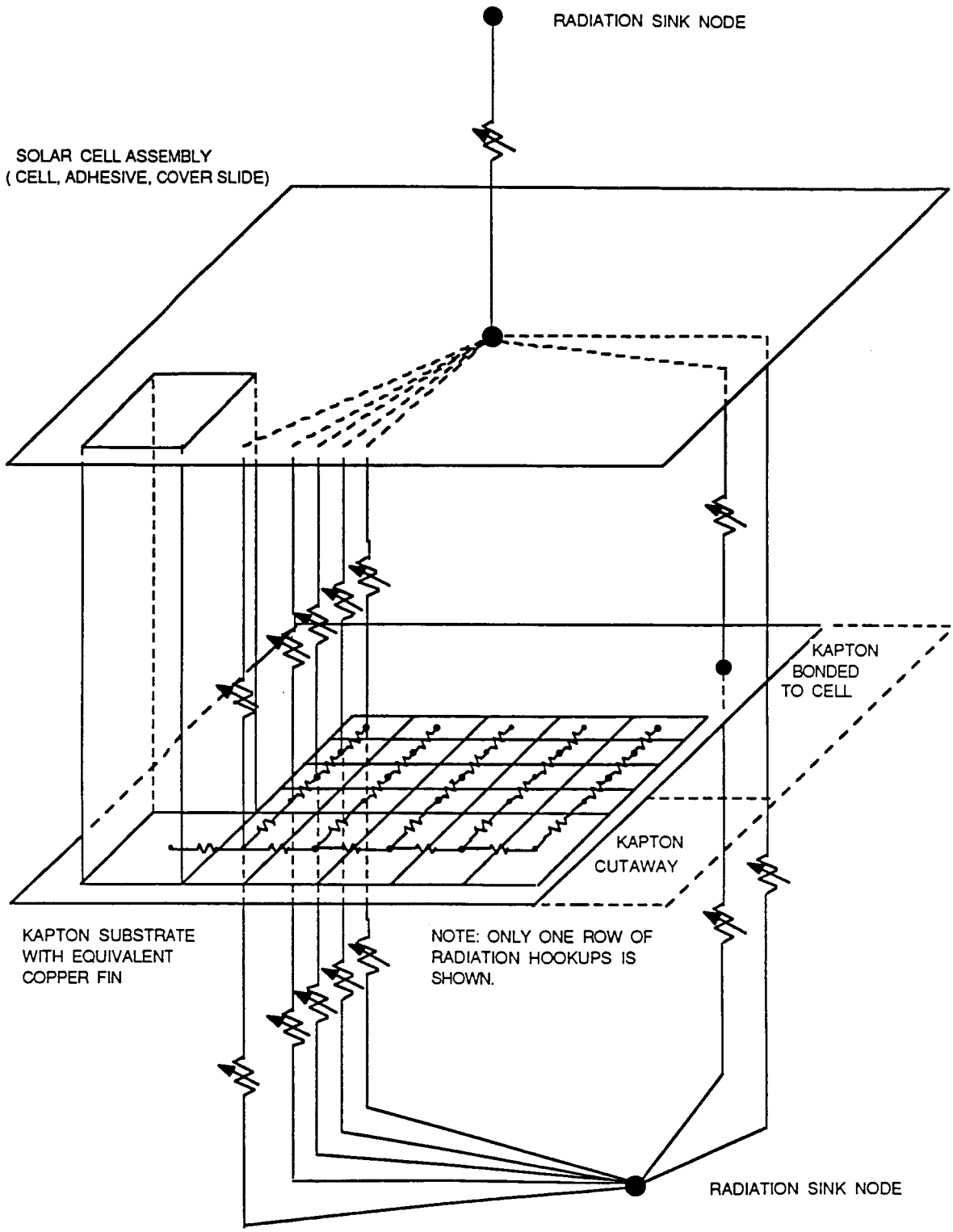

Figure 4-18 Cell Thermal Model

For the two test modules with full substrates, the radiation directly from the cell back face to the cone was due to the partial transparency of the substrate to infrared radiation ($\tau_{IR} = .13$). In sections where the substrate is bonded to the cell back face or cutaway, the cell radiates directly from its back face.

The thermal surface properties of test modules used in modeling were based on spectral measurements of material reflectance and transmittance. Measurements were made for several solar cells. Average values were used in the model. The spectral distributions of energy supplied by the A1200 solar simulator and the X25L albedo simulator did not match the true solar distribution. The thermal surface properties of solar cells and the kapton substrate were corrected by integrating absorptance, reflectance, and transmittance with respect to the spectral energy distributions of the simulators. Table 4-4 provides a summary of the thermal surface properties used in the analysis. The total solar and albedo heat load absorbed in the cell and substrate nodes included the secondary terms stemming from reflection and transmission of energy within the test module. The electrical power extracted from the cell was subtracted from the total absorbed solar and albedo to arrive at a net heat load in the cell.

4.2.6.2 Results. Figure 4-19 shows one case for the opaque cell with full substrate. The model results and test data matched within 3°F at steady state. From 138 minutes to 155 minutes, the power circuit was open. From 155 minutes to the 203 minutes there were four different resistances in the electrical circuit. The minimum temperature around the 170 minute mark corresponded with the maximum electrical power extracted from the cell. The transition to the next test case (1.0 solar, 0.30 albedo) began at the 203 minute mark. There were 20 total cases for the opaque cell with full substrate. In 17 of the cases, the model results matched the test data within 5°F at steady state. The remaining three cases matched within 10°F.

TABLE 4-4

SUMMARY OF THERMAL SURFACE PROPERTIES

	Solar Spectrum (A1200)			Albedo Spectrum (X25L)				
	α	ρ	τ	α	ρ	τ	ϵ_{IR}	τ_{IR}
• Opaque Cell Assembly Front Face (Opaque Solar Cell, Adhesive, Superstrate)	0.72	0.28	0	--	--	--	0.85	0
• Opaque Cell Assembly Back Face	--	--	--	0.08	0.92	0	0.1	0
• Transparent Cell Assembly Front Face (Transparent Solar Cell, Adhesive, Superstrate)	.686	.135	.179	--	--	--	0.85	0
• Transparent Cell Assembly Back Face	--	--	--	0.57	0.295	0.135	0.60	0
• Kapton and Polyester Laminate	--	--	--	0.173	0.144	0.683	0.75	0.13
• Kapton Side of a Kapton, Polyester, and Copper Laminate	--	--	--	--	--	--	0.73	0
• Copper Side of a Kapton, Polyester, and Copper Laminate	--	--	--	0.26	0.74	0	0.04	0

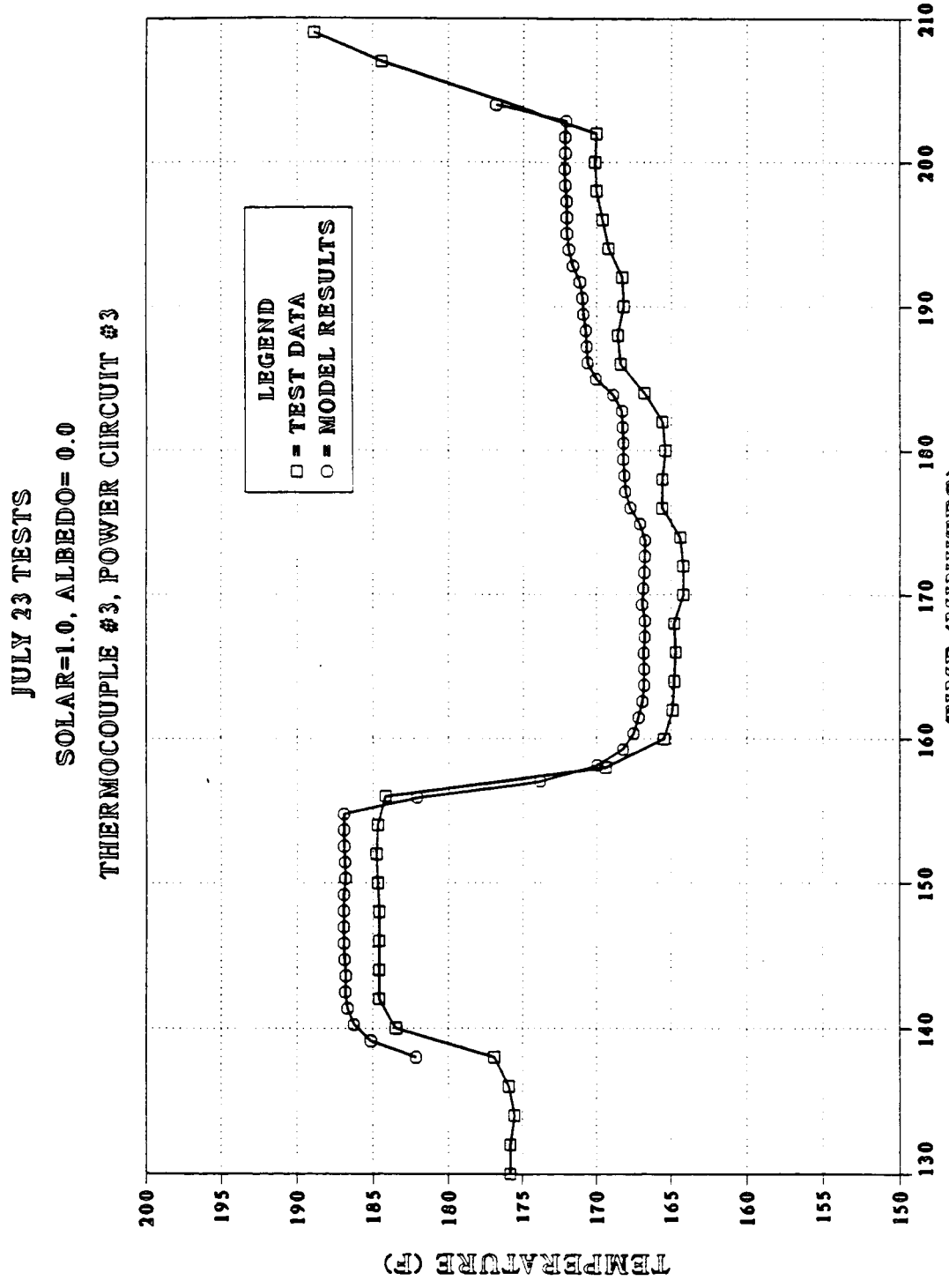

15-APR-87, *Thermodynamics*

Figure 4-19 Opaque Cell with Full Substrate

Figure 4-20 gives some typical results for the transparent cell with cutaway substrate. At steady state the model results were within 3°F of the test data for all power settings. The electrical circuit was open between 308 and 352 minutes, followed by three different electrical resistance settings between 352 minutes and 405 minutes. Between 372 minutes and 386 minutes the electrical circuit had a resistance of 0.45 Ω . During this period the model results and the test data responded in opposite manners. The electrical power data indicated a decrease in cell electrical power during this period. An increase in cell temperature should be expected. The test data showed a temperature decrease. This same discrepancy occurred throughout the tests of the two transparent cell test modules (July 24 and 25 tests). The phenomenon always occurred with the 0.45Ω resistance setting. The model predicted rapid temperature changes for the transparent cell with cutaway substrate. Rapid temperature changes were not found in the test data. The model underestimated either thermal capacitance of the test module or the effective resistance from the test module to the sink nodes of the chamber. Model results for all 20 test cases with the transparent cell and cutaway kapton were within 5°F of the test data at steady state.

Figure 4-21 shows one case for the transparent solar cell with full substrate. The electrical power circuit was open between 70 minutes and 97 minutes followed by three resistance settings between 97 minutes and 161 minutes. The 0.45Ω resistance setting produced the same contradictory results described earlier. In this case the model results and test data were within 10°F during all steady state periods. In all cases with this test module, the test data indicated lower operating temperatures than the model predicted. In 12 of 15 cases for this test module, the test data and model results were within 10°F at all steady state conditions. The remaining 3 cases were within 15°F. The five cases for power circuit #1 were not considered, because a disconnected thermocouple resulted in erroneous test data.

The differences in thermal performance between the three module designs are illustrated in Figures 4-22 and 4-23. Model results for a case with no albedo load are plotted in Figure 4-22. At maximum cell power the transparent cell with the cutaway substrate operates 12°F cooler than the transparent cell with the full substrate and 42°F cooler than the opaque cell with the full substrate. The temperature

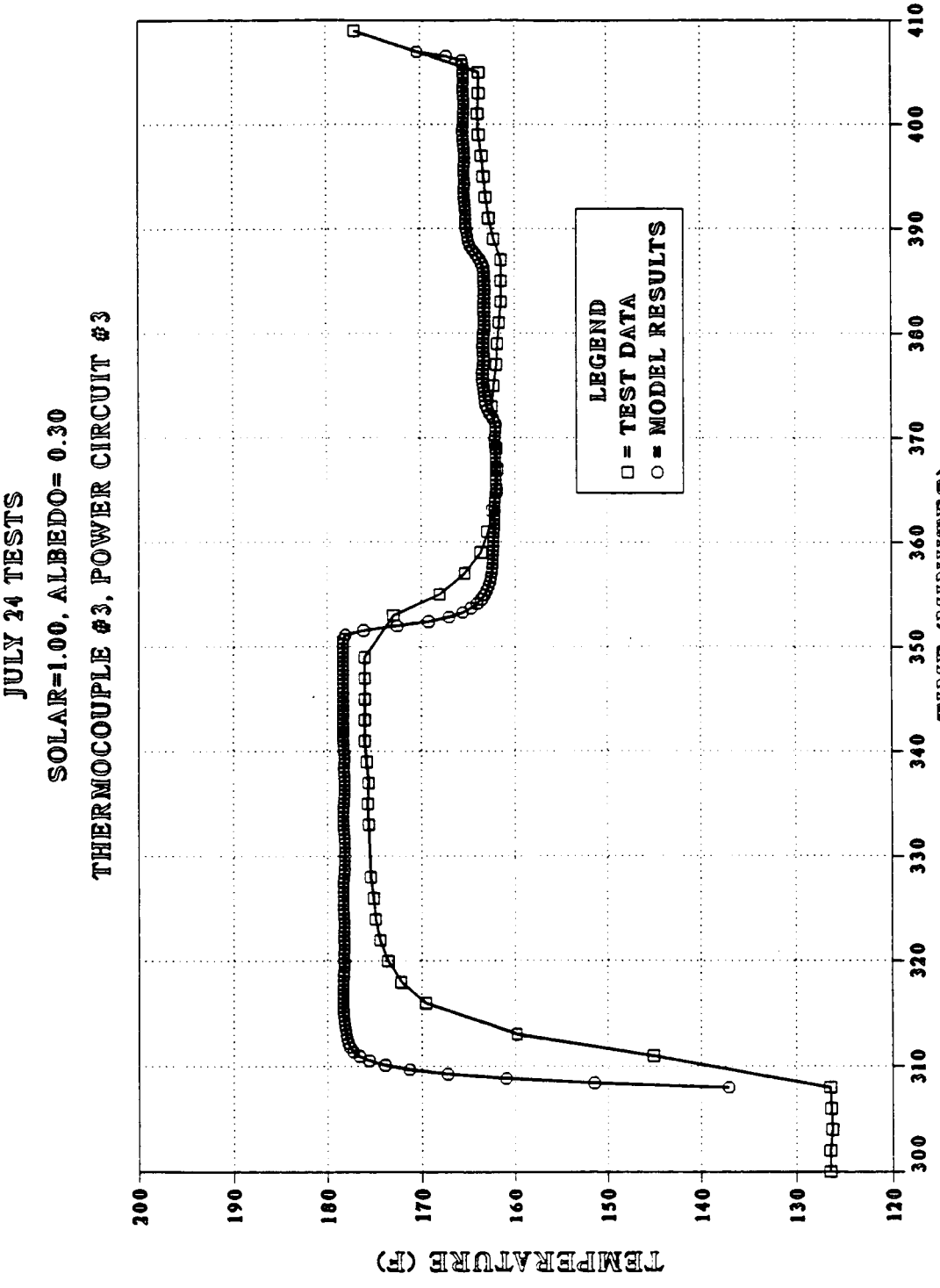

15-APR-87, *Thermodynamics*

Figure 4-20 Transparent Cell with Cutaway Substrate

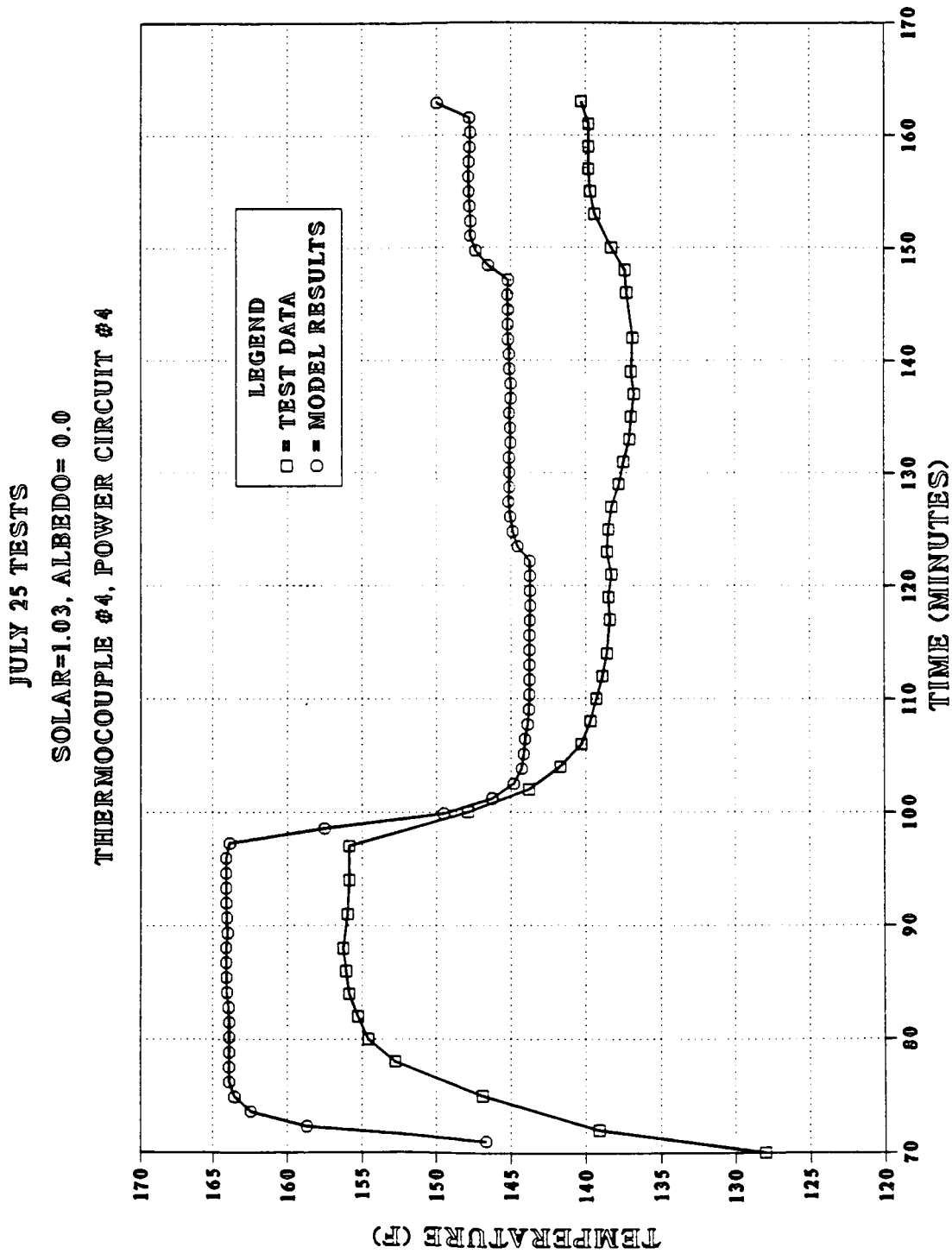

15-APR-87, *Thermodynamics*

Figure 4-21 Transparent Cell with Full Substrate

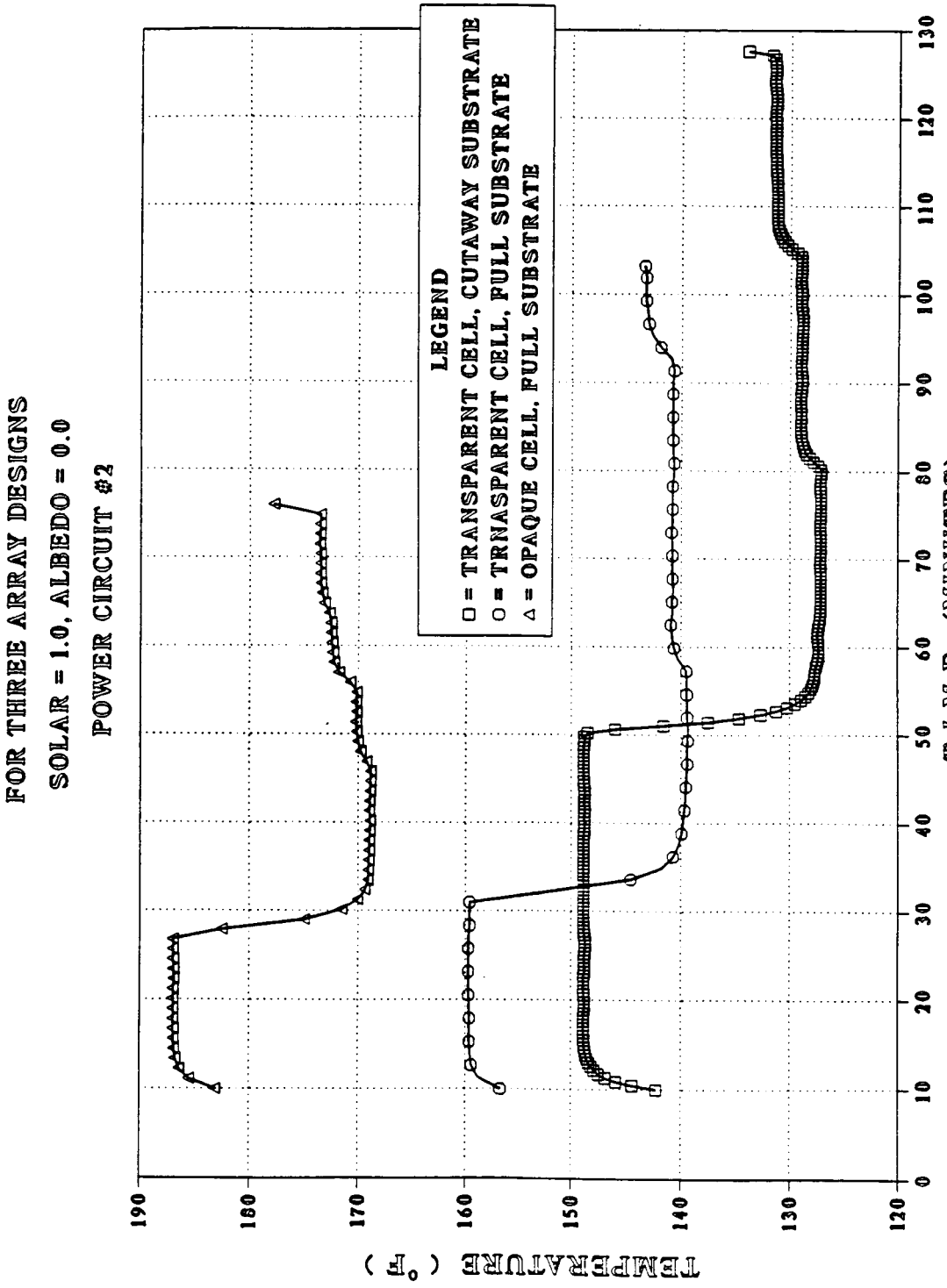

28-APR-87, *Thermodynamics*

Figure 4-22 Predicted Solar Cell Test Temperatures

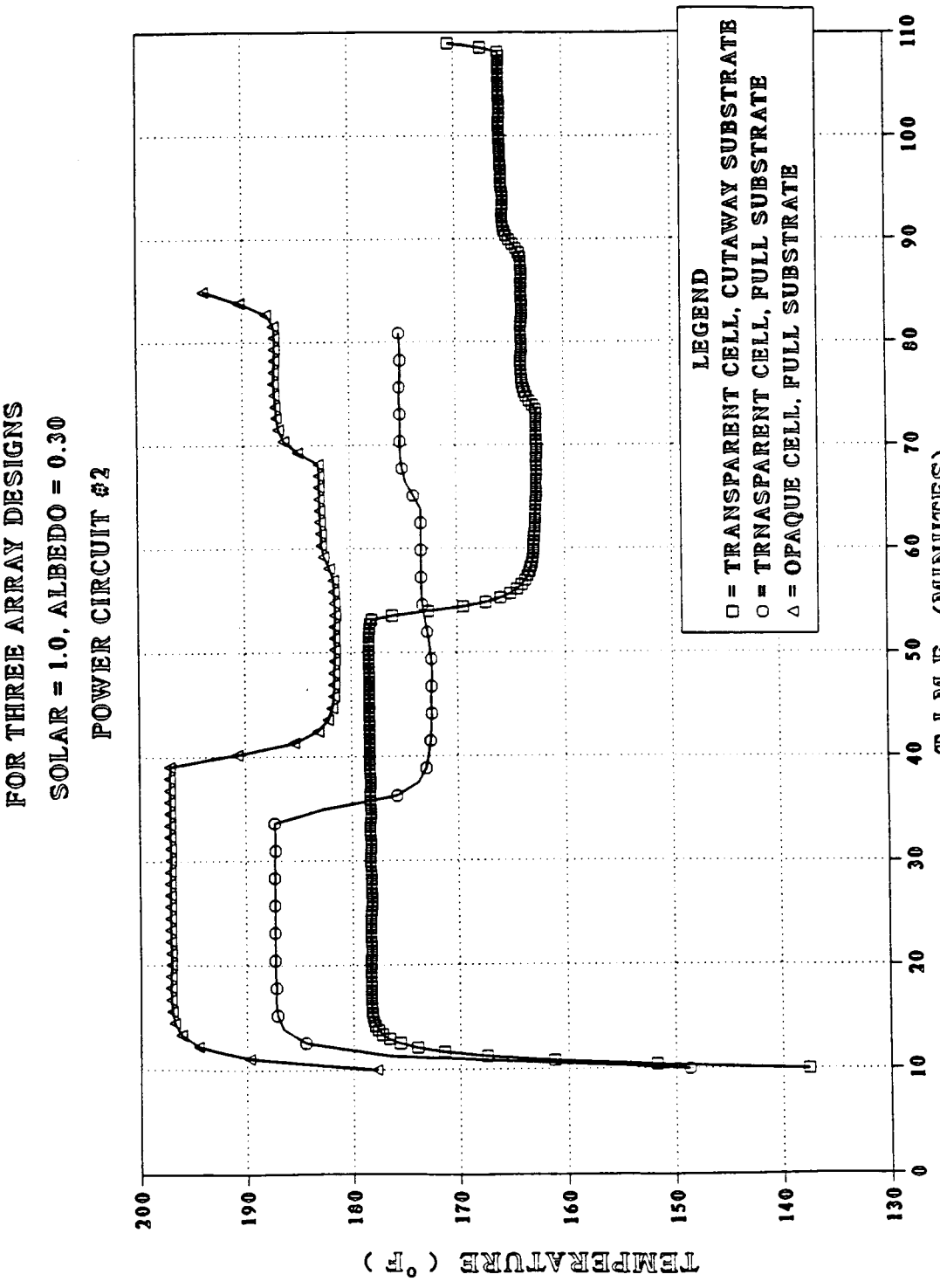

Figure 4-23 Predicted Solar Cell Test Temperatures

differences result from two factors: the solar absorptance of the cells and the radiation of heat off the back face of the cells. The solar absorptance of the opaque cells is 0.72 versus 0.69 for the transparent cells. The opaque cell absorbs some wavelengths that the transparent cell would transmit. The .03 increase in absorptance results in a 6°F increase in cell temperature. The opaque cell test module is the worst of the three designs in terms of radiation off the back face. The cell back face has an emittance of 0.1. As a result, radiation between the cell and substrate is negligible. The copper interconnects provide a conduction path between the cell and substrate, but the low conductivity and thin cross-section of the kapton keep most of the substrate isolated from the copper interconnects. The transparent cell with the full substrate performs somewhat better than the opaque test module because the cell back face has 0.6 emittance. However, radiation from the back face is limited due to the presence of the full substrate. Heat radiated from the cell is absorbed by the substrate and then re-radiated at lower temperature. The cutaway substrate design keeps this radiation shield effect to a minimum.

With an albedo load on the back face, the solar absorptances of the substrate and of the back surface of the cell become significant. Figure 4-23 shows model results for the three module designs for a case with an albedo load. At maximum power conditions, the temperature difference between the opaque cell module design and the cutaway substrate module design is only 19°F versus a 42°F temperature difference with no albedo load. The metallic back surface of the opaque cell (α = .08) absorbs less solar energy than the gridded back surface of the transparent cell (α = .57).

Some design changes could be made to enhance cell thermal performance. Bonding the substrate to the back of the cell over part or all of the back face would enhance heat rejection off the back of the cell. The bonding would be most beneficial in designs incorporating a full substrate. Designs with a cutaway substrate would be improved by application of a 3 to 5 mil layer of a high IR emittance, low solar absorptance coating to the back of the cells. The material would have to be transparent to wavelengths from 1 μm to 3 μm for use with the transparent gridded back cells. The DC 93-500 adhesive would satisfy all these requirements.

Figure 4-24 shows predicted orbital temperatures for four array designs that are similar to the test modules. The orbital designs include the changes listed above. The thermal surface properties were integrated with respect to the true solar spectrum for this analysis. There were important differences in some thermal surface properties:

Opaque cell assembly front face solar absorptance = 0.68

Transparent cell assembly solar absorptance (front and back) = 0.62

With the cutaway substrate, the exposed area of the back of cells was assumed to have an enhanced 0.85 emittance. The electrical conversion was governed by the equation:

$$e = .132\ (1-.0044\ (T_{Cell} - 28°C))$$

The thermal surface properties and the electrical conversion efficiency are beginning of life values.

From 34 minutes to 93 minutes the array has full normal sun. The peak temperatures at 65 minutes occur when the array is at the sub-solar point in the orbit, where there is full earthshine and albedo on the back of the cells.

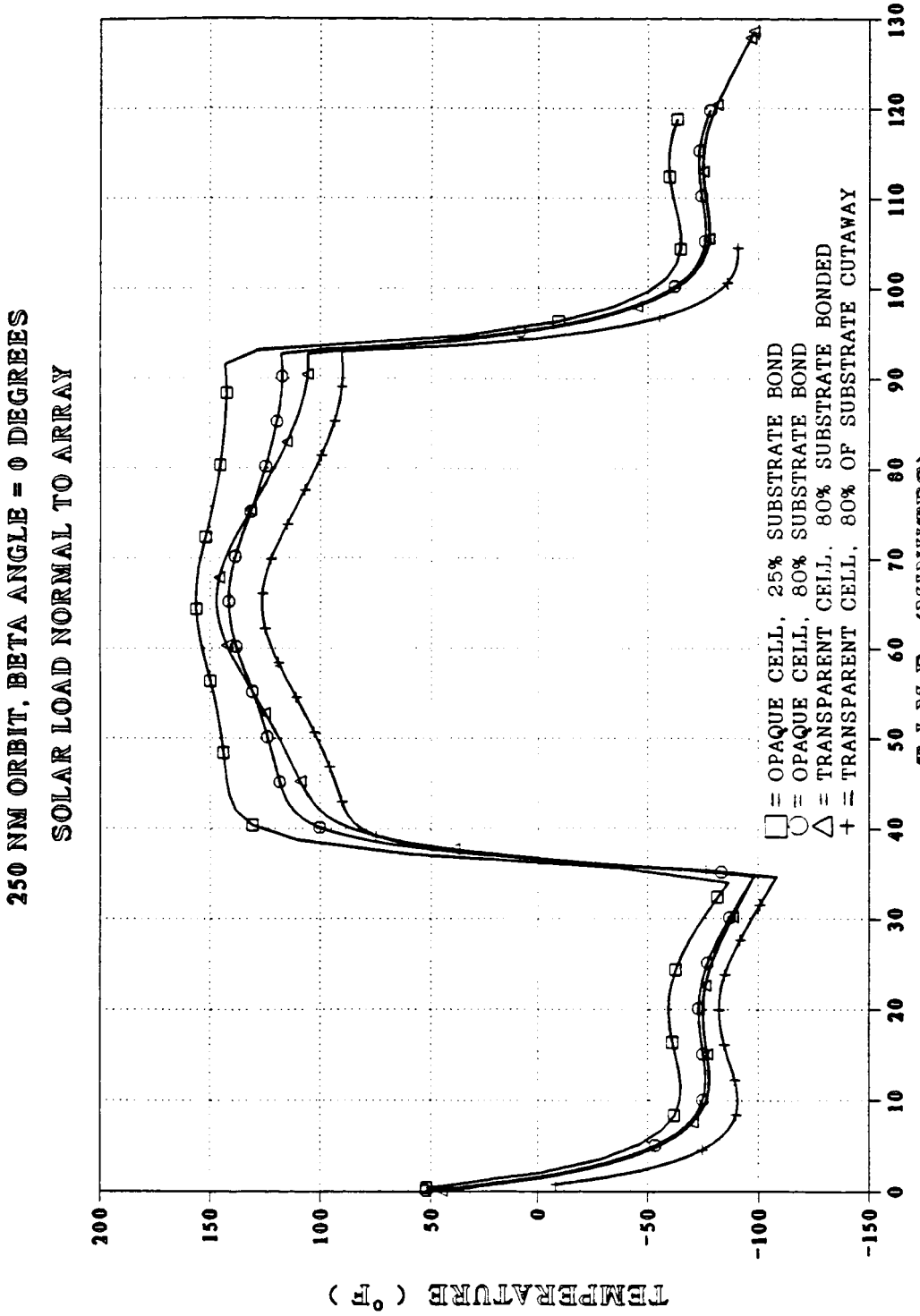

Figure 4-24 Predicted Cell Temperatures on Orbit

4.3 PANEL SEGMENT ASSEMBLY (TASK 2.3)

4.3.1 Description of Panel Segment Assembly

A five unit panel segment was fabricated and appears in Figure 4-25. All five modules are identical. The superstrate glass used to fabricate the modules was .020 inch thick. IR transparent solar cells were used and most of the copper/kapton interconnect was cut away to allow for maximum IR transmission. Figure 4-26 shows the back side of the panel segment.

The panel segment has two electrical circuits, an upper and a lower. This is achieved by dividing each module into two separate twelve cell strings. The module terminations are located so that electrical jumpers can connect to adjacent module interconnects. When all jumpers were installed the panel segment became two circuits with each circuit being a sixty cell string. Figure 4-27 shows a closeup of a jumper on the superstrate modules installed in the panel segment.

A closeup of the completed superstrate panel segment is shown in Figure 4-28. Figure 4-29 shows a disassembled superstrate panel segment. The panel segment frame which was made of aluminum channel is shown in Figure 4-30. The superstrates were attached to the frame using springs. In order to use the superstrate hinge, special fiberglass/moly hinges were fabricated as shown in Figure 4-31. By using these fiberglass/moly hinges, the hinge simulates being installed on a deployed superstrate wing assembly. Figure 4-32 shows a closeup of the cut-away kapton interconnect welded to the superstrate assembly.

4.3.2 Panel Segment Acceptance Test

The panel segment was acceptance tested by thermal cycling each superstrate assembly separately. All five superstrates experienced 100 thermal cycles from -90°C to +50°C. The superstrate assemblies were electrically tested both before and after thermal cycling. After the panel segment was assembled, the unit was electrically tested and shipped. Figure 4-33 shows the acceptance test sequence. Figure 4-34 shows two of the five superstrate assemblies being acceptance tested in one of LMSC's thermal cycle chambers. Figure 4-35 shows the electrical test setup of LMSC's pulse light test system.

ORIGINAL PAGE IS
OF POOR QUALITY

Figure 4-25 Superstrate Panel Segment - Front Side

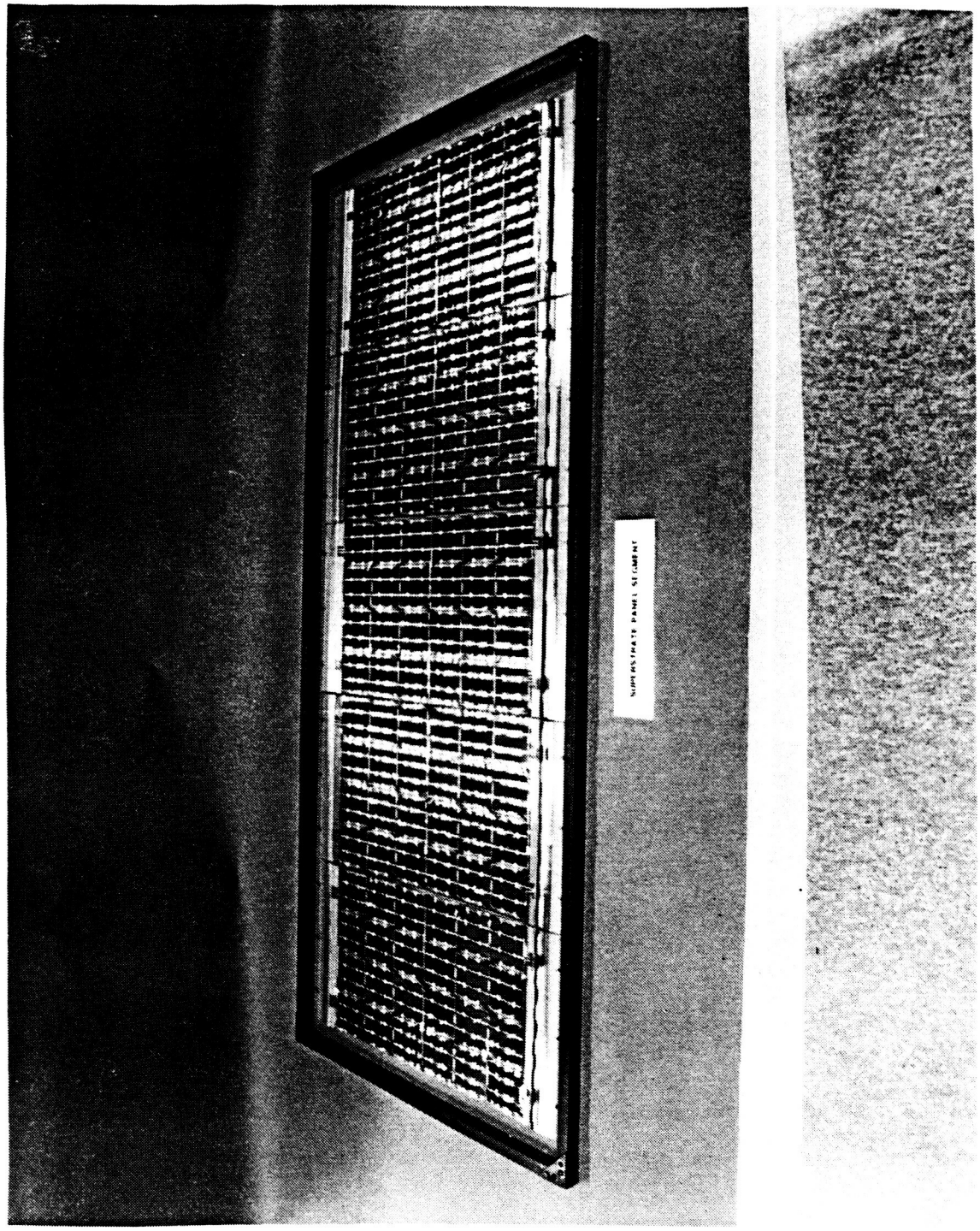

Figure 4-26 Superstrate Panel Segment - Back Side

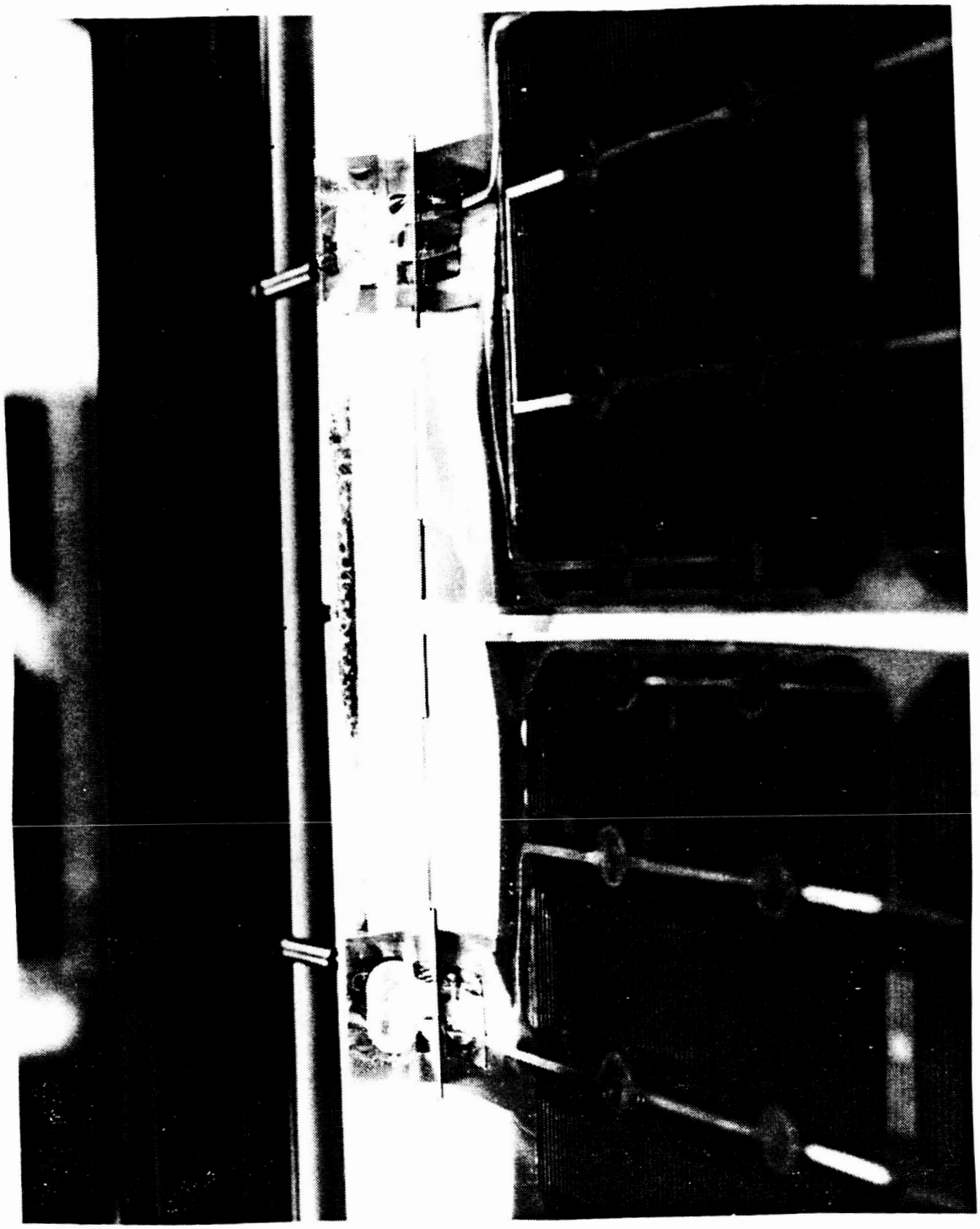

Figure 4-27 Electrically Connecting Two Superstrate Modules With Jumper - Back Side

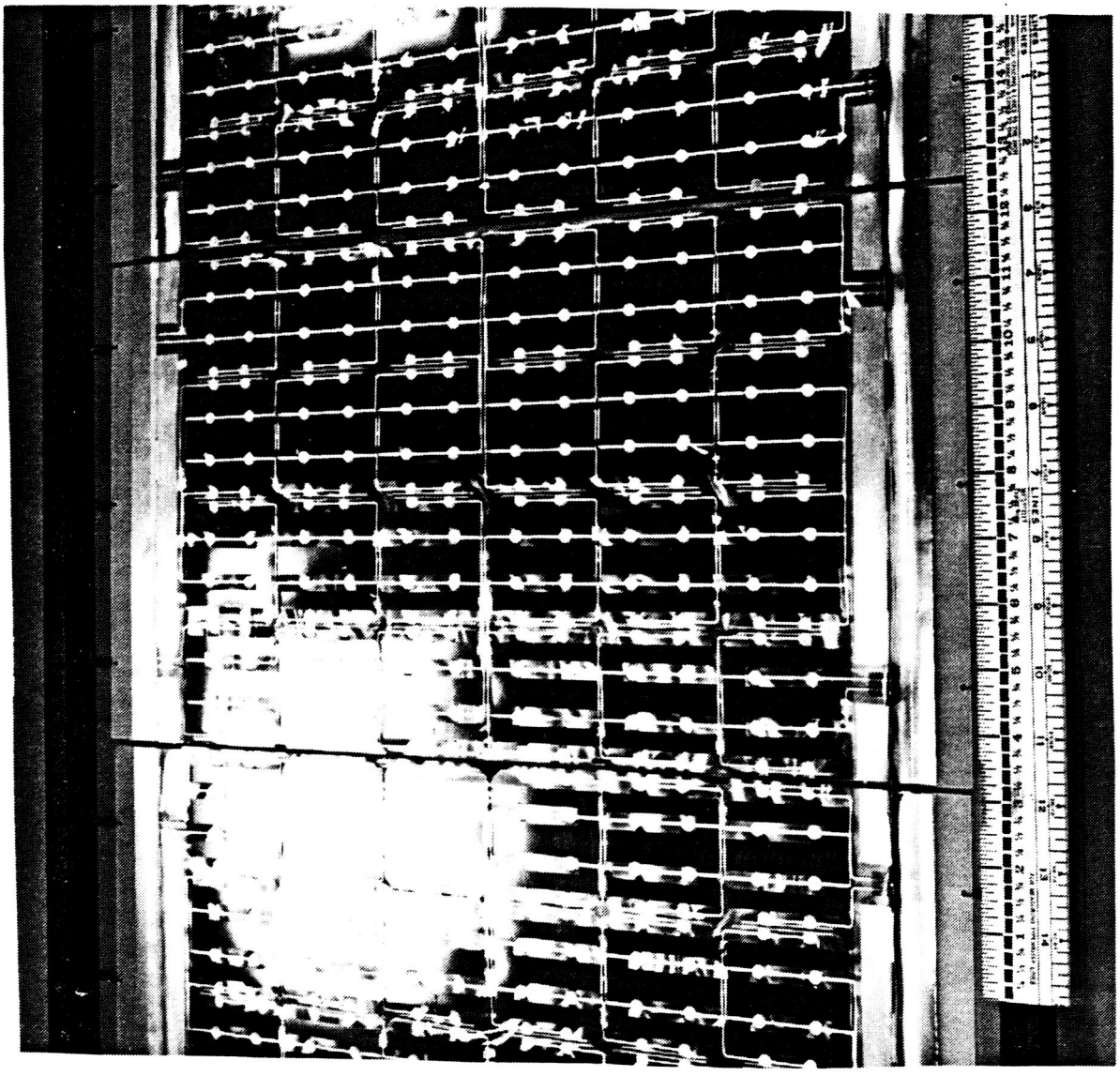

Figure 4-28 Closeup of Completed Superstrate Panel Segment

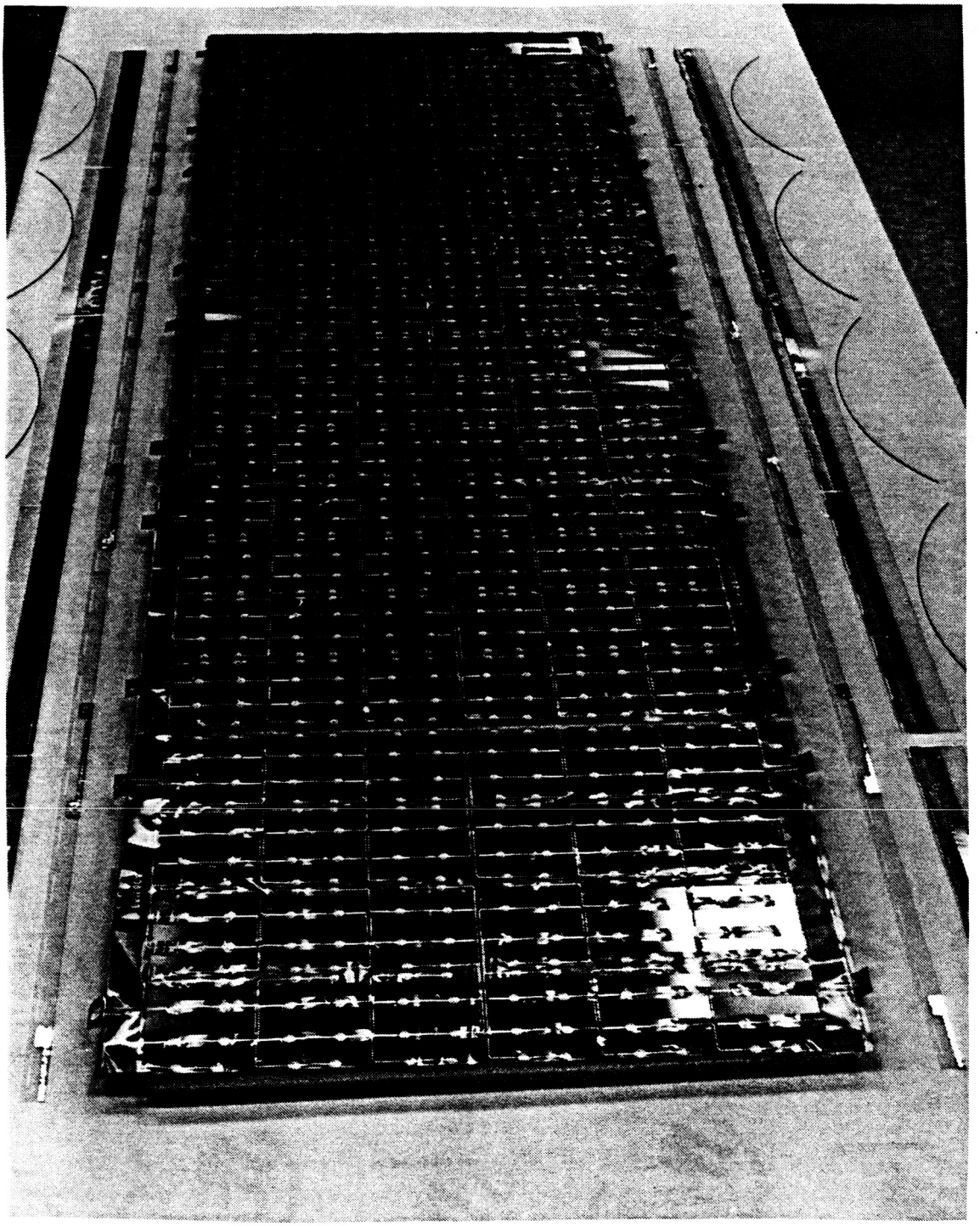

Figure 4-29 Disassembled Superstrate Panel Segment

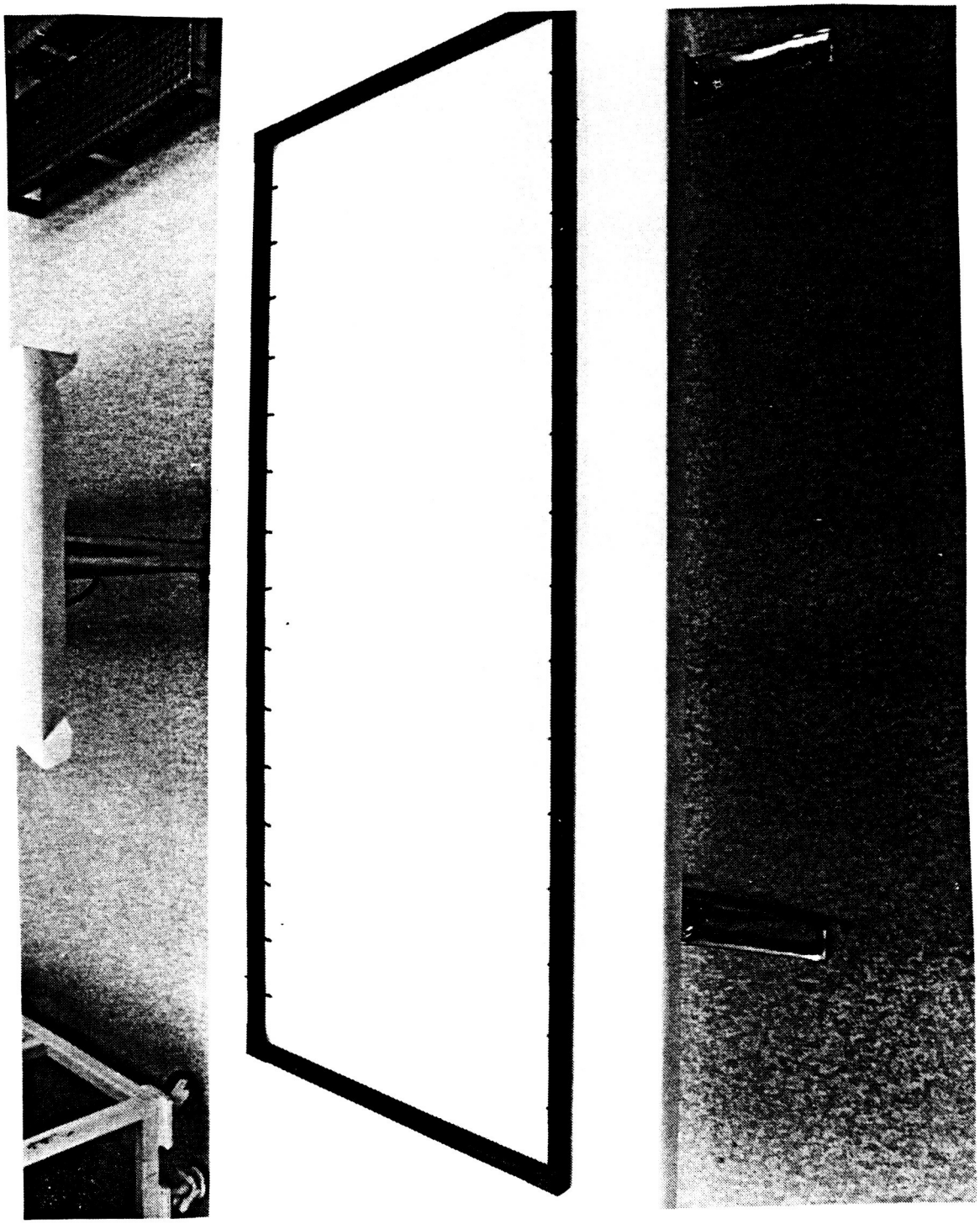

Figure 4-30 Superstrate Panel Segment Frame

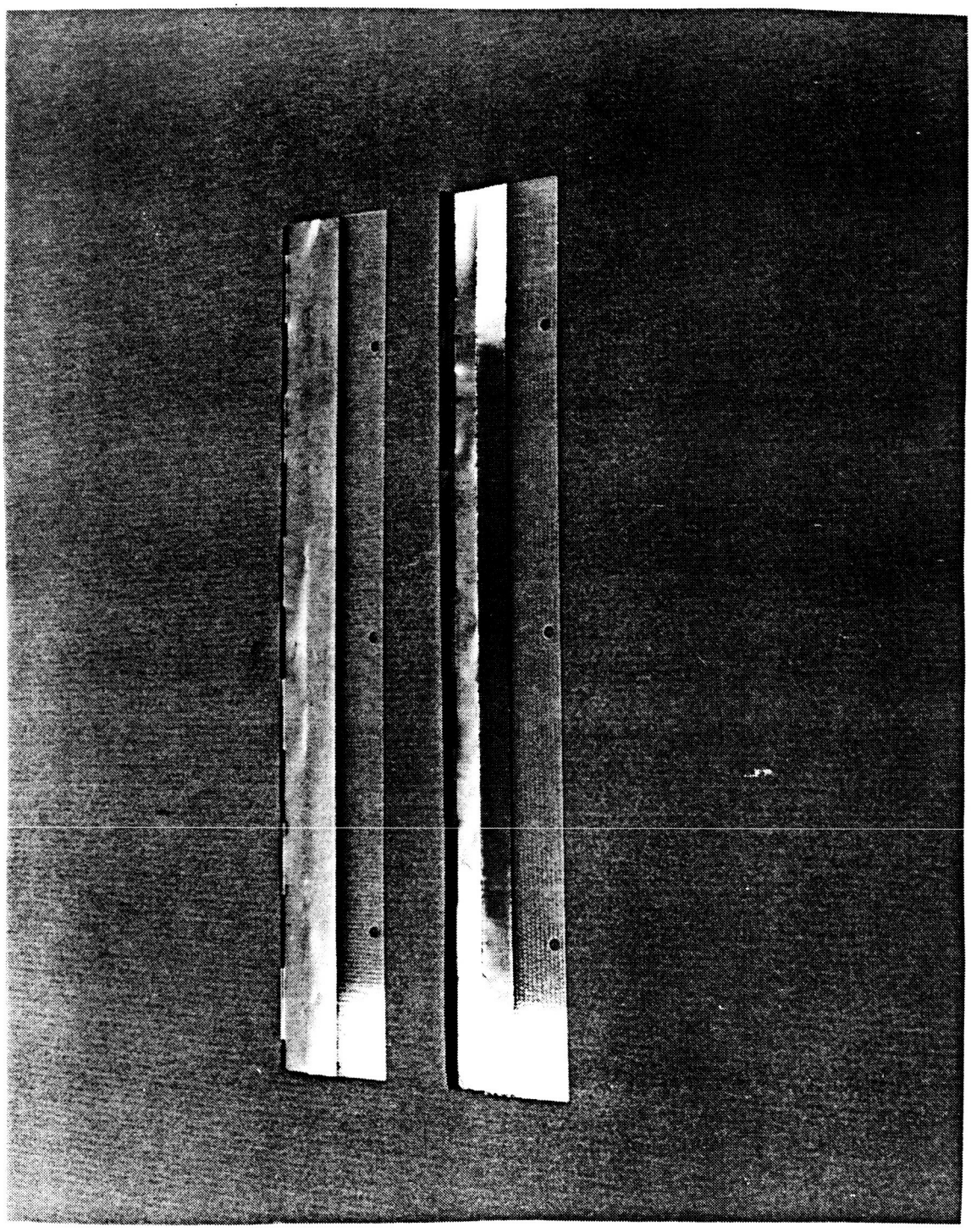

Figure 4-31 Formed Fiberglass/Moly Hinges for Panel Segment

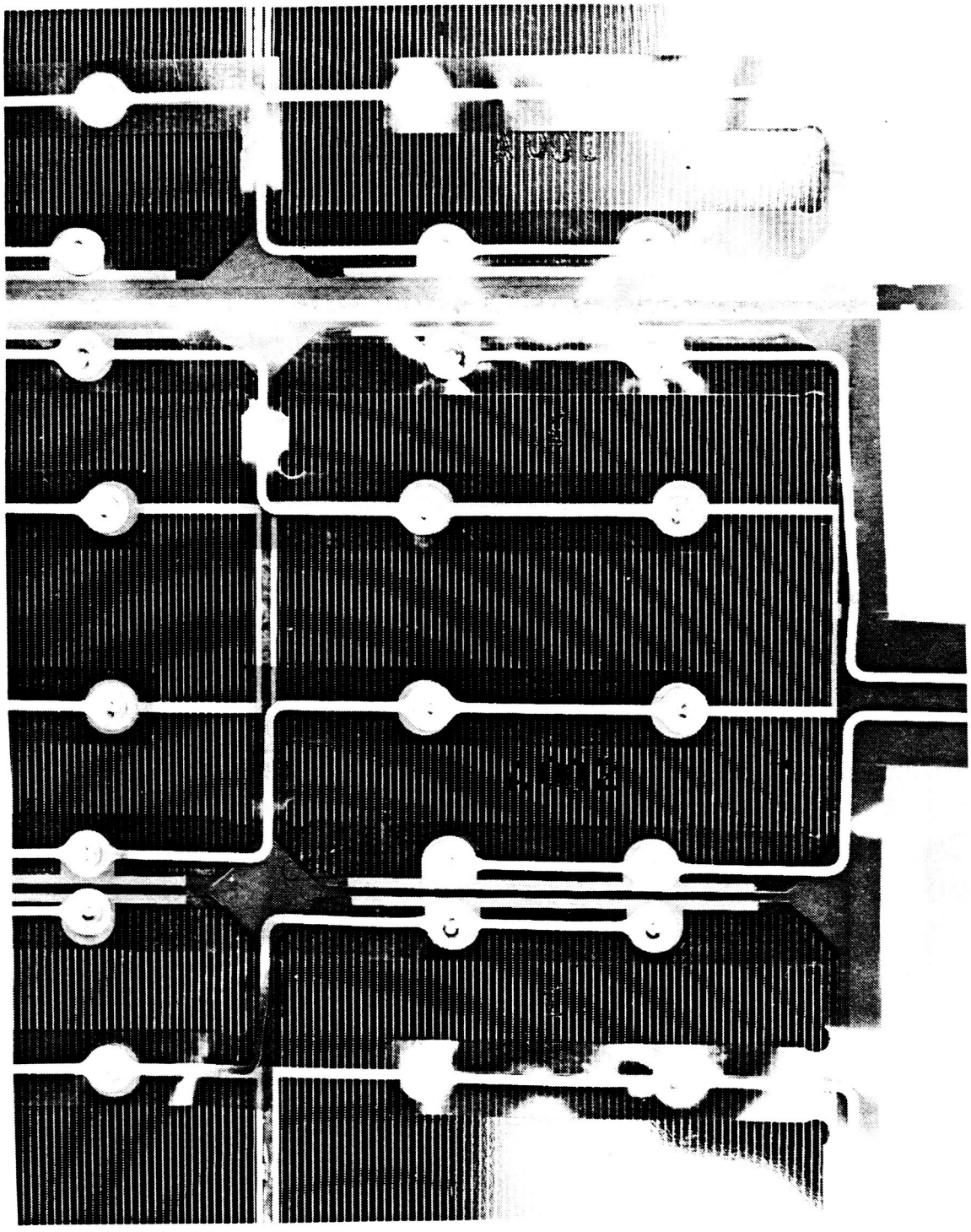

Figure 4-32 Closeup of Cut-Away Kapton Interconnect Welded to Superstrate Assembly

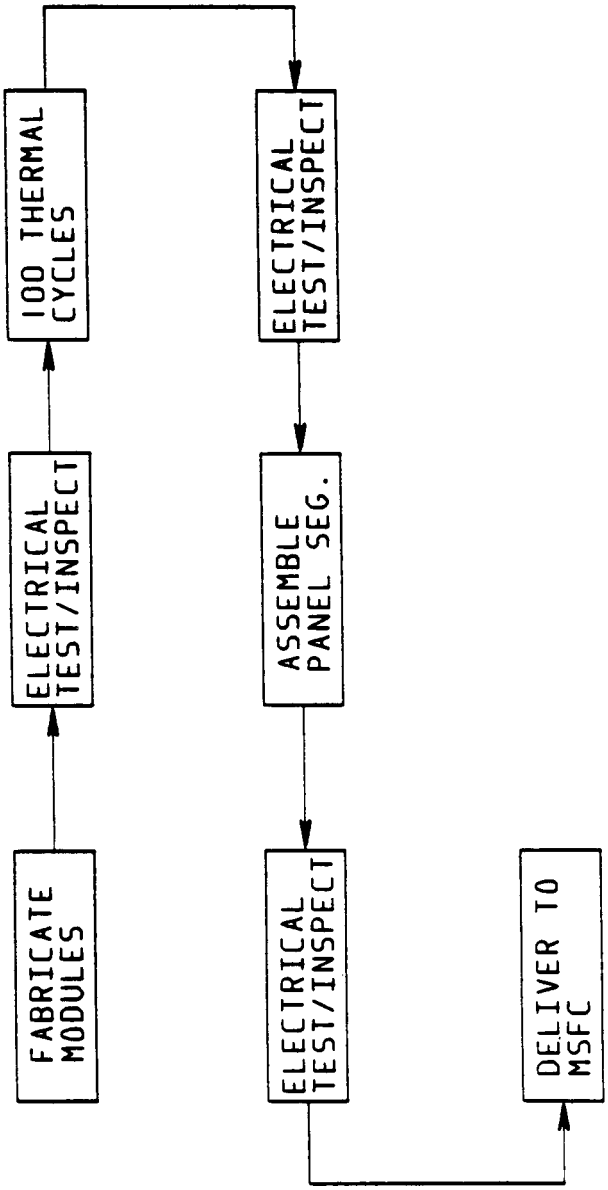

Figure 4-33 Panel Segment Acceptance Test

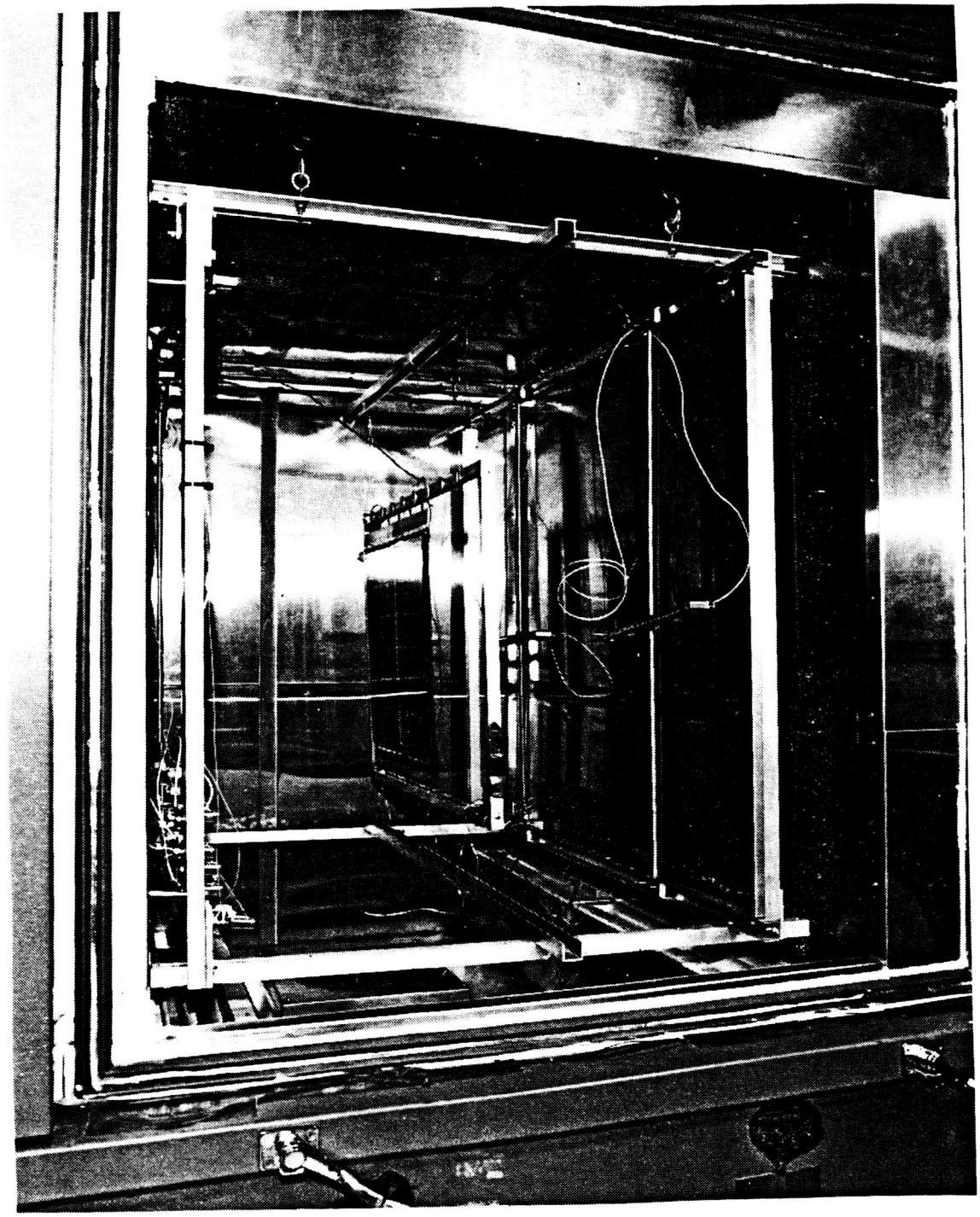

Figure 4-34 Panel Segment Acceptance Test - Front Side

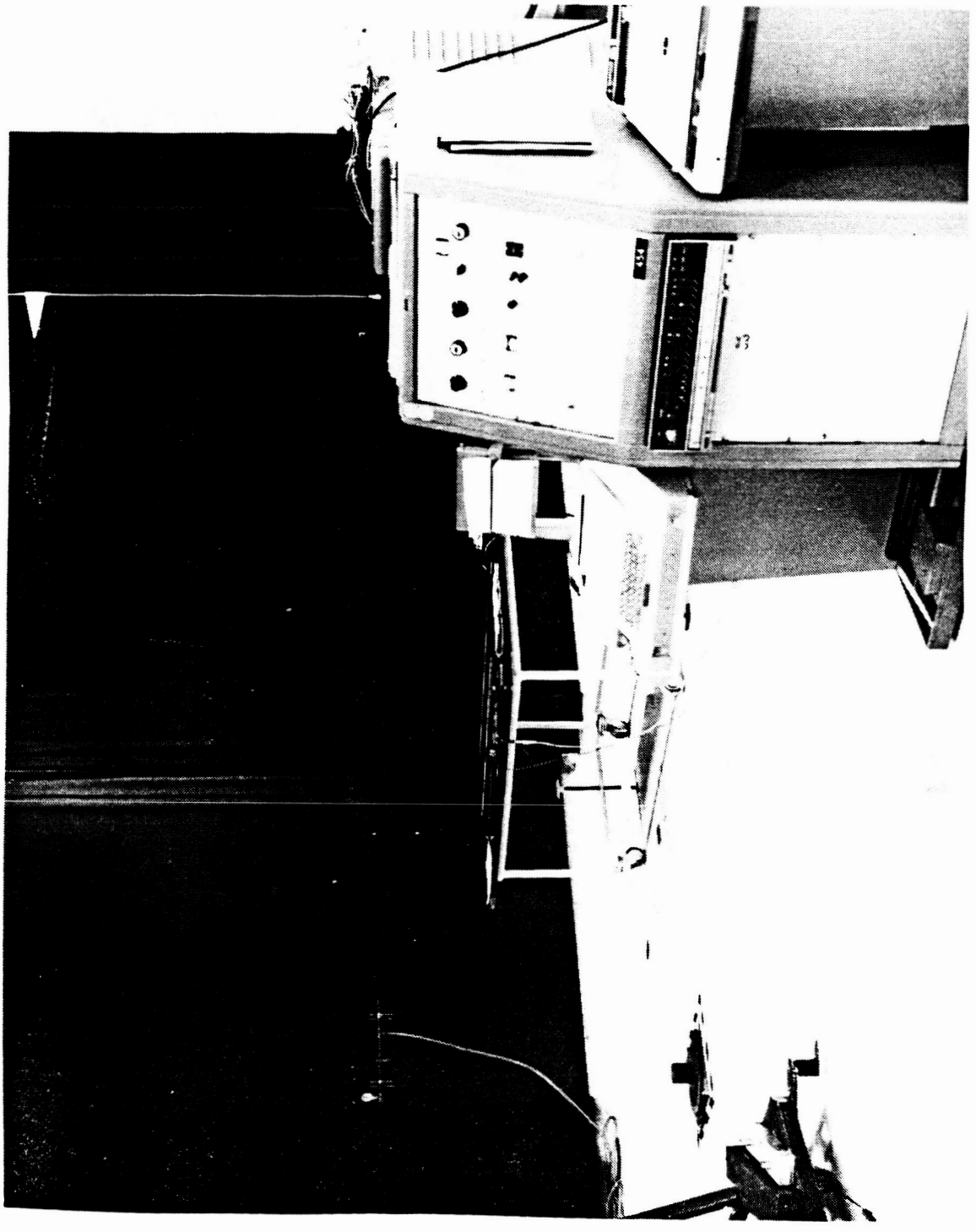

Figure 4-35 Setup for Electrical Testing of Panel Segment

Section 5
SUMMARY

The work completed under this contract included developing a process for manufacturing superstrate assemblies, fabricating ten superstrate modules and two conventional modules, thermal cycling four modules for 2000 cycles, performing a thermal balance test at Boeing, and delivering a panel segment to MSFC. The results of the above mentioned tests are contained within this report. As expected, the operating temperature of a superstrate module is less than the operating temperature of a SAFE-type module. The temperature difference between an optimum superstrate design vs an optimum SAFE-type design would be approximately 30°F.

Section 6

ADDITIONAL WORK

With the completion of this contract, the superstrate technology is now at a technology readiness level of 5 as defined by Table 6-1. For additional work, LMSC would like to reach level 6 by building a superstrate prototype wing. The scope of the original contract included building a prototype wing, but funding cutbacks resulted in MSFC eliminating the prototype wing from the contract.

TABLE 6-1
TECHNOLOGY READINESS LEVELS

LEVEL 1	BASIC PRINCIPLES OBSERVED AND REPORTED
LEVEL 2	CONCEPTUAL DESIGN FORMULATED
LEVEL 3	CONCEPTUAL DESIGN TESTED ANALYTICALLY OR EXPERIMENTALLY
LEVEL 4	CRITICAL FUNCTION/CHARACTERISTIC DEMONSTRATED
LEVEL 5	COMPONENT/BREADBOARD TESTED IN RELEVANT ENVIRONMENT
LEVEL 6	PROTOTYPE/ENGINEERING MODEL TESTED IN RELEVANT ENVIRONMENT
LEVEL 7	ENGINEERING MODEL TESTED IN SPACE

By building a prototype wing, LMSC could demonstrate the superstrate array benefits of low cost and increased efficiency over the SAFE-type array which is the current baseline for the Space Station solar array. The Space Station solar array costs could be significantly reduced by using superstrate technology. By bonding multiple solar cells to a sheet of glass at one time, the overall piece part count for fabricating a solar array is reduced. In addition, the modular design of a

superstrate array allows for easy production of modules and assembly into a wing. The superstrate array's lower operating temperature than the SAFE-type array means the superstrate array would be more efficient. This means the overall size of NASA's Space Station solar array would be reduced.